ABSTRACT

Walter Alex Smith, Jetting Techniques for Pile Installation and Environmental Impact Minimization. (Under the direction of Dr. Mohammed A. Gabr and Dr. Roy H. Borden)

Development of a comprehensive laboratory experimental program provided insight into the effects of jetting parameters (i.e. water volume flowrate and jet nozzle velocity) on maximum pile insertion depth, pile insertion rate, volume of debris transported to the ground surface, and the extent of the debris zone area (installation characteristics). This research is a two-part process involving laboratory and full-scale field jetting applications to determine the environmental impacts of jetting and the possibility of minimizing these impacts through jetting parameter optimization. The laboratory experimental program involved jetting installations in several soil types with unique grain-size distribution characteristics. Installation characteristics were compared for different sand types for the various jetting parameters investigated in order to develop a model for full-scale jetted pile installations. Results of the experimental program show that optimizing the jetting parameters for a given soil type may have positive effects on decreasing the surface impact of jetted pile installations. Recommended design procedures for using the jetted pile model are presented.

JETTING TECHNIQUES FOR PILE INSTALLATION AND ENVIRONMENTAL IMPACT MINIMIZATION

By

WALTER ALEX SMITH

A thesis submitted to the Graduate Faculty of
North Carolina State University
In partial fulfillment of the requirements for the
Degree of Master of Science

CIVIL ENGINEERING

RALEIGH, NORTH CAROLINA
2003

APPROVED BY:

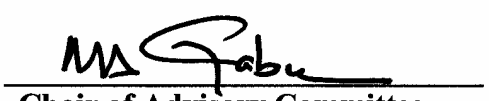

Chair of Advisory Committee
M.A. Gabr, Ph.D., P.E.

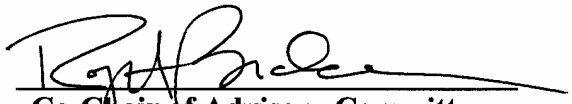

Co-Chair of Advisory Committee
R.H. Borden, Ph.D., P.E.

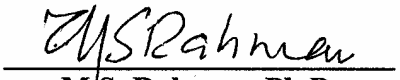

M.S. Rahman, Ph.D.

DEDICATION

The following work presented is dedicated to my grandparents; Lester Carl Smith Sr., Doris Atkinson Smith, James Corby Johnson Sr., and Mamie Lou Roberts Johnson. Carl Smith taught me the importance of family values, quality workmanship, and desire to move forward in life no matter what obstacles are in your path. Doris Smith's faith in God and constant prayers for her children and grandchildren have been felt and appreciated. The smile on her face when she sees her family burns constantly in my heart. The work ethic instilled in James Johnson is overwhelming. I hope that I have acquired some of that trait and utilize it for the betterment of my future. The importance of faith, love, and education has been taken from Mamie Lou Johnson. Her words of encouragement, knowledge, and understanding of the importance of education have challenged me to strive to become the person I am today.

BIOGRAPHY

Walter Alex Smith was born on November 21, 1978 to Lester Carl Smith Jr. and Helen Hudson Johnson Smith of Micro, North Carolina. He was raised in a small town where family and friends were always near and glad to see you. He has an older brother named Lester Carl Smith III whom has been a best friend throughout his life. As an Eagle Scout, he has learned to appreciate and protect the resources that God has provided and the responsibilities and importance of citizenship. He attended school at Micro-Pine Level Elementary, North Johnston Middle, and North Johnston High School. He decided to enroll at North Carolina State University for his secondary education and pursue a degree in Civil Engineering. Upon working as a technician in several fields of civil engineering during school, he decided to further his studies in Geotechnical Engineering. He enjoys outdoor sporting activities, conservation, and is thankful that his country allows him this freedom.

ACKNOWLEDGEMENTS

I thank God for the abilities and the opportunities that He has given me. I thank Him for a loving family and group of close friends whom have supported me throughout my life. Without many answered prayers from above, I could not be where I am today.

I would like to thank Dr. Mohammed Gabr for the opportunity he gave me to achieve this educational goal. Without the confidence, support, and knowledge that he has contributed to me, I could not have completed this work. I would also like to thank Dr. Roy Borden for the effort he contributes in teaching students to convey their thoughts and develop their minds in order to become better engineers. The guidance, knowledge, and friendship contributed by these two individuals are greatly appreciated. I would also like to thank Dr. Shammur Rahman for his role on my research committee and review of my work.

I thank my family for their continuous love, support, and prayers which they have provided in my favor. You have allowed me to set my own goals and expectations and provided the means and necessities to achieve these ambitions. I hope that someday I can return your investment to make your lives even more pleasant than they already are.

Several personal friends have been influential in helping me achieve this goal. The friendship that I have developed with Levi Denton has helped me in many aspects of this achievement. First, the ability for us to work together towards a common goal and the power of mutually reasoning through this research has at times even surprised us. Without the many hours that you have spent in fabrication, testing, analysis, and support, this research could not have been completed. Thank you for all that you have done, and good luck in continuing this research. I would also like to thank Jodie Nixon for

inspiring me to continue my education. He has led me to understand that knowledge does not come from memorization of facts alone, but that true knowledge evolves from understanding and implementation of the principles behind the facts. I will never forget your patience, friendship, and guidance that you provided to me through these past few years. Luke Menius and Adam Browning have been helpful in conducting many of the characterization tests required in this research. Their work ethic and work quality have allowed me to contribute more time to the development of this thesis. Finally, to Kelly Gardner, my newest best friend. We began this journey at the same time. Through all that we have been faced with over the past two years, we never faltered. I look forward to continuing and growing in our love and support for one another. Thank you.

TABLE OF CONTENTS

LIST OF TABLES

LIST OF FIGURES

CHAPTER 1 - INTRODUCTION

1.1 Background

With the increased demand for public transportation, rural development, and leisure activities, it has become likewise demanding for engineers to produce innovative methods to assure safe and economic designs for civil structures. This demand has also impacted environmentally sensitive areas which ensure stability in the environment and achieve balance within our ecosystems. Achieving balance between public demand and environmental stability becomes more difficult with public expansion into undisturbed regions. This balance and continuation of development can only be ensured by close interaction between federal and state environmental agencies and engineers.

North Carolina has a diverse environmental landscape; possessing the Smokey Mountains in the western and the Atlantic Ocean in the eastern regions of the state. This environmental diversity has become a key influence in the tourism industry as well as urban and rural developments. The variation in surface environment compares favorably with the disparities in the underlying geological conditions spanning from the mountain region to the coastal plains. The mountain and piedmont regions within the state consist largely of residual soils underlain by weathered and crystalline rock, whereas the coastal plain region consists mainly of sedimentary soils. Practicing geotechnical engineers must possess knowledge and experience in assessing and implementing engineering properties of an array of soil types to ensure cost-effective construction throughout the state.

As demand for quality road systems and structures in the coastal plain region escalates, the North Carolina Department of Transportation (NCDOT, research sponsor) is faced with maintaining the balance between development of sound economic transportation systems as well as insuring minimal environmental impact on its ecosystems. In the estuarine regions in eastern North Carolina, brackish waters flourish due to tidal flushing of the sounds and river basins. Therefore, bridges and structures erected in this region must possess foundations which are competent in resisting weathering from saline environments during service life. Accordingly, NCDOT *Soils and Foundations Design Section Reference Manual* version 2001 specifies use of pre-stressed concrete piles in the coastal plain region of North Carolina due to the high corrosion resistance properties of concrete, as compared to steel piles.

Concrete piles can be driven into subsurface profiles consisting of relatively low blow count (0-20 bpf) "Standard Penetration Test" material by dynamic methods or jetting. However, in soil stratums in which the design pile tip elevations are deep due to poor bearing material in the upper subsurface, dynamic methods used for concrete pile installation may become ineffective. Dynamic driving of concrete piles occurs due to displacement of soil beneath the pile tip and along the pile skin into subsequent soil layers. The displacement of this soil and vibrations from the dynamic driving cause densification of the material with each depth increment and hammer blow. As densification of the soil stratum increases, overstressing and cracking of concrete piles is inevitable if changes in engineering properties of the soil are not considered in the pile driving analysis. Traditionally, pile driving in material with N-value greater than 20 bpf is difficult. Therefore, it has become common practice to use pile jetting or drilled shaft

construction techniques when dynamic pile driving methods are deemed inappropriate. This is especially true in layered soil profiles where a hard layer is encountered at relatively shallow depth. Without the application of jetting, pile installation may not be possible. Installation of concrete piles by jetting is an economic benefit as compared to drilled shaft construction for foundations. The cost per foot and time rate of installation of drilled shaft foundations is greater than jetted pile foundations. Therefore, it is often economically feasible to use jetted, then driven concrete piles in lieu of drilled shaft foundations.

However, previous discussions and comparison of jetted pile construction with more costly or time-consuming foundation installation methods rarely encompass the possible adverse effects on the environment surrounding jetted pile installations. While there exists much literature on the performance and design of jetted pile foundations, little is published on the environmental effects and mechanics of installation of jetted piles. Tsinker (1988) presents empirical relationships for jetting piles in various soil types and a general understanding of the mechanics of installation. Gunaratne et al. (1999) presented comparisons of load tests conducted on driven, bored and jetted piles. The effect of fluid velocity on transport characteristics of particles has been reviewed to provide general insight to the jetting process. However, the literature review yielded no documentation on the correlations between jetting parameters and surface disturbance adjacent to pile installations.

At the present, United States Army Corps of Engineers (USACOE), North Carolina Division of Water Quality, United States Fish and Wildlife Services, Division of Coastal Management, and Environmental Protection Agency restrict or prohibit jetting as

a construction technique in eastern North Carolina. This is predominantly due to insufficient data and lack of specification-based contracts directing foundation contractors to controlled and engineered jetting parameters. Knowledge of the debris zone created by the jetting process is currently unavailable to the regulatory agencies, engineers, and contractors who use jetting construction methods.

Upon completion of jetting a pile, the original ground surface surrounding the pile is normally inundated with water and overlain by debris exhumed from the annulus around the pile. In coastal or environmentally sensitive areas, debris from the annulus affects essentially the hydric soil layer adjacent the pile. These hydric soils are considered by federal regulation 40456 (August 14, 1991) to be layers that are saturated, flooded, or ponded long enough to develop anaerobic conditions in the upper stratum of the soil profile. The soils are composed of organic and mineral constituents necessary for many organisms to reproduce and develop. The environmental impacts of debris extruded from the jetted holes can be evaluated using present assessment techniques such as the Habitat Evaluation Procedure (HEP) and the Wetland Evaluation Technique (WET). However, the knowledge regarding the extent of such debris zone is missing. Therefore, in order to provide information for environmental evaluation, it is necessary to investigate the effects of jetting parameters on the volume and area of material debris due to pile installations.

1.2 Problem Statement

In order to investigate the impact of pile jetting on environmentally sensitive areas and the size of debris zone, it is necessary to first evaluate jetting parameters on a laboratory scale prior to conducting full scale field jetting applications. It is important to

understand mechanics of installation using water jets as well as determining installation parameters such as jet water flow rate and jet nozzle velocity. It is also necessary to determine the combined affect of varying these parameters on the debris zone developed from the jetting process. In order to determine variations in installation mechanics and debris zone profiles, an array of soil types consisting of various material type and engineering properties will be implemented into an experimental program. This research is conducted to investigate the size and extent of the debris zone and achieve an understanding of mechanisms and jetting parameter effects in pile jetting applications.

1.3 Objectives

The main objective of this research is to parameterize jetted pile installations and develop evaluation techniques of the disturbance zone from numerous laboratory jetting experiments. The results from this research will be used to develop a model for jetting piles in environmentally sensitive areas while minimizing ecological impact. The following objectives are pursued in this research:

1) Develop an experimental testing program and analysis method to evaluate debris zone characteristics and understand mechanics of jetted pile installations.
2) Characterize and define disturbance due to jetted pile installations.
3) Discover effects of varying jetting parameters on pile installation rates, debris zone volumes, debris zone areas, and installation depths.
4) Develop a model for jetted pile installations while minimizing impact to the surrounding environment.
5) Recommend state of practice modifications to current pile jetting practices if feasible.

1.4 Scope of Research

1.4.1 Chapter 1 – Introduction

An introduction to the jetting problem as related to ecologically sensitive areas is given. The effects of pile jetting have been characterized as harmful to environmentally sensitive areas due to the displacement of subsurface materials to the ground surface.

1.4.2 Chapter 2 – Literature Review

The current state of practice of pile jetting and the effects of pile jetting on pile performance is reviewed. Design equations and methodology for effectively installing jetted piles are summarized. Also, the effect of jetting implementation on pile performance and generalizations of particle transport due to water jets is reviewed.

1.4.3 Chapter 3 – Experimental Program

The experimental program is developed and presented providing insight on the materials implemented in the testing program. The index properties of the soil types and the classification tests conducted to obtain these properties are described. The methodology behind construction of the test pit is presented as well as an investigation into the mechanics of jetting presented.

1.4.4 Chapter 4 – Data Acquisition and Test Monitoring

Methods of data acquisition are presented to gather quality information from lab testing. A data analysis procedure was developed so that test results could be compared in an efficient and accurate manner.

1.4.5 Chapter 5 – Results of Laboratory Pile Jetting

All tests conducted in the experimental program were analyzed and presented. The relationship between jetting characteristics such as debris zone surrounding jetted piles, pile insertion rate, and the mechanics of installation are developed based on the various soil types used in the program.

1.4.6 Chapter 6 – Model Development

A universal model for pile jetting is developed for implementation to full-scale jetted pile installations. The model requires input of soil index properties and allows the engineer to predict the debris zone characteristics and pile insertion rate for a set of jetting parameters and given pile dimensions. Model validation is conducted by back-calculating insertion characteristics of actual laboratory tests. A design example and method for model implementation is provided.

1.4.7 Chapter 7 – Summary and Conclusions

Conclusions derived from the experimental program are suggested to quantify the disturbance zone due to jetting parameters and soil type for jetted pile installations.

1.4.8 Chapter 8 – Recommendations for Future Research

Recommendations for future research are provided due to the inability of laboratory jetting to cover all soil types encountered in the natural environment.

CHAPTER 2 - LITERATURE REVIEW

The practice of using water jets to install piles is not a premature process. Water jetting of piles is an effective means of installing both displacement piles and sheet piles in an economic, time efficient manner. Pile jetting has been predominantly used in areas consisting of sands and gravels to install bridge foundations, dock piles, bulkheads and fence posts. However, after an extensive search for literature on the environmental impacts of jetting, it is realized that environmental disturbance due to pile jetting has not been reported in past literature. The purpose of this research is not to perfect the art of pile jetting, but to enhance and modify the jetting process to produce a more environmentally favorable jetting system. In order to understand the fundamental practice of jetting, literature from Tsinker (1988) and Matlin (1983) has been reviewed. Their research consists of performance monitoring of jetted piles as well as installation guidelines for jetting piles in various soil profiles with the main objective being assuring full depth installation. An in-depth investigation into capacity and performance monitoring of bored, driven, and jetted piles has been conducted by Gunaratne et al. (1999) demonstrating the effect of installation method on the service integrity of structural piles. Their research encompasses a detailed small-scale experimental program as well as a detailed dimensional analysis and evaluation of their findings. A study on the hydraulic effects of fluid velocity on particle transport is presented to provide an understanding on how particles are initially suspended and transported by fluids.

2.1 State-of-the-art of Pile Jetting

Pile jetting in its current form is an effective means of installing piles for many structural applications using pile foundations. However, as stated by NCDOT, the state-of-practice of pile jetting is no longer accepted as a suitable means for pile installation in environmentally sensitive areas. This has stemmed from non-regulated and specification deficient contracts encompassing the jetting installation processes. It has been realized by NCDOT officials that control of pile installation methods is necessary to ensure minimal disturbance to ecologically sensitive areas.

2.1.1 Efficiency and Comparison of Pile Installation Methods

A comprehensive review of pile jetting has been conducted by Tsinker (1988). Tsinker realizes the significance in time savings from pile jetting as compared to dynamic methods of pile installation. As expected, the energy savings and noise reduction in using pile jetting as opposed to dynamic driving methods is a positive component of jetting practices. Noise pollution from dynamic and vibratory pile installation methods is believed to divert migrating fish species from traveling to spawning estuaries. This negative effect yields support for the jetting process which is understood as a quiet driving technique.

Pile installation using jetting is nearly the only method for driving “wide flange, T-shaped” steel or concrete piles (McGregor 1973; Matlin 1983). Jetted piles can be effectively installed in most sand and gravel soil stratums as well as subsurface profiles encompassing clay and peat materials. Jetted piles can easily be positioned on land or over water with appropriate driving templates. Also, jetted piles can be removed and

aligned if installed incorrectly from the design grade. Water jetting of piles is beneficial as compared to dynamic driving in that piles are installed before any stress conditions develop within the pile section. If not efficiently controlled and designed, driving piles with dynamic methods may lead to development of stress increases within the pile section above the allowable stresses considered in design and fabrication. This effect may lead to damage in sections and will require implementation of Pile Driving Analysis (PDA) systems.

The cost and time factors realized with dynamic driving methods is basically non-existent with jetted pile applications. Jetted pile applications consist basically of discharging a stream of water at the base of the pile and/or along the pile sides to erode the surrounding soils (Tsinker 1988). Continued water erosion and removal of the surrounding soils allows the pile to penetrate through soil layers until a sufficient distance above the permanent tip elevation is reached. At this point, dynamic methods are implemented for the last few feet of installation to achieve final pile set and to densify soil surrounding the pile.

2.1.2 Variation of Subsurface Characteristics

In jetting piles within sand formations, Tsinker realizes that water flow rate is more important than the jet velocity, whereas in gravel or clay materials, the jet velocity is vital in loosening soil particles from around the pile. In both conditions, an effective jetting program is only successful if the jet velocity is sufficient to loosen soil and an appropriate flow rate of water is used to displace the soil from below the pile tip and carry them along the pile sides to the ground surface (Tsinker 1988). If either of these two characteristics of the jetting parameters is insufficient, the pile will not penetrate the

soil column. Air is often implemented into jetting applications to insure that soil particles are effectively transported to the ground surface.

Variation in soil type also affects the dimensions of the jet-effected zone surrounding the pile. Layers of clay encountered in predominantly uniform sand profiles may cause a blanketing effect of the return water streaming from the jet pipe nozzles (Tsinker 1988). Due to this phenomenon, downward movement of the pile would discontinue at lesser depth than would a similar pile in a uniform sand stratum without the clay layer. It is therefore inferred that sufficient volume of return water must be maintained in any soil stratum to insure continual pile insertion. Also, in cemented sands and clay materials, the jet velocity must be sufficient to fracture the matrix into smaller diameter masses in which the flow of water can transport the material above ground. A schematic of pile jetting through various soil stratums along with variation in return water annulus dimensions are shown in Figure 2.1 below (Tsinker, 1988).

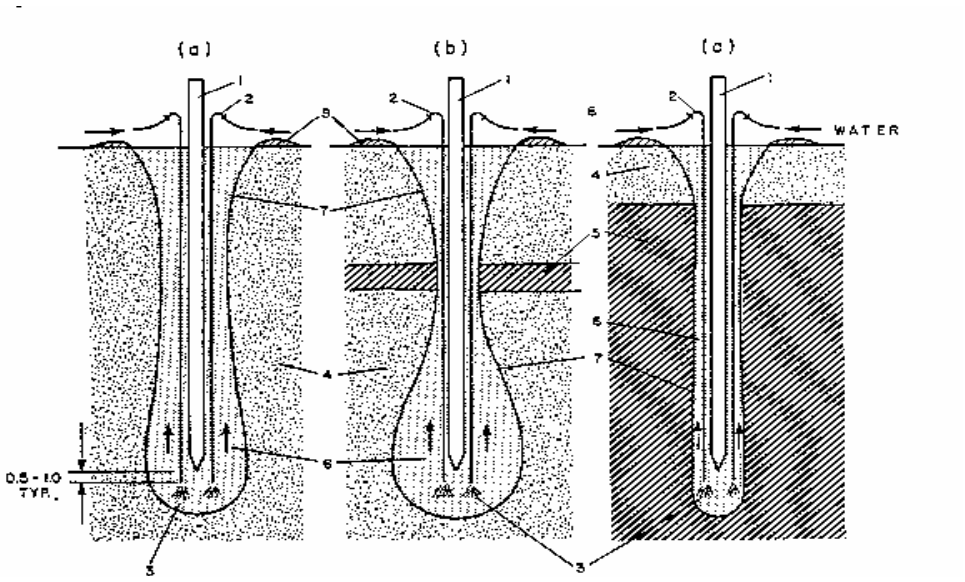

Figure 2.1 Variation in Annulus Dimensions for Various Foundation Soils (Matlin 1983).

(a) Uniform Sand; (b) Sand with Clay Stratum; (c) Sand with Underlain Clay: 1 – Pile; 2 – Jet Pipe; 3 – Water Jet; 4 – Sand; 5 – Clay; 6 – Loose Sand; 7 – Return Annulus; 8 – Particle Deposition

Tsinker also recognizes effects of large boulders, cobles, or debris on the effectiveness of pile jetting. These discrepancies in soil profiles may obstruct the return water annulus, preventing extraction of soil from beneath and from the sides of the pile. Tsinker stresses the importance of achieving essential volume flow rates of water to maintain adequate transport of subsurface materials to the ground surface.

2.1.3 General Installation Procedure (Tsinker 1988)

Pile jetting is a relatively simple application involving equipment such as a "centrifugal pump equipped with a flow meter and pressure gage, a minimum of two steel jet pipes connected to the pump….and a winch for handling the jet pipes" (Tsinker 1988). Tsinker suggests that pipe diameters between 2 and 4 inches (50 and 100mm) are

sufficient to carry the flow of water to the jet nozzles to increase the velocity of water exiting the jet hose. The two jet pipes are often mounted on either side of the pile to achieve balance and symmetry during pile installation. Prior to lowering the pile to the driving location, the pump is engaged and the jet pipes are lowered to the ground surface and allowed to penetrate the soil stratum. Operators then successively lower and raise the jet pipes through the soil column to loosen material within that section. The pile is then lowered into position and allowed to penetrate the soil column freely.

2.1.4 Pile Installation Design Guidelines (Shestopal 1959)

Shestopal (1959) conducted numerous jetting investigations for pile installation using steel pipes as model test piles. Through correlations gathered from research data, he developed empirical equations for determining water quantities and jet water velocities to install piles of various length and diameter. He also considered the effects of jetting piles in soil stratums with elevated and deep ground water profiles.

Shestopal gives the following empirical equation for installation of jetted piles in a uniform sand stratum (groundwater table below pile tip):

$$\frac{Q}{D} = 530\left(d_{50}\right)^{1.3} l^{0.5} + 0.1\pi l k \qquad \text{Eq. 2. 1}$$

Where: Q = flow rate of water, (m^3/h)
D = pile diameter or width, (m)
d_{50} = average size of soil particles, (mm)
l = installation depth of pile, (m)
k = filtration coefficient, (m/day)

The following empirical equation is for installation of jetted piles within a uniform saturated sand stratum (Shestopal 1959):

$$\frac{Q}{D} = 530(d_{50})^{1.3} l^{0.5} + 0.017\pi l k \qquad \text{Eq. 2. 2}$$

For jetting piles in non-uniform soil stratums, the average filtration coefficient should be determined from the following:

$$k = \frac{\sum k_n l_n}{l} \qquad \text{Eq. 2. 3}$$

Where: k_n = filtration coefficient for soil layer n, (m/day)
l_n = length of soil layer n, (m)
l = installation depth of pile, (m)

In order to determine the required pump capacity, head loss in the jetting system water supply hoses may be calculated from the following equation:

$$H = \frac{Q^2 l_h}{K_T} \qquad \text{Eq. 2. 4}$$

Where: H = head loss in jetting system, (m)
Q = flow rate of water, (m^3/h)
l_h = length of water supply hoses, (m)
K_T = empirical coefficient due to hose material obtained from Table 2.1

Table 2.1 K_T factor for various jet pipe material (Marine Structures Handbook 1972)

Jet Pipe Internal Diameter (mm)	Rubberized Hose Material	Rubber Hose Material
33	33	50
50	133	200
65	567	850
76	1333	2000

In order to select an efficient jetting system Tsinker (1988) suggests 1) selecting the appropriate water volume flow rate and head to drive the proposed pile (Table 2.2, or Eqs. 1-4); 2) determine pressure losses foreseen in the hoses and jet pipes of the system; 3) select competent pump.

Table 2.2 Volume of Water and Head Required for Pile Jetting (Marine Structures Handbook 1972)

Soil Type	Depth of Pile Driving (m)	Head at Nozzle Tip (MPa)	Pile Section Diameter			
			300-500 mm		500-700mm	
			Jet Pipe Internal Diameter (mm)	Flow Rate of Water (m^3/min)	Jet Pipe Internal Diameter (mm)	Flow Rate of Water (m^3/min)
Silt; Silty Sand	5-15	0.4-0.8	37	0.4-1.0	50	1.0-1.5
Fine Sand; Soft Clay; Sand	15-25	0.8-1.0	68	1.0-1.5	80	1.5-2.0
Sand and Hard Sand Loam	5-12	0.6-1.0	50	1.0-1.5	68	1.5-2.0
Sand with Gravel	15-25	1.0-1.5	80	1.5-2.5	106	2.0-3.0
CONVERSIONS MPa to psi: multiply by 145.04 m^3/min to ft^3/min: multiply by 35.31						

2.1.5 Summary of State-of-the-Art of Pile Jetting

A review of literature on installation of piles yielded some findings beneficial to the research conducted in this report. Fundamental mechanics of a jetted pile installation in sand is shown in Figure 2.2. Tsinker (1988) describes the structure of the jet hole with three distinctive zones. Immediately beneath the pile tip, the sand structure is significantly altered from in situ conditions. Infiltration of jet water into this zone results

in a mixture of sand particles and water. Within Zone 2, excess water from the sand-water mixture rises to the surface while lubricating the pile sides. Tsinker also realized a third zone in the jet hole structure consisting of a sand-water mixture at high pore pressures stemming from water infiltration into the hole sides.

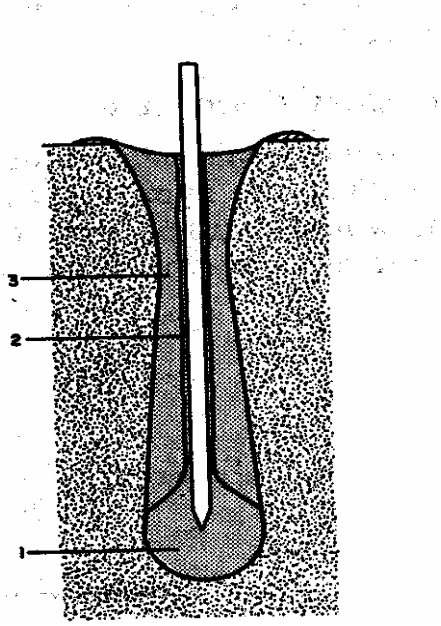

Figure 2.2 Structure of Typical Jetted Pile Installation (Matlin 1983)

Tsinker (1988) also conducted research on capacity effects of jetting piles within dry and water-bearing sands. From that research, Tsinker (1988) suggests "concrete piles jetted into dry sand have six to nine times more capacity than identical piles jetted into water-bearing sand." Tsinker (1988) also stated that implementation of dynamic pile driving methods does not increase capacity of piles jetted in dry sand stratums significantly. This is due to the inability of dry sands to densify by liquefaction. Densification in unsaturated profiles transpires due to settlement of loose sand around the pile and subsequent compaction of the material due to water force from the jets. This densification is not as profound as that seen in saturated sands where dynamic driving

methods invoke liquefaction. Also, although washing of some fines from the jetted column occurs, Tsinker (1988) states that "sandy soils granulometric composition" is not altered significantly.

2.2 Model Techniques for Determining Affects of Jetting on Pile Performance (Gunaratne et al. 1999)

An investigation into the effects of pile jetting on pile capacity was conducted by Gunaratne et al. (1999) under sponsorship by Florida Department of Transportation. This study encompasses model piles installed using jetting techniques, preforming and dynamic driving methods. The purpose of the report is to determine the effect of jetting pressure and process on the lateral behavior and skin friction of piles; determine the zone of influence of jetting on soils adjacent to existing foundations; explore strength variation in soils due to jetting and preforming; develop an analytical model encompassing the effect of jetting on lateral and frictional behavior of piles. The scope of the aforementioned study differs from the research in the present report however, in that surface effects of jetting and installation practices and procedures were not considered. Attention to the jetting installations of the model test piles and experimental findings are considered in this literature review.

2.2.1 Experimental Program for Model Testing

Gunaratne et al. (1999) conducted an experimental program using model aluminum piles driven into a 90% sand + 10% kaolin mixture with jetting, preforming, and dynamic installation methods. Quality testing of soil material used in the experimental program yielded the results shown in Table 2.3.

Table 2.3a-b Engineering Properties of Foundation Soil (Gunaratne et al. 1999)

	Masonry Sand	Kaolinite
D_{50} (mm)	0.25	N/A
γ_d Max, (lb/ft^3)	111.7	N/A
γ_d Min, (lb/ft^3)	88.0	N/A
PI	N/A	22
LL	N/A	60

a)

Soil Material	% Passing No. 40 Sieve	% Passing No. 200 Sieve	Spec. Gravity, Gs	Opt. Moist. Content, OMC (%)	γ_d @ OMC. lb/ft^3	ϕ @ γ_d = 94.7 lb/ft^3	ϕ @ γ_d = 103.7 lb/ft^3
90% Masonry Sand + 10% Kaolinite	88.2	10.2	2.68	10.2	112	35	38
CONVERSIONS: lb/ft^3 to kN/m^3 divide by 6.4 mm to inch multiply by 0.0394							

b)

2.2.2 Testing Matrix and Pile Installation Methods

The experimental program consisted of an excavated 26.26 ft^2 (2.44 m^2) by 7.0 ft (2.13m) deep test pit filled to 5.97 feet (1.82 m) in successive lifts with the mixture of masonry sand and kaolinite. Each lift was compacted to 103.2 lb/ft^3 (16.2 kN/m^3) or 94.3 lb/ft^3 (14.8 kN/m^3) based on the desired relative density of the test protocol. Next, two

5.0 ft (1.52 m) long aluminum shafts, 2 in. x 2 in. (50.8 mm x 50.8 mm) and 1/16 in. (1.6 mm) thickness were instrumented with strain gauges and installed into the testing medium through dynamic driving and jetting. Piles were jet driven through saturated and unsaturated test specimens at various jetting pressures to expedite installation due to increased flow rate and velocity of the jet water. The nomenclatures for tests within the testing program are shown in Table 2.4 below.

Table 2.4 Nomenclature for Piles in the Testing Program (Gunaratne et al. 1999)

Unit Weight (lb/ft^3)	Condition	Driven Pile	Jetted Pile Identification			
			25 psi	50 psi	75 psi	100 psi
103.7	Unsaturated	UD_1	UJ_{11}	UJ_{12}	UJ_{13}	UJ_{14}
	Saturated	SD_1	SJ_{11}	SJ_{12}	SJ_{13}	SJ_{14}
94.7	Unsaturated	UD_2	UJ_{21}	UJ_{22}	UJ_{23}	UJ_{24}
	Saturated	SD_2	SJ_{21}	SJ_{22}	SJ_{23}	SJ_{24}
CONVERSIONS: lb/ft^3 to kN/m^3 divide by 6.4 psi to kPa multiply by 6.895						

The water jet system used to install jetted piles consisted of two stainless steel pipes with inside diameters of 0.16 in. (4 mm) extending to the pile tip and fastened to the pile head. Water was pressurized with a "booster" pump and fed into a 0.75 in. (19.05 mm) reinforced hose which was reduced and coupled to the two steel jet pipes. Each pile was jetted to 2.5 ft (0.75 m) and then impact driven 0.833 ft (0.254 m) to the required tip elevation.

Upon completion of model pile installation and dissipation of excess pore water pressure, lateral load testing of the piles were conducted. The piles were monitored with Linearly Varying Displacement Transducers (LVDT) and strain gauges connected to a data acquisition system to monitor the displacement and loading information. From Figure 2.3, it is realized that lateral load capacity for jetted piles decreases with increased

jetting pressure as compared to driven piles in the same soil stratum. This holds true for both saturated and unsaturated conditions. Also, lateral capacity for saturated conditions is significantly less than for unsaturated conditions with similar jetting parameters. Overall, for similar jetting parameter tests, lateral displacements at failure with saturated conditions seem to be greater than for lateral load tests conducted unsaturated.

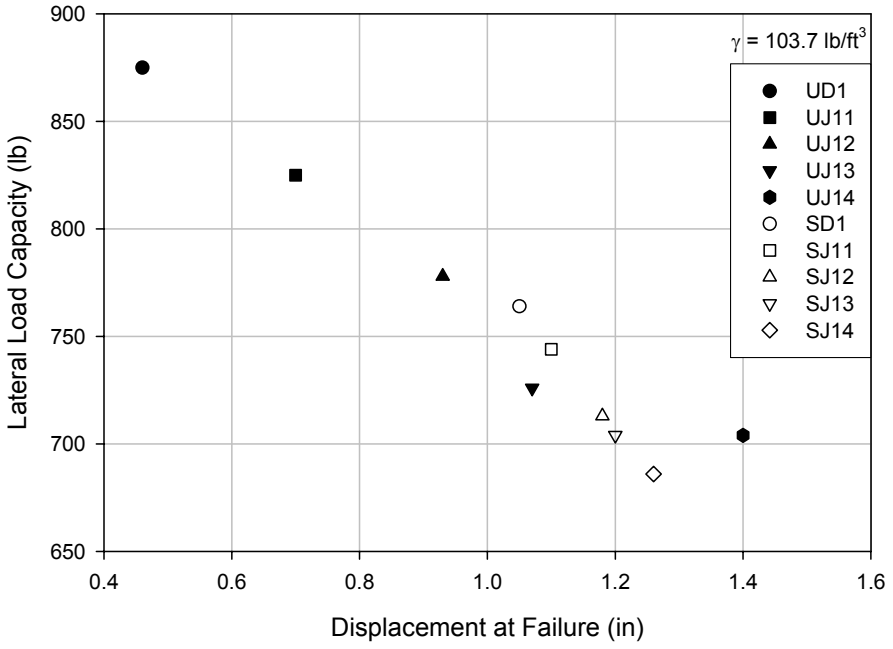

Figure 2.3 Lateral Load Capacity vs. Lateral Displacement at Point of Load Application (Gunaratne et al. 1999)

Figure 2.4 displays the required jetting time to reach the required pile tip elevation (0.75 m) prior to impact driving to final pile set for lateral load testing (Gunaratne et al. 1999).

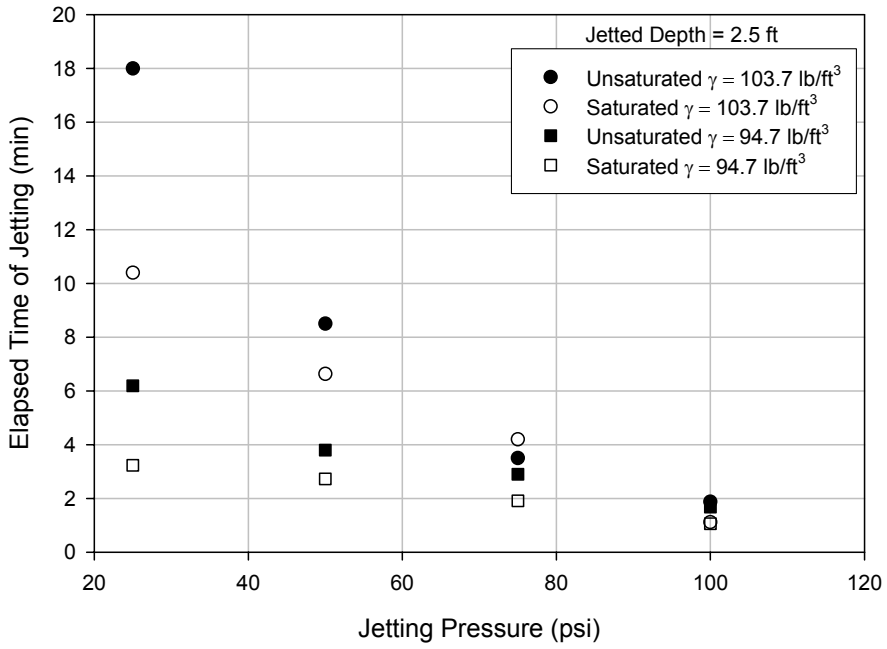

Figure 2.4 Elapsed Time of Jetting vs. Jetting Pressure – 2.5 ft Depth (Gunaratne et al. 1999)

From Figure 2.4, it is shown that for equal depth of driving, the pile installation rate is dependent on both material density and saturation conditions. For equal material density at low jetting pressures, installation rates through saturated soils are nearly double than for unsaturated soils. However, as jetting pressure is increased, installation rate seems to become more dependent on soil density in the jetting stratum.

2.2.3 Lateral and Axial Load Testing of Jetted Piles (Gunaratne et al. 1999)

Lateral and axial load testing of both jetted and dynamically driven piles were conducted to determine effects of spacing and the installation methods on pile capacity. The piles were tested at axial displacements of 0.5 in (0.13 mm) and laterally tested to displacements of 1 inch (25.4 mm). Axial capacities of piles driven with jetting and dynamic driving were shown to have higher capacities at spacing of 3D than similar piles driven at spacings of 5D in unsaturated conditions. This is believed to be due to the overlapping influence of densification zones surrounding the piles at closer spacing. Dynamic driving of the piles to achieve final set at this close spacing was believed to have overridden the jetting effects. Gunaratne et al. (1999) also states that axial capacity of jetted piles in saturated soil conditions does not affect adjacent driven pile axial load behavior.

Lateral load testing of the model piles was conducted under saturated and unsaturated conditions. In general, Gunaratne et al. (1999) suggest that lateral load capacity in unsaturated conditions increases with greater spacing between jetted piles tested in the experimental program. Higher lateral load capacities were also obtained in existing piles where jetting was implemented in installing piles at a spacing of 5D rather than 3D (Gunaratne et al. 1999). At closer spacing, reduction in lateral confinement surrounding existing piles occurs due to the effects of jetting.

2.2.4 Summary of Experimental Modeling of Jetted Pile Installations

Through research funded by Florida Department of Transportation, Gunaratne et al. (1999) developed design charts for piles installed with various installation methods. The scope of research conducted through Gunaratne et al.'s (1999) study differs from the

scope of the present research. However, through reviewing their literature, the current research has benefited by realizing the importance of a quality controlled experimental program and specimen preparation procedure. Conclusions drawn from their research include; lateral stability of jetted piles are significantly less than lateral stability of piles mechanically driven to the same installation depth; jetting further than 5D from existing piles in unsaturated conditions and 3D in saturated conditions seem to have little effect on axial and lateral load capacity; installation rates of jetted piles are influenced by jetting pressures and flow rates as well as material density and saturation conditions within the jetting stratum.

2.3 Hydraulic Effects on Transport of Sedimentary Particles

In order to understand the effects of fluid and flow properties on sediment transport, a review of literature provided by Allen (1985) was conducted. This review was undertaken to determine if available jetting parameters from the experimental program could effectively be used to initiate erosion of a conglomeration of soil particles and displacement of the soil particles from the jetting annulus to the specimen surface. The hydraulic properties of pile jetting are similar to the hydraulic characteristics involved in sediment transport due to water currents. Transport of soil particles by fluids involves two distinct characteristics. First of which consists of an initial force required to initiate particle motion. The next characteristic involves forces necessary to move soil particles along a velocity vector. These forces must initiate movement and entrain the soil particles within the fluid current for successful transport (Allen 1985). Allen (1985) states that grain size, fluid properties, and flow characteristics together determine the "entrainment threshold and the modes and rate of sediment transport." Considering

Figure 2.5, the forces acting on an idealized spherical particle of greater density than the shearing fluid, in contact with a bed of similar spherical particles, is acted on by a fluid drag force F_D, lift force F_L, particle buoyant weight F_W, and interparticle cohesion F_C from grain to grain contact.

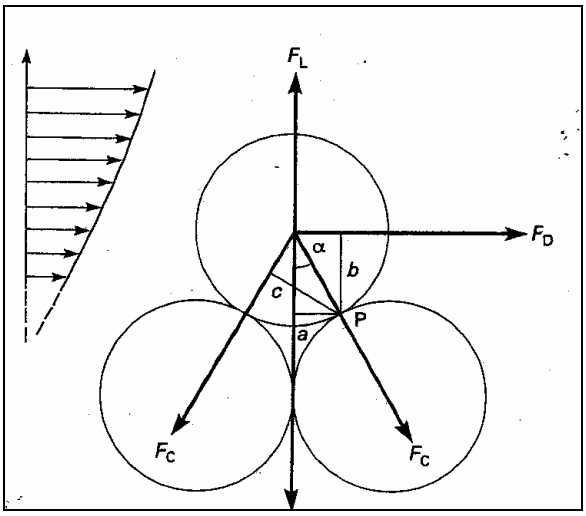

Figure 2.5 Forces acting on a particle resting on a granular bed subject to a steady current (Allen 1985)

Applying Newton's First law, the following force balance is given (Allen 1985):

$$aF_L + bF_D = aF_w + cF_C \qquad \text{Eq. 2. 5}$$

where: a, b, and c are the moment arm lengths from P
P is the downstream pivot point on grain surfaces

The effects of inter-particle cohesion between sand and gravel particles is neglected which results in only the fluid drag, fluid lift, and particle buoyant weight acting on the soil grain. Within clay or silt profiles, the inter-particle forces become important due to adhesion of particles through van der Waals or electrostatic forces (Allen 1985).

The fluid drag force may be specified as the mean bed shear stress or through definition of the drag coefficient involving mean fluid velocity at the particle-fluid interface (Allen 1985). The lift force may be defined through application of the Bernoulli

equation. Since the velocity on the upper surface of the soil particle in Figure 2.6 is greater than at the particle interface between the soil particles, a pressure gradient exists which provides a lifting force beneath the upper soil particle (Allen 1985). Therefore, the particle weight or specific gravity, particle size, and interparticle cohesion all contribute to efficiency of a given fluid velocity to initiate soil particle transport.

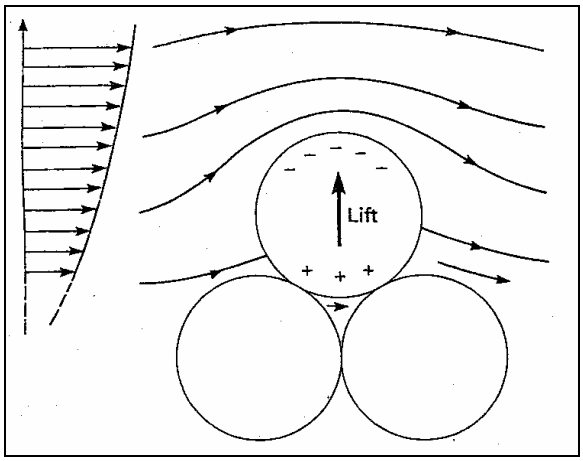

Figure 2.6 Lift force due to Bernoulli effect on granular bed subject to fluid shear (Allen 1985)

The jetting velocities used in the laboratory testing program range from approximately 180 ft/min (55 m/min) to 1200 ft/min (365 m/min). Based on the average particle diameters of soils used in the testing program (0.15 mm to 0.75 mm) it is inferred from Figure 2.7 (Open University. Oceanography Course Team 1999) that effective erosion of soil particles will take place during laboratory jetting of piles. The jet nozzle velocities of water extend well above the referenced zone for initiation and transport of soil particles for the given diameters. It is therefore inferred that higher velocity of the water jets will provide both increased erosion efficiency and transport of soil particles from beneath jetted piles to the ground surface.

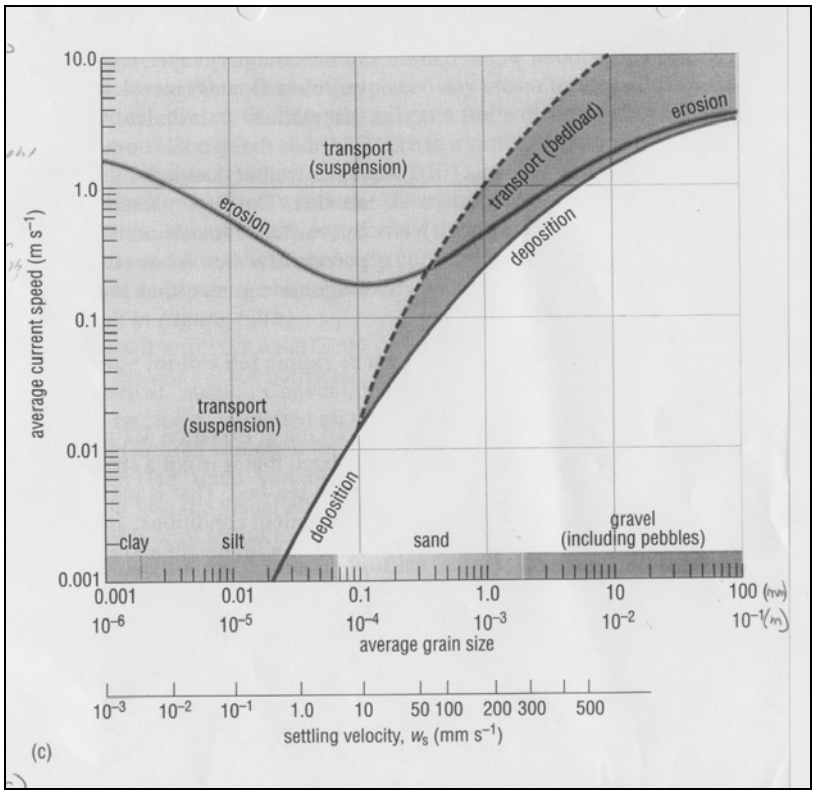

Figure 2.7 Effect of Current Speed on the Erosion and Deposition Characteristics for Specified Bed Particle Diameter (Open University. Oceanography Course Team 1999)

2.4 Summary of Literature Review

The literature review presented the state-of-the-art of pile jetting techniques implemented for installation of various length and diameter piles as presented by Tsinker (1988). These techniques encompassed several variations in subsurface material as well as jetting pump capacity requirements. Research conducted by Gunaratne et al. (1999) brought forth important aspects of model testing and experimental program development for conducting research programs. Lateral load test results from jetted and driven piles were presented and compared as well as pile installation rates due to jetting pressure and flow rate variation. Literature reviewed on the effects of fluid currents and the initiation of erosion and transport ensured adequate jetting parameters could be obtained in the lab

to allow successful pile jetting. However, there was no information attained from a literature investigation on the impacts of pile jetting on surface debris zone volumes, debris zone areas and the effects of these characteristics on surface environments. The focus of the current research is to quantify the debris characteristics due to variation in soil type and jetting parameters for successful pile installation.

CHAPTER 3 - EXPERIMENTAL PROGRAM

An experimental program was developed to quantify jetting induced disturbance and pile insertion characteristics for jetted pile installations. The purpose of the laboratory testing program is to provide a setting in which a detailed study of jetting parameters can be conducted in various soil types. The program involved an exclusive quality control program to ensure uniform specimen preparation and accurate index properties of soils. The quality control program is crucial in developing a model for full scale jetted pile installations. The model developed for this research requires index properties of underlying soils consistent with routine subsurface investigations for deep foundations. This program enabled the researchers to vary jetting parameters in a controlled setting to determine the relationship between jetting parameters with zone of disturbance and pile insertion characteristics.

3.1 Laboratory Testing Medium

A variety of sand types and a mixture of Kaolinite (Huber 90) and sand were used to formulate a method of analysis for jet-driven pile installations. A jetting system as well as model concrete piles were fabricated in the laboratory to simulate jetting practice. The concrete piles were jetted into the various soil specimens prepared in a permeable containment system described later in this section. These soil types exhibited unique properties necessary to develop a jetting model for various soil conditions. The sand types included a well-graded coarse Concrete Sand, a uniform graded Mortar Sand, a uniform Cherry Branch Ferry Basin dredged sand, and a 90/10 Mortar Sand/Kaolinite mixture. The natural sand materials provided a broad spectrum of engineering and index

properties that may be directly compared to subsurface environments in eastern North Carolina.

3.1.1 Grain Size Distribution of Testing Material

Selections of soils used in this research were predominantly based on the particle size distribution and characteristics of the distribution curves. The soils used in this research demonstrated a range of characteristics that are necessary in developing the full-scale model for jetted pile installations. From literature reviewed by Allen (1985) it is inferred that soil particle size and gradation will have an impact on pile insertion depth, pile insertion rate, and debris volume characteristics due to variations in jetting parameters. With this point understood, the importance of quality particle size analyses is realized. Particle-size analyses for each material were conducted in accordance with ASTM D 422. The grain size distribution curves for each material used in the testing program are shown in Figure 3.1.

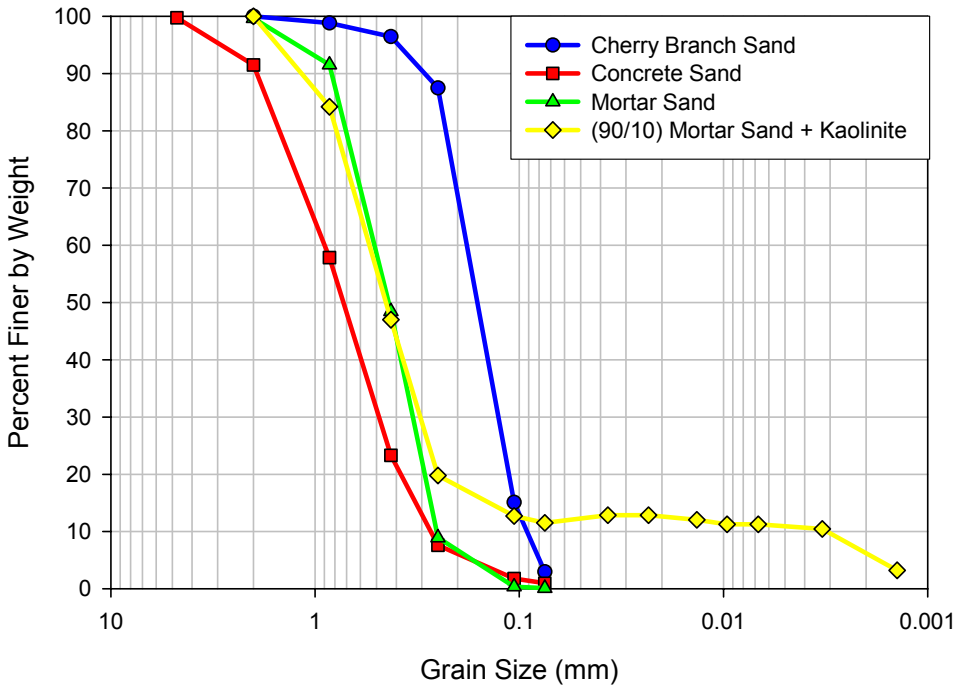

Figure 3.1 Grain Size Distribution Curves for Laboratory Jetting Tests

From the particle-size analyses, certain grain diameters were used to represent specific characteristics of each soil type. These characteristics are defined as the Coefficient of Uniformity (C_u) and Coefficient of Curvature (C_c). The equations for the Coefficient of Uniformity and Coefficient of Curvature are given as:

$$C_u = \frac{D_{60}}{D_{10}} \qquad \text{Eq. 3. 1}$$

$$C_c = \frac{(D_{30})^2}{(D_{10})(D_{60})} \qquad \text{Eq. 3. 2}$$

Where: D_{60} = grain diameter corresponding to 60% passing by weight
D_{30} = grain diameter corresponding to 30% passing by weight
D_{10} = grain diameter corresponding to 10% passing by weight

R. D. Holtz et al. (1981) states that "a soil with a coefficient of curvature between 1 and 3 is considered to be well graded as long as the coefficient of uniformity is also greater than 4 for gravels and 6 for sands". Based on the GSD properties and uniformity coefficients, USCS classifications were made for each soil type. The USCS classification and particle size information for each soil type used in laboratory pile jetting is given in Table 3.1 below.

Table 3.1 Material Classification and Particle Size Information for Laboratory Specimens

Material →	Concrete Sand	Mortar Sand	Cherry Branch Sand	Mortar Sand + Kaolinite (90/10)
USCS	SW	SP	SP	SW-SM
D_{60} (mm)	0.95	0.60	0.18	0.53
D_{50} (mm)	0.75	0.50	0.15	0.53
D_{30} (mm)	0.54	0.35	0.13	0.30
D_{10} (mm)	0.18	0.28	0.09	0.003
C_u	5.28	2.14	2.00	176.67
C_c	1.71	0.73	1.04	56.60

3.1.2 Maximum and Minimum Index Densities of Testing Material

The maximum and minimum index densities were determined for each natural occurring material (Concrete Sand, Mortar Sand, and Cherry Branch Sand) used in the testing program. The maximum dry densities of the soils were determined in accordance with ASTM D 4253 using a vibratory shake table. The minimum dry densities for the natural soils were determined in accordance with ASTM D 4254 using the "funnel pouring device" to fill the specified material mold Also, specific gravities of the soils were determined in accordance with ASTM D 854. The maximum and minimum index densities of all materials are shown in Table 3.2 below.

Table 3.2 Index Properties for Natural Soils Used in Laboratory Testing Program

Soil Type	Max. Dry Density, ρ_{dmax} (pcf)	Min. Dry Density, ρ_{dmin} (pcf)	Min. Void Ratio, e_{min}	Max. Void Ratio, e_{max}	Specific Gravity
Concrete Sand	114.81	94.10	0.44	0.76	2.65
Mortar Sand	107.98	90.10	0.49	0.79	2.58
Cherry Branch Sand	102.00	82.00	0.60	0.99	2.61

Knowing the index densities for each soil type, each test specimen prepared in the laboratory could easily be compacted to equal relative density. This provided a basis of comparison between test results for the different sand types. Upon completion of data analysis and test comparison, model development was undertaken and behavioral characteristics of the jetted piles in sands were correlated to the physical properties of the soils.

3.1.3 Effective Angle of Internal Friction of Testing Material

To determine strength properties of the testing soils, direct shear tests were conducted in accordance with ASTM D 3080. Each natural soil specimen was compacted to dry densities corresponding to 50% relative density. This relative density was the minimum allowable dry density for jetting in the testing program. This minimum density requirement was based on an evaluation of subsurface conditions at jetting test sites selected for full-scale field jetting tests. The relative densities for each test site were determined from correlations with Standard Penetration Test (SPT) results. Relative densities ranged from 50 to 70 percent within the upper soil stratums where jetting would routinely be used for pile installation. Therefore, all test specimens constructed in the laboratory were compacted to relative densities between 50 and 70 percent.

Shear Tests were conducted with a Wykeham Farrance direct shear apparatus (Model 27401). Normal stresses ranging from 250 psf (12 kPa) to 2000 psf (96 kPa) were used to develop the failure envelope for each sand type. Upon application of incremental normal stress, the natural specimens were allowed to consolidate for five minutes to insure 90% consolidation. For each shear test, the normal stress was doubled from the previous test until the failure envelope was clearly defined. These normal stresses envelop the range of effective stress within a saturated soil stratum of 20 to 40 feet (6.1 to 12.2 m) below the ground surface. These depths are consistent with jetted pile installations that will be conducted in field settings as an extension to the laboratory research.

Strain rates used in direct shear testing were set at 0.04 in/min (1 mm/minute) for the sands, whereas strain rates for the Mortar + Kaolinite (90/10) mixture were set at 0.008 in/min (0.2 mm/min). The strain rates for sands were based on reference elapsed time to failure values (t_f = 10 min), given for quick draining sands with less than 5% fines, and estimated horizontal displacement at failure values (d_f), of 0.5 inch (12 mm) for normally consolidated soils (ASTM D 3080). For the Mortar + Kaolinite (90/10) mixture, the estimated elapsed time to failure (t_f = 60 min), was used due to the increased percentage of fines. The effective angles of internal friction for each test are shown in Figure 3.2 below.

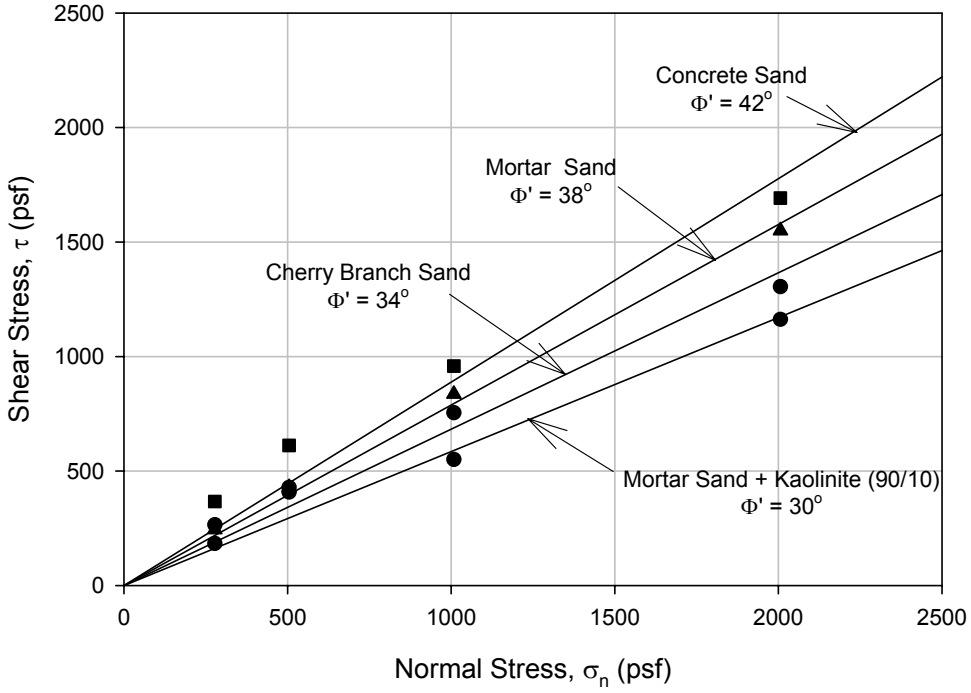

Figure 3.2 Direct Shear Test Results for Material Used in Laboratory Jetting

3.1.4 Permeability of Testing Material

Falling head permeability tests were conducted on samples of material used for model development. Specimens were prepared in permeability cells manufactured by Trautwein Soil Testing Equipment. The upper and lower drainage platens constrained the specimen diameters to 2.835 in (72 mm). Based on this constraint, permeability specimens were constructed at a minimum of 5.76 inches (145 mm). With these dimensions, required masses of each soil material were determined to yield relative densities between 50% and 70%. These relative densities were consistent with threshold values deemed appropriate for the experimental program. Required densities were obtained by constructing the specimens in five equal thickness lifts while firmly tamping each lift forty times with a rubber tamp (dia. = 1.44 inches (36.6 mm)).

Upon completion of specimen preparation, each permeability, head, and tail water cell were filled with deaired water. Deaired water was obtained using the Soiltest Water Deairing Device System (Model LT-150). Each specimen was exposed simultaneously to 10 psi (69 kPa) confining pressure and specimen pressure (headwater) to prevent volume change. These confining stresses envelop the range of effective stress within a saturated soil stratum of 20 to 40 feet (6.1 to 12.2 m) below the ground surface. Upon application of confining stress, specimens were allowed to equilibrate for thirty minutes. Upon completion of the thirty minute equilibrium stage, the top specimen valve was opened to the atmosphere and the headwater pressure was increased to 11 psi (76 kPa). Pore water was allowed to permeate through the specimen until continuous permeability values were reached. Permeability values along with pertinent test information are shown in Table 3.3.

Table 3.3 Permeability Information for Soils Used in Laboratory Testing

Soil Type →	Concrete Sand	Cherry Branch Sand	Mortar Sand	Mortar Sand + Kaolinite (90/10)
Relative Density, D_r (%)	57	72	63	
Void Ratio, e	0.56	0.71	0.65	0.56
No. of Pore Volumes for Constant k	11	21	10	4
Permeability, k ft/s (cm/s)	1.5×10^{-4} (10^{-2})	2.8×10^{-4} (10^{-2})	5.2×10^{-4} (10^{-2})	2.7×10^{-5} (10^{-3})

3.1.5 Laboratory Testing Medium Summary

An exclusive soil property testing program was conducted to determine engineering properties of the various materials used in the laboratory jetting program. Based on these properties, comparisons of the jetted pile installations between various sands were investigated, and a model was developed for full-scale jetting applications.

3.2 Laboratory Testing Methodology

The laboratory jetting program was developed in the Constructed Facilities Laboratory on North Carolina State University's Centennial Campus. The jetting program consisted of fabrication of model test piles, a jetting test chamber, and jetting apparatus. This program involved an elaborate design process that stemmed from hours of conversation with contractors and NC Department of Transportation officials whom have been involved with full-scale jetting operations for bridge foundation construction. It was the desire of the researchers to develop a laboratory scale jetting system that contained all aspects of full-scale jetting processes. Also, of key importance was development of a method to repeatedly construct specimens with similar index densities. This provides a basis of comparison for each jetted pile insertion with various jetting parameters. Therefore, a quality control program was initiated and maintained throughout the testing program.

3.2.1.1 Fabrication of Model Test Piles

After consulting with contractors and NC DOT officials, it was realized that concrete piles would be most beneficial in the laboratory jetting program. Due to similar unit weights of concrete (approximately 150 pcf (23.4 kN/m^3)) and pile skin friction

characteristics, a basis of comparison between the laboratory test piles and full-scale concrete piles is strengthened.

Three model test piles were constructed of 5000 psi (34500 kPa), 28 day compressive strength concrete, formed with 0.667 ft (0.204 m), 0.5 ft (0.153 m), and 0.333 ft (0.102m) inside diameter PVC water pipe. Each test pile was 8 feet (2.438 m) in length and reinforced with A36 steel No. 8 rebar extending the entire length of the test pile. Steel hooks were placed in the top of each test pile. These hooks extended from the pile head so each could be mobilized with an overhead crane. The steel reinforcement provided sufficient tensile support to the pile so each could be lifted at the head without excessive cracking of the concrete. After finishing, the test piles were allowed to cure for seven days to develop adequate strength before the forms were removed.

Each test pile was marked from the pile tip at 2-inch (50mm) increments so that insertion rate information could be obtained during each jetting procedure. These insertion rates were compared between each test to determine jetting parameter effects and installation and debris characteristics in the various soil types.

3.2.1.2 Fabrication of Jetting Test Chamber

The jetting test chamber is located in the Geotechnical Testing Lab within the Constructed Facilities Laboratory. This chamber is a 6 ft wide x 12 ft long x 8 ft tall (1.82 m x 3.66 m x 2.44 m) concrete walled chamber. The test chamber is shown below in Figure 3.3.

Figure 3.3 Jetting Test Chamber

The chamber had been used in past research where Aggregate Base Course (ABC) was used to fill the chamber. To modify the chamber for jetting purposes, the surface of the ABC was excavated to a depth of 3.5 feet (1.07 m) below the top of the pit walls. Upon removal and surface leveling of the ABC, a 5 ft x 5 ft x 4.5 ft (1.52 m x 1.52 m x 1.37 m - length x width x height) steel box was fabricated. The steel panels were 0.375 inch (9.5 mm) thick and were fastened together with hinges welded on each side 1.5 ft (0.46 m) from the top and bottom of each panel. Next, a 5 ft x 5 ft x 3 ft (1.52 m x 1.52 m x 0.91m - length x width x height) excavation was completed at the back of the pit. The steel box was placed at a depth in which the researchers could efficiently conduct jetting tests without unnecessary climbing and bending over the box sides. After lowering the steel box in place, the corners were waterproofed with silicone caulk and painted to prevent future water leaks. This box was fabricated as a tank used to saturate large soil specimens used in the laboratory jetting program.

A 3 ft x 3 ft x 4 ft (0.91 m x 0.91 m x 1.22m - length x width x height) steel frame was fabricated with steel ell channel for specimen containment. The frame allowed routine mobilization of large soil specimens with an overhead crane. The interior of the frame was wrapped with Tensar BX 1200 Geogrid and lined with a non-woven geotextile to form a basket-like membrane. The specimen basket was then placed within the saturation box where 4 ft tall (1.22 m) soil specimens were created for each jetting test. After each specimen was constructed, the saturation box was filled with water until the water table was level with the specimen surface. The geotextile allowed the saturation water to permeate the soil specimens. During testing, the geotextile allowed free drainage of jetting water while preventing escape of fine particles through the basket. The saturation tank and specimen basket are shown in Figure 3.4 and Figure 3.5.

Figure 3.4 Saturation Tank and Specimen Basket

Figure 3.5 Overhead View of Saturation Tank with Specimen Basket in Place

3.2.1.3 Fabrication of Jetting Apparatus

To install model test piles in the various testing media, it was necessary to fabricate a jetting apparatus that would allow controlled water flow rates and jet nozzle velocities. Variations in jetting parameters provided a means of comparison between tests for final depth of installation, volume and area of debris zones, and pile insertion rate. The data obtained from each controlled test was used to develop the jetting model for predicting insertion characteristics of full-scale jetted pile installations.

The jetting apparatus consists of two 5 ft (1.52 m) long, 0.8125 inch (20.6 mm) inside-diameter jet pipes connected with galvanized tees, forming a single jetting system. The jetting system was connected to the model test pile and fed with two 0.75 inch (19.1mm) diameter water hoses. The water hoses were fed from an industrial water

supply under a pressure of 87 psi (600 kPa). The flow rates available from the water supply were 1.337 ft^3/min (0.038 m^3/min) and 2.674 ft^3/min (0.076 m^3/min).

A series of nozzles were implemented into the jetting system providing variation in jet nozzle velocities under the available flowrates. Variations in these two parameters were seen to have significant impact on the insertion depth, insertion rate, and debris zone characteristics of the model jetted piles. In order to model field jetting applications, the jetting apparatus was fabricated to produce jet streams parallel to the length of the test piles. This was consistent with full-scale jetting systems determined from discussion with contractors and NC DOT officials. However, a modified version of the jetting system involved angled jets below the pile tip to determine if direction of water flow from the jet nozzles contributed positive or negative installation effects. The jetting apparatus used in laboratory testing and the various nozzles implemented in the program are shown in Figure 3.6. Also, the available flow rates and nozzle velocities for each nozzle configuration are shown in Table 3.4.

Figure 3.6 Laboratory Jetting Apparatus and Various Nozzles

Table 3.4 Available Flowrate and Nozzle Velocity Configurations

	Water Flow Rate 1.337 ft^3/min	Water Flow Rate 2.674 ft^3/min
Nozzle Diameter (inch)	Jet Nozzle Velocity (ft/min)	Jet Nozzle Velocity (ft/min)
0.500	490	980
0.625	313	326
0.813	186	372

CONVERSIONS:
ft^3/min to m^3/min multiply by 0.0283
inch to mm multiply by 25.4
ft/min to m/min divide by 3.281

3.2.2 Test Setup and Quality Control

Construction of quality specimens in the experimental program was important so installation comparisons could be developed. These comparison tests involved jetting piles with various jetting parameters through specimens compacted to equal relative densities. From these tests, optimum jetting parameters were determined to minimize debris zone characteristics while maintaining acceptable insertion rates.

The test specimens were constructed in a specific manner to ensure quality and uniformity. A quality control program was initialized to establish a compaction schedule meeting relative density requirements (50-70%). The program was initially a trial and error procedure. The specimens were composed of four one-foot lifts producing a specimen with dimensions 3 ft x 3 ft x 4 ft (0.91 m x 0.91 m x 1.22 m - length x width x height). Each soil layer was placed in one-foot lifts using a material box with a sliding door mechanism. The density and moisture contents of each lift were determined using a Troxler Nuclear Density Gage. Density and moisture contents were taken at depths of six inches in each lift. Thus, an average density of the top and bottom of each layer was assumed from the midpoint of each lift.

Each specimen lift was compacted with a Bosch 11304 Electric Jackhammer with a 12 inch x 12 inch steel foot. After many trials, the optimum procedure to produce 50-70 % relative density for one lift thickness was as follows:

1. Allow soil to free-fall from material box producing an un-compacted height of approximately 18 inches. Level the surface.
2. Compact the lift for five minutes starting from the edge of the specimen basket while following a circular motion until the center is reached.

3. Adjust the moisture content accordingly to aid in compaction.
4. Determine dry density from the midpoint of the layer (6 inches).

This method produced repeatable relative densities for each specimen and soil type used in the laboratory testing program. This specimen preparation sequence is shown in Figures 3.7 through 3.9.

Figure 3.7 Free-fall of Specimen Soil for Desired Lift Height

Figure 3.8 Compaction of Individual Lift Height

Figure 3.9 Density Check at Midpoint of Lift Height

Upon completion of specimen preparation and quality control, the saturation tank was filled with water until the water surface and specimen surface coincided. The Concrete, Cherry Branch, and Mortar sands were allowed to inundate for an hour, whereas the Mortar Sand/Kaolinite mixtures were allowed to inundate for 24 hours. This modeled field conditions consistent with coastal groundwater conditions found in Eastern North Carolina. It was assumed that this attempt at saturation was adequate due to the rather large size of the specimens.

3.2.3 Testing Program

The testing program consisted of a series of tests conducted on the four various soil types. Initial tests conducted using the four-inch and six-inch diameter piles resulted in insertion depths equal to the depth of the specimen basket. Therefore, there was no refusal depth information gained from the tests. It was deemed necessary to utilize the larger eight-inch diameter pile with the available flowrates and jet nozzle velocities. Upon jetting of the larger pile, depths to refusal were less than the specimen basket height for all flowrates and jet nozzle velocities.

3.2.3.1 Vertical Jet Testing Program

The majority of laboratory jetting involved the vertical jetting apparatus. As mentioned before, this method is most widely used by contractors to install full-scale concrete piles in sandy profiles. The purpose of the research was to develop a model for jetted pile installations by determining optimum jetting parameters while minimizing debris zone disturbance and insuring an adequate insertion rate for a given pile length. In order to quantify disturbance and insertion rate due to jetting parameters, a series of "full-

depth" tests were conducted. These full-depth tests involved maintaining a consistent water flowrate and jet nozzle velocity for each test. After completion of specimen preparation and inundation, the jetting apparatus was connected to the pile so the jet nozzles were flush with the pile tip. The jetting nozzles were located at the center of the pile on opposite sides. The pile was then lowered into place and allowed to settle under self weight at the specimen surface. During jetting, the test pile penetrated the specimens until refusal. From these tests, maximum insertion depth and debris zone characteristics for given jetting parameters were acquired. The following flowchart demonstrates the test matrix for vertical jet testing in the laboratory program.

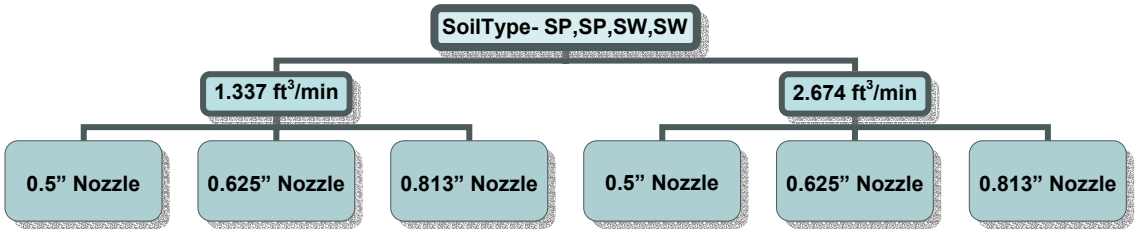

Figure 3.10 Flowchart for Test conducted with Vertical Jets – Full Depth

After several full depth tests with the vertical jets, realization that debris zone characteristics of tests with different water flowrates and jet nozzle velocities were incomparable. This conclusion was based on the variation in refusal depths for the jetted pile under constant water flowrates with various jet nozzle velocities. Therefore a series of "depth-controlled" tests were undertaken in each soil type. These tests utilized the same water flowrates and jet nozzle velocities as the full-depth tests. However, the piles were jetted to a given depth based on the minimum water flowrate and minimum jet nozzle velocity. From this series of tests, correlations between debris zone characteristics

due to various water flowrates and jet nozzle velocities were developed based on a specified depth constraint. Therefore, for a given depth, the optimum jetting parameters could be determined to minimize debris zone surrounding jetted piles.

3.2.3.2 Angled Jet Testing Program

A modification to the current practice was implemented into the laboratory jetting program. This modification involved jet nozzles angled at 45° from the vertical pipes. These nozzles were oriented so the jet water flowed directly under the pile tip. These tests were conducted to determine if jet nozzle orientation affected the insertion and debris zone characteristics of jetted piles. The orientations of the jet streams used in these tests are shown in Figure 3.11. Data produced from these tests were compared to similar jetting parameter tests using vertical nozzles.

Figure 3.11 Angled Jet Nozzles for Jetting Modification

3.3 Investigation of Pile Jetting Mechanism

Previous literature on pile jetting revealed that pile insertion is attained only when soil is liquefied beneath the pile tip and moved to the ground surface by return water. This mechanism of liquefaction was investigated with the aid of a transparent plexi-glass box. The box was 3 ft x 3 ft x 4 ft (0.91 m x 0.91 m x 1.22 m - length x width x height) with one inch-thick side walls. The box was reinforced laterally with ratchet straps secured at one-third points from the bottom of the box prior to soil placement.

Surface effects of pile jetting appeared to be symmetric with respect to the east and west axes as shown in Figure 3.12. It was decided that an eight inch diameter pile cut in half along the east-west axis and jetted against the box face would have similar insertion mechanics of a "full-pile." A view of the "half-pile" against the plexiglass box face is shown in Figure 3.13.

Figure 3.12 Symmetry of Surface Effects of the Vertical Jet System

Figure 3.13 View of Half-pile Used in Mechanics Investigation

Cherry Branch Sand and Mortar Sand were used to investigate the mechanics of pile jetting. These two sands were chosen due to similar GSD shape parameters but differing average particle diameters. For each test, testing material was placed in four lifts and tamped with the Bosch Jackhammer to relative densities of 50 to 70%. The specimens were then inundated with water and allowed to soak overnight. The jetting apparatus was then fixed to the half-pile and placed on the specimen surface at the box face. Jetting tests were performed with various water flowrates and jet nozzle velocities while the insertion mechanism was witnessed.

As Tsinker (1988) mentions, an annulus forms along the edges of the jetted pile. In this transition zone, the soil matrix was in a liquefied state while being transported from the annulus to the specimen surface. However, it was recognized that the insertion mechanism was due to erosion of a sufficient area of soil to cause a bearing capacity

failure beneath the pile tip. As failure occurred, the soil beneath the pile tip was displaced into the annulus and the erosion process continued. The piles were seen to incrementally move through the soil profile with a "jerking" motion. This was attributed to the "erode and fail" mechanism. It was also realized that as the pile moved further into the soil profile, the insertion rate slowed considerably. This characteristic is due to the decreased bearing pressure and increased bearing capacity beneath the pile tip as it moves deeper into the inundated soil stratum. To continue penetration, the jetting system must erode greater amounts of soil with depth to cause a bearing capacity failure. The particles which displace from beneath the pile tip must also be transported to the specimen surface for continual insertion. After tip failure the jetting mechanism is then governed by particle transport theory from hydraulics. In conclusion, for pile insertion, adequate water flowrate and jet nozzle velocity is required to erode a specific area of soil beneath the pile tip while transporting these soil particles to the ground surface. Figure 3.14 demonstrates the annulus caused by jetting and the element of soil providing bearing resistance to pile insertion.

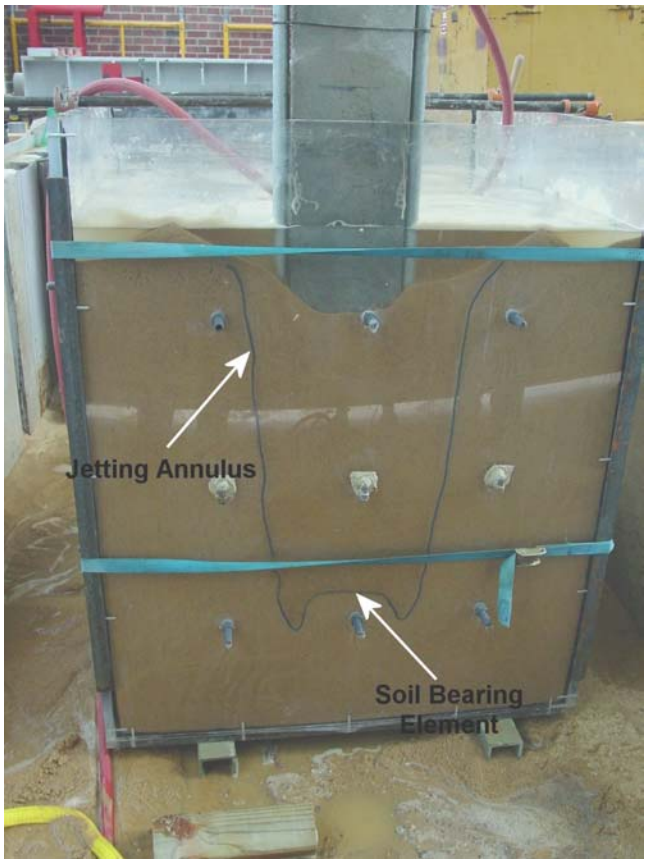

Figure 3.14 Jetting Annulus and Soil Bearing Element

CHAPTER 4 - DATA ACQUISITION AND TEST MONITORING

A data acquisition program was developed to obtain pertinent information from each laboratory jetted pile installation. The data acquisition program was implemented identically for each of the tests so comparisons of test results could be made. The data acquisition program involved the following; determining grain size distributions prior to jetting and of the debris zones, surveying the specimen surface before and after application of jetting, recording pile insertion rate, and determining a cutoff standard for test termination. The data acquisition program covered all aspects necessary for development of a jetting model for large scale applications.

4.1 Grain Size Distribution Monitoring

Grain size distributions were used to determine particle size of soils protruding from the annulus around jetted piles. These size distributions were used to quantify amounts of specific-sized soil particles that could extend beyond the pile location within return water from the jetting stratum. Pre-test and post-test grain size distributions of specimen materials were also used as a quality control method to ensure that sufficient quantities of fines were not removed by the jetting applications. This enabled the researchers to recycle specimen soils, thus minimizing stockpile volumes needed to construct new specimens for each test.

Samples of the debris zone were taken from north, south, east and west directions at distances within and extending six inches from the pile edge and at depths in the upper and lower sections of the debris profile. An elevation view of the debris zone is shown in Figure 4.1 demonstrating grain size distribution sampling technique. Symbols E-1 and S-

1 represent locations of sampling near the pile edge (within 6 inches (150mm)) whereas symbols E-2 and S-2 represent locations of sampling beyond six inches from the pile edge.

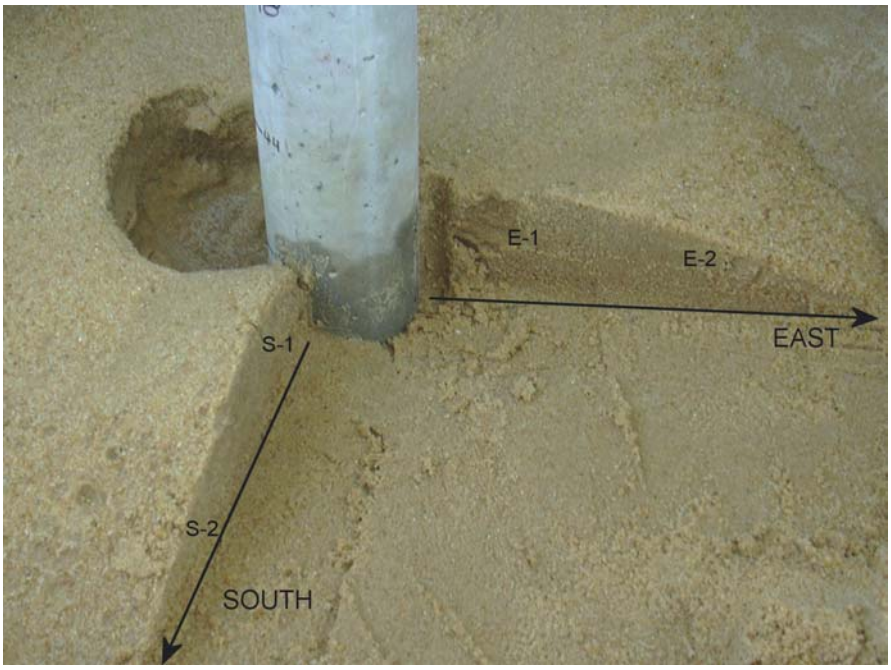

Figure 4.1 View of Debris Zone and Sampling Locations

The grain size distributions from debris zone material produced curves similar to initial grain size distributions of the specimens prior to jetting. Therefore a sufficient volume of material, regardless of size, must be removed from around the pile for productive jetting. However, there exists some discrepancy in the pre and post grain size distribution curves. From the grain size distribution curves shown in Figure 4.2, the debris zone consists of the entire range of particle sizes from the initial grain size distribution. However, the amount of coarse particles within the debris zone will vary depending on the nozzle velocity of the jet water. The GSD of the debris zone (South and East) and the pre-jet specimen GSD in Figure 4.2, reveal greater quantities of fine

grained soil particles on the specimen surface as compared to larger soil particles for given jetting parameters. The property was true for all lab jetting tests.

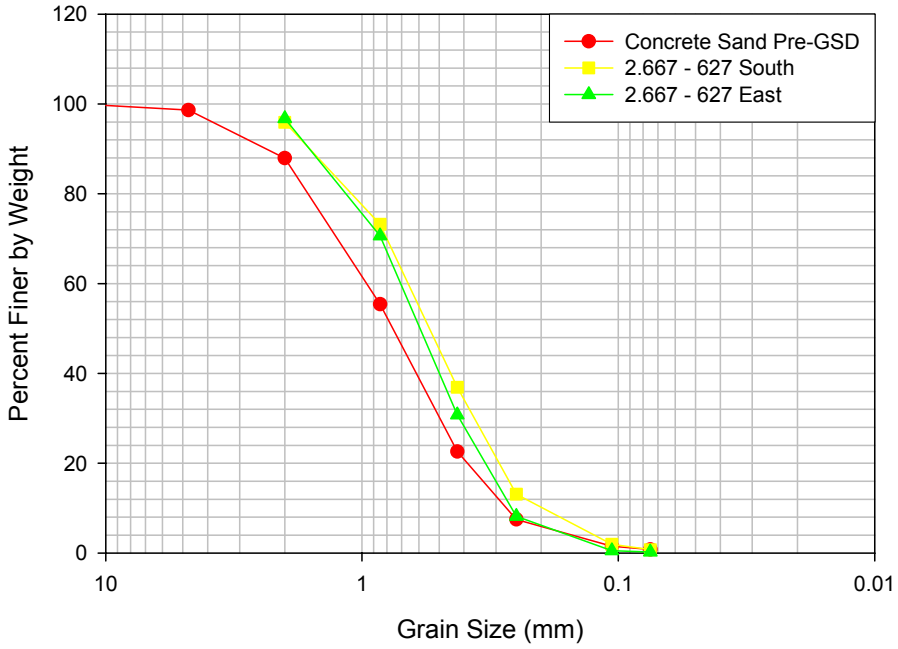

Figure 4.2 Grain Size Distribution Curve for Debris Zone Comparison

4.2 Debris Zone Delineation and Debris Volume Acquisition

In order to determine surface effects of jetted pile installations, it was necessary to develop a method to survey the initial and final surface profile upon cessation of jetting. Therefore, a reference beam was fabricated to conduct the profile inspections. The reference beam was an aluminum, T-shaped beam which rested on supports and spanned the specimen basket side rails. The supports were leveled so the reference beam remained truly horizontal. After lowering and centering the pile on the specimen surface, the reference beam was centered in the direction for which initial ground surface readings were required (north, south, east or west directions). The reference beam was constructed

with notches at every 0.5 inch (12.7 mm) along the survey line. These notches provided exact locations where elevation measurements from the reference beam were taken. Upon completion of jetting, elevations were again taken in each direction to delineate the debris zone height and radial distance of debris zone from the pile. A typical section of a jetted pile installation is shown in Figure 4.3.

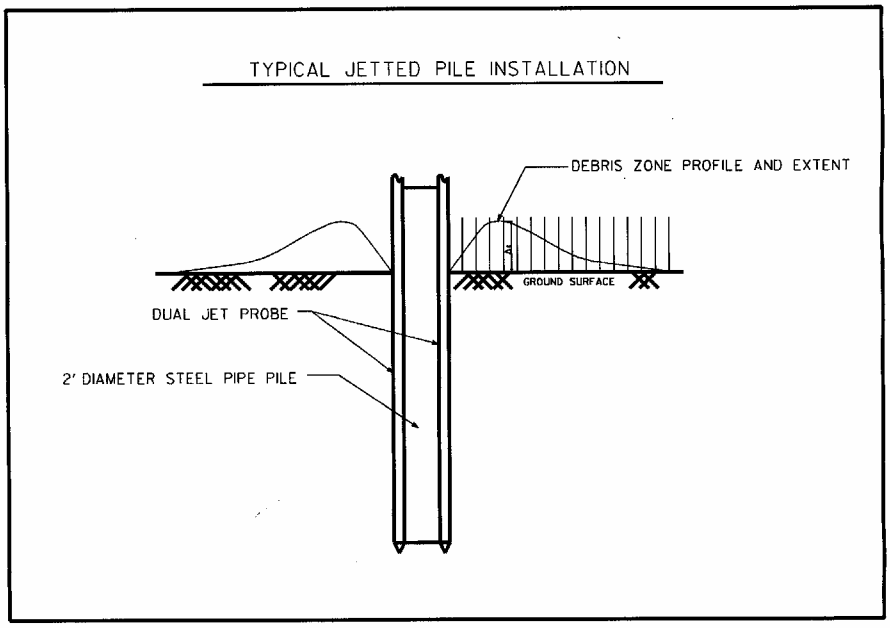

Figure 4.3 Debris Zone Delineation of Jetted Pile Installation

The initial and final elevations at each point along the specimen surface were tabulated in data sheets in Microsoft Excel™. With this information, the elevation change at each location along the specimen surface was determined by the difference in initial and final elevations. To determine the volume of material deposited within the debris zone, numeric integration of the average height of deposited material between divisions on the reference beam was conducted 360º around the pile center. The volume integration was conducted in all four coordinate directions (north, south, east and west) and averaged. The pile volume within this zone was deducted from the average volume

approximation to yield the average debris zone volume (V_{debris}) for each test. The area of the debris zone (A_{debris}) was calculated from the following equation for an elliptical area as shown in Figure 4.4:

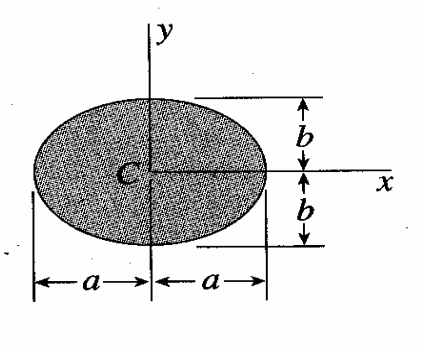

Figure 4.4 Elliptical Distribution of Debris Area

$$A_{debris} = \pi ab \qquad \text{Eq 4. 1}$$

where: a = radial distance of debris zone extent in east and west direction
b = radial distance of debris zone extent in north and south direction

Therefore, the surface effects of pile jetting could be quantified and compared with tests employing different jetting parameters.

4.3 Pile Insertion Rate Acquisition

To determine pile insertion rate due to various jetting parameters and soil type, test piles were marked from the pile tip at two-inch increments. Upon initiation of jetting, a reference datum was chosen corresponding to a given point along the test pile. A stopwatch was used to record the elapsed time of jetting for each depth increment of pile insertion from the reference datum. The pile template shown in Figure 4.5 provided a reference datum for pile insertion data acquisition.

Figure 4.5 Reference Datum (Pile Template) Used for Insertion Data Acquisition

The insertion rate data obtained from each test demonstrate the dependency of insertion characteristics on Q_w and V_j. These relationships had to be evaluated to develop a model encompassing these variations.

4.4 Test Termination

After several pile installations, it was noticed that pile insertion reached refusal when return water from the pile annulus was lost. This attribute was used as a termination point for each test within the various sand types. These termination depths varied between tests based on jetting parameter fluctuation. Therefore, it is evident that debris zone characteristics as well as insertion and pile termination depth are related to the water flowrate and jet nozzle velocity used in jetted pile applications.

4.5 Summary of Data Acquisition and Test Monitoring

A quality data acquisition program was invoked for all tests conducted in the experimental program. Quality data obtained from the testing program provided a means of comparing all test results between the various soils. With these test results, model development was undertaken to provide a tool that geotechnical engineers may use to predict the insertion rates, insertion depths, and debris characteristics of larger scale jetted piles.

CHAPTER 5 - RESULTS OF LABORATORY PILE JETTING

Jetting of model concrete piles was conducted within the soil profiles previously mentioned. Since all tests were performed in soils at similar relative densities, comparing the results between the various soil types were used to develop the jetting model. Initial jetting of the four inch and six inch diameter piles penetrated the entire stratum where boundary conditions were introduced. Therefore, a majority of the jetting procedures were conducted on the eight inch diameter pile which consistently reached insertion refusal prior to encountering the specimen depth limit. The water flow rates (Q_w) and jet nozzle velocities (V_j) varied between tests under constant pressure of 87 psi (600kPa). The water flow rate and jet nozzle velocities fluctuated between tests to determine the effects of these parameters on pile installation and debris zone characteristics. Table 5.1 provides information on pile jetting tests conducted in the experimental program. The following sections present the results from the laboratory experimentation.

Table 5.1 Description of Tests Conducted in Experimental Program

Concrete Sand		Mortar Sand		Cherry Branch Sand		Mortar + Kaolinite	
Full Tests	Depth Control Tests	Full Tests	Depth Control Tests	Full Tests	Depth Control Tests	Full Tests	Depth Control Tests
(Q_w–V_j) (ft^3/min – ft/min)	(Q_w–V_j) (ft^3/min – ft/min)	(Q_w–V_j) (ft^3/min – ft/min)	(Q_w–V_j) (ft^3/min – ft/min)	(Q_w–V_j) (ft^3/min – ft/min)	(Q_w–V_j) (ft^3/min – ft/min)	(Q_w–V_j) (ft^3/min – ft/min)	(Q_w–V_j) (ft^3/min – ft/min)
1.337-313	1.337-490	1.337-186	1.337-313	1.337-186	1.337-186	1.337-186	1.337-186
1.337-313	2.674-372	1.337-186	1.337-490	1.337-313	1.337-313	1.337-313	1.337-490
1.337-490	2.674-626	1.337-490	2.674-372	1.337-490	1.337-490	1.337-490	2.674-372
2.674-372	2.674-980	2.674-626	2.674-980	1.337-490	2.674-372		2.674-980
2.674-626		2.674-626		2.674-372	2.674-626		
2.674-626		2.674-980					
2.674-980							
CONVERSIONS: ft^3/min to m^3min multiply by 0.0283 ft/min to m/min divide by 3.281							

5.1 Refusal Depth and Insertion Characteristics

After conducting several full-depth tests, data analysis revealed insertion rate and penetration depth characteristics. Piles were jet-driven into various sand specimens compacted to consistent relative densities to provide a basis of comparison between tests with variation in water flow rate (Q_w) and jet nozzle velocity (V_j). It was seen that insertion properties (i.e. Pile Insertion Rate, and Refusal Depth) rely on both water flow rate (Q_w) and jet nozzle velocity (V_j). Tests conducted under equal Q_w but with higher jet velocities produced higher insertion rates at a given depth as compared to tests with lower V_j. This trait was also true for refusal depth characteristics. This is attributed to the increased erosion efficiency of higher jet nozzle velocity beneath the pile tip. Also, it is expected that water returning from the pile annulus at higher V_j has the ability to lift larger size or quantities of particles thus aiding in insertion.

5.1.1 Insertion Rate Characteristics – All Tests

The following figures provide insertion rate characteristics of all tests conducted in the experimental program. It may be inferred from the depth versus time graphs (Figures 5.1a-d) for each soil type, that with equal Q_w, higher jet nozzle velocities enable the pile tip to extend to greater depths as compared to lower jet nozzle velocities. This is true for both water flowrates used in laboratory testing. The insertion characteristics due to similar jetting parameters between sand types are also shown in Figure 5.1.

Based on the variation in material and engineering properties of the soil types presented in Chapter 3, it is expected that equal jetting parameters produce dissimilar insertion characteristics between the soil types. It was stated earlier that for effective jetted pile insertions, a sufficient quantity of soil particles must be eroded from beneath

the pile tip and transported out of the jetting annulus. Therefore, erosion efficiency and particle lifting ability increases with higher jet velocities for a given soil type. It was noticed during laboratory experimentation that insertion diminished when return water from the annulus ceased. At this point the ability of return water to transport eroded soil from beneath the pile tip to the specimen surface was lost. From the literature review on sediment transport, it is recognized that particle lift by a fluid medium is dependent on the velocity of fluid, particle diameter, and specific gravity of the particle. Therefore, for equal jetting parameters, it is expected that greater insertion depths may be obtained in soil profiles with smaller average particle sizes as opposed to soil profiles with larger average particle sizes. For example, the two tests conducted in Cherry Branch Sand (5.1c) with Q_w and V_j of 1.337ft^3/min (0.039 m^3/min) and 490 ft/min (149 m/min), respectively, achieved an average final insertion depth of 2.9 ft (0.88 m), whereas implementing the same jetting parameters in the Mortar Sand profile, a final insertion depth of 1.25 ft (0.38 m) was achieved. The corresponding average particle sizes (D_{50}) are 0.006 in (0.15mm) and 0.02 in (0.5mm) respectively.

The insertion rate characteristics may also be attributed to the material and engineering properties. For example, consider the elapsed time of jetting required to reach a depth of one foot (0.30 m) in the Concrete and Cherry Branch Sand specimens at Q_w and V_j of 1.337ft^3/min (0.039 m^3/min) and 490 ft/min (149 m/min), respectively. For the two tests conducted in Cherry Branch Sand, the average insertion rate at one foot insertion is approximately 0.7 ft/min (0.20 m/min), whereas the insertion rate at one foot insertion in the Concrete Sand is approximately 0.3 ft/min (0.08 m/min). The effective angle of internal friction (ϕ') determined by direct shear testing is 42^o and 34^o for the

Concrete and Cherry Branch Sand, respectively. Thus, tip bearing capacity of the Concrete Sand at this depth increment is greater than tip bearing capacity of the Cherry Branch Sand. For equal depths of insertion, a larger eroded area must be removed from beneath the pile tip in Concrete Sand to cause a bearing capacity failure. With equal jetting parameters, longer time intervals are necessary to erode greater areas of bearing soils in the higher friction angle materials, therefore decreasing the pile insertion rate.

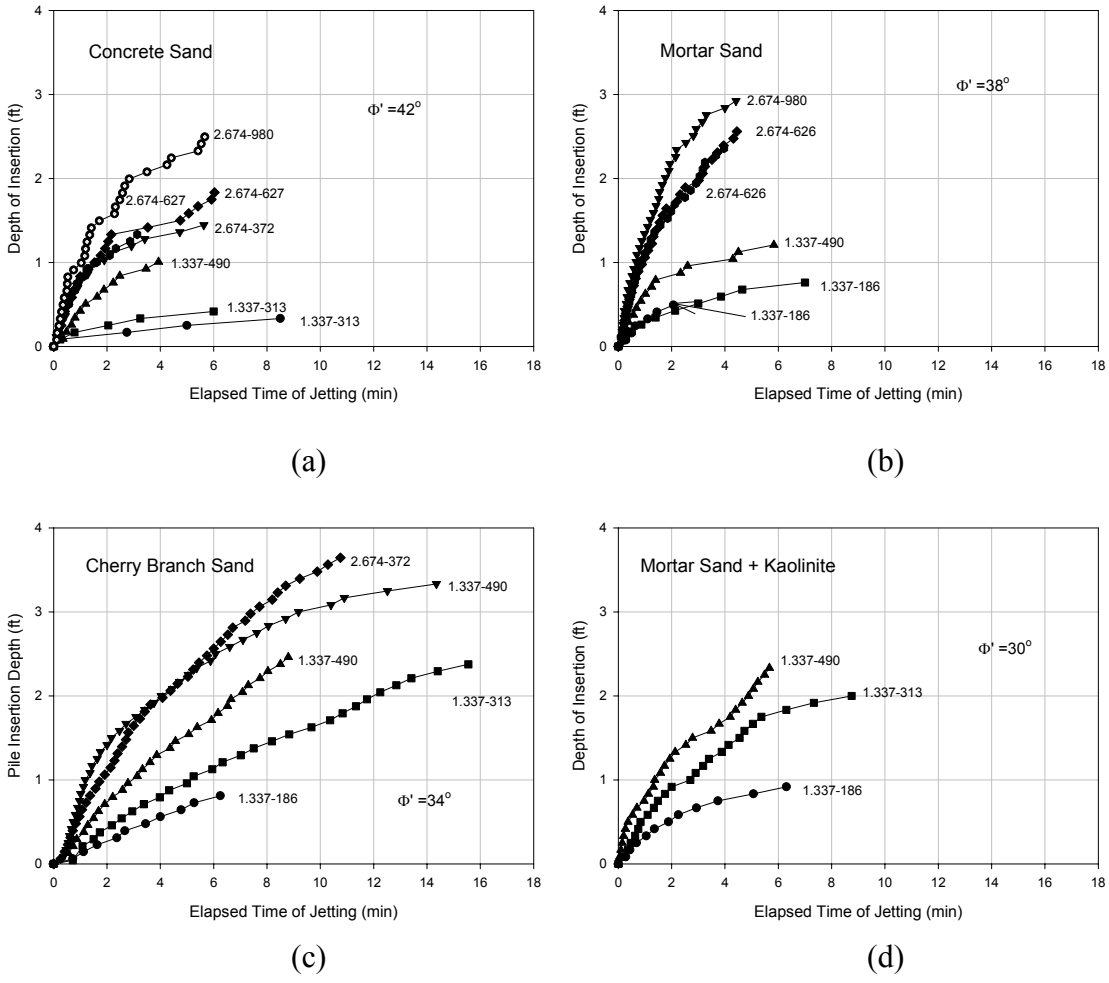

Figure 5.1 Depth of Insertion as a Function of Time for Various Water Flowrate and Jet Nozzle Velocity.

Referring to Figure 5.1, the derivative of pile insertion depth with respect to elapsed time of jetting was taken at given depths to compare pile insertion rates due to

jetting parameters (Figure 5.2). Depths of insertion were chosen for each soil type based on the attainable insertion depth of the lowest Q_w and V_j relationship. For example, in Concrete Sand, to better illustrate pile insertion rate as a function of Q_w and V_j, it was recognized that the lowest value of Q_w and V_j were 1.337 ft^3/min (0.038 m^3/min) and 313 ft/min (95 m/min) respectively. These values correspond to a final depth of insertion of 0.25 ft (0.076 m). For comparison with other Concrete Sand tests with higher Q_w and V_j values, the pile insertion rates were determined at a depth of 0.25 ft (0.076 m) for each test. From Figure 5.2 it is realized that for a given depth, the pile insertion rate is dependent on both Q_w and V_j. For equal Q_w, increases in V_j will provide higher insertion rates for any depth of insertion.

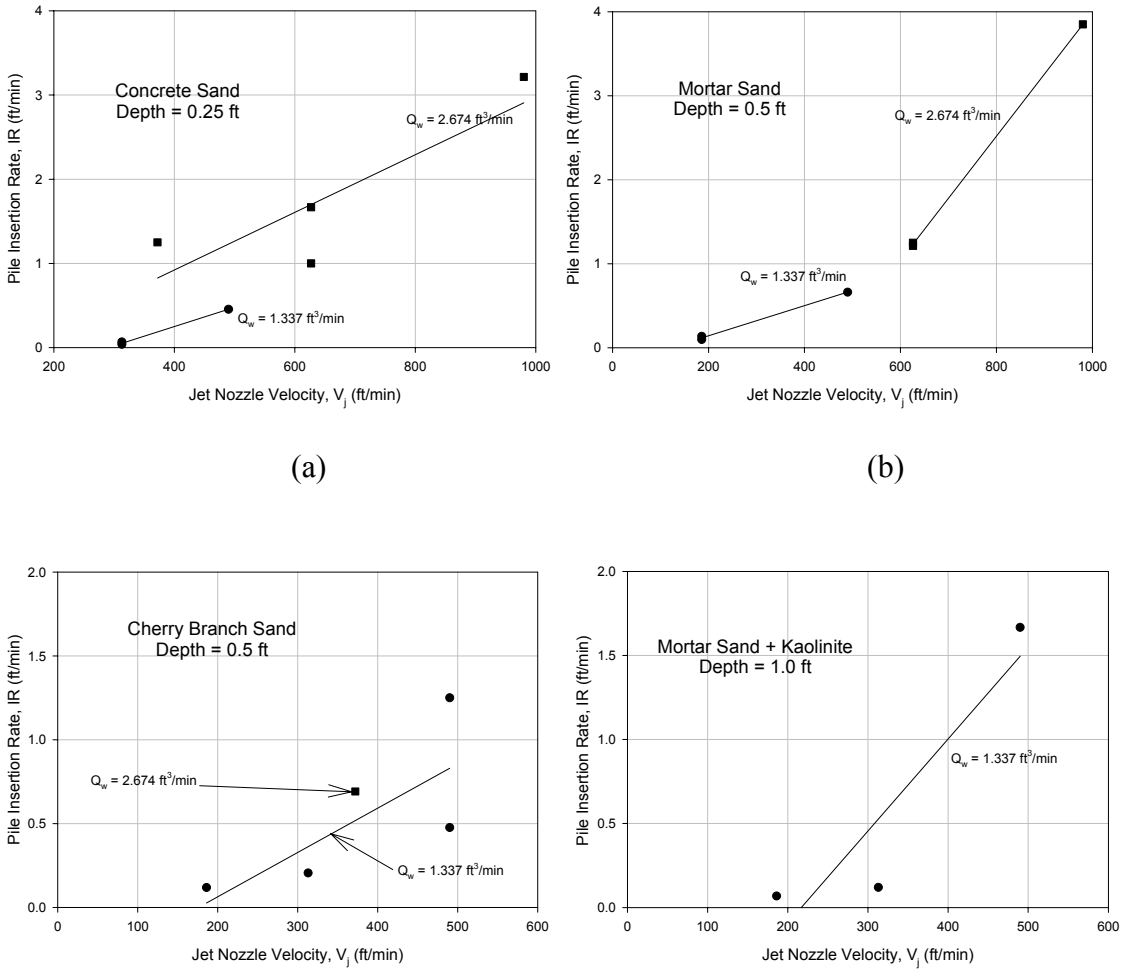

Figure 5.2 Comparison of Pile Insertion Rates at Given Depths Due to Variation in Jetting Parameters

From Figures 5.1 and 5.2, pile insertion depth and insertion rate for a given soil type is dependent on both Q_w and V_j. Assuming continuity, jet nozzle velocity is linearly dependent on the jet nozzle area and water flow rate through the nozzle by the following equation:

$$Q_w = A_j V_j \qquad \text{Eq. 5. 1}$$

where: Q_w = water volume flowrate (L^3/T)
A_j = jet nozzle area (L^2)
V_j = jet nozzle velocity (L/T)

The pile insertion rate, IR, is based on both Qw and Vj for a given depth in the soil stratum. Since the bearing resistance of a uniform soil profile increases with depth, the dimensions of the jetted pile are important when comparing installation characteristics. Therefore, the pile volume flowrate, Q_p, is presented in equation 5.2. This term provides a direct relationship between the pile dimensions, insertion rate, and the jetting parameters at a specified depth within the soil profile.

$$Q_p = IR \times A_p \qquad \text{Eq. 5. 2}$$

where: Q_p = pile volume flowrate (L^3/T)
IR = pile insertion rate (L/T)
A_p = pile area (L^2)

Normalizing the water volume flowrate with pile volume flowrate (Q_w/Q_p) at each depth increment of jetted pile provides a direct relationship between the jetting parameters and insertion rate for that depth increment. For example, as depth increases, Q_p decreases due to the decrease in applied bearing pressure (q_{app}) of the pile (*groundwater table at specimen surface*) and the increase in bearing capacity. The decrease in q_{app} requires removal of a greater quantity of soil particles beneath the pile tip into the jetting annulus to cause a bearing capacity failure. Therefore, if the jetting parameters are held constant throughout the pile insertion, an increase in required erosion time to cause failure results in a decrease in Q_p with depth. Figure 5.3 provides a relationship between insertion properties of jetted piles due to the jetting parameters at various depths within the soil profiles.

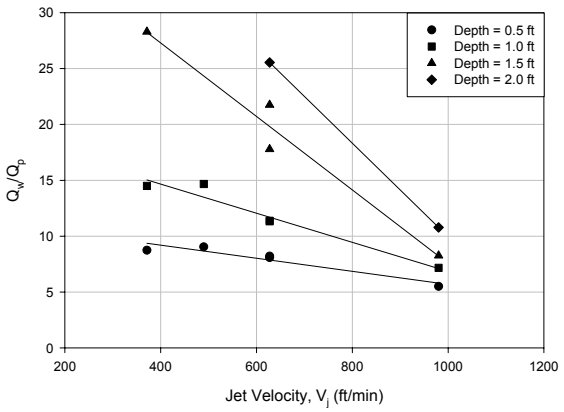

(a) Concrete Sand

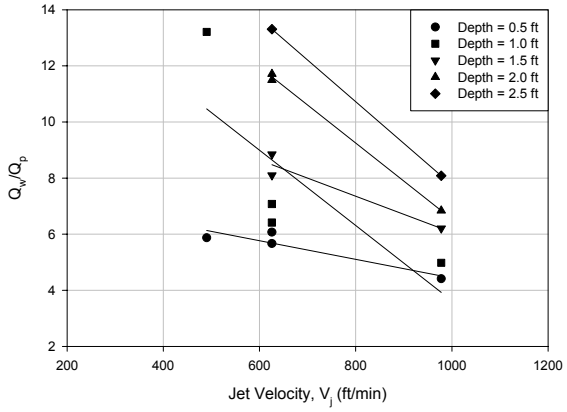

(b) Mortar Sand

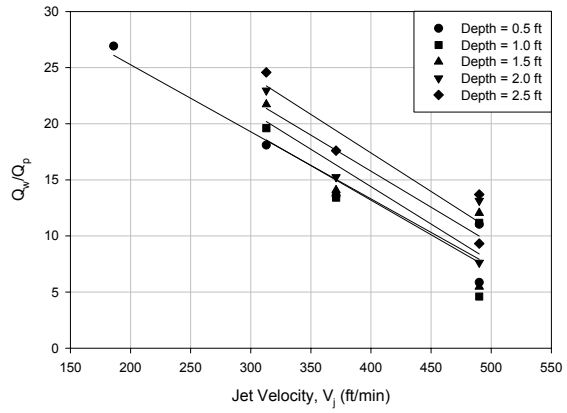

(c) Cherry Branch Sand

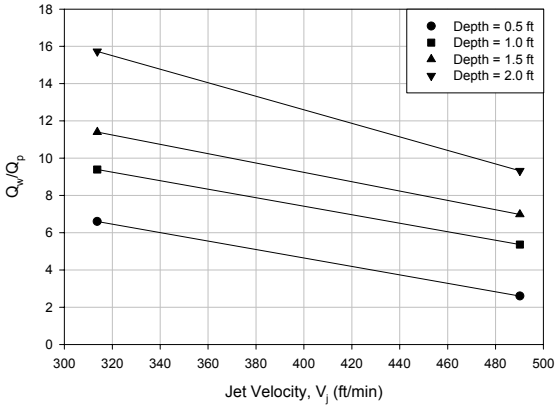

(d) Mortar Sand + Kaolinte

Figure 5.3 Insertion Rate Characteristics of Laboratory Tested Soils

For each soil type displayed in Figure 5.3, the pile volume flow rate is linearly dependent on Q_w and V_j for a given depth increment. As mentioned before, Q_p decreases with depth for constant jetting parameters contributing to an increase in the Q_w/Q_p ratio with depth. These Q_w/Q_p ratios were determined at depth increments to provide an understanding of the insertion characteristics for jetted piles in each soil type and the jetting parameters. It should also be realized from Figure 5.3 that penetration depth for soils with larger percentages of fine particles, i.e. Cherry Branch Sand and Mortar Sand +

Kaolinite, require lower values of Q_w and V_j to insert a pile to equal depths in soil profiles with greater average particle size. These relationships are defined by a specific slope and intercept of the regression line through all the data points for a given depth increment. The regression properties in Figure 5.3, relating Q_p at depth for given Q_w and V_j for all soil types, are given in Table 5.2.

Table 5.2 Regression Coefficients for all Soil Types from Figure 5.3

Concrete Sand				**Mortar Sand**			
Depth (ft)	Slope (m_0)	Intercept (b_0)	R^2	Depth (ft)	Slope (m_0)	Intercept (b_0)	R^2
0.5	-0.006	11.52	0.90	0.5	-0.003	7.76	0.86
1.0	-0.010	19.88	0.95	1.0	-0.013	17.04	0.59
1.5	-0.030	40.44	0.96	1.5	-0.006	12.50	0.93
2.0	-0.040	51.78	-	2.0	-0.014	20.08	0.99
				2.5	-0.015	22.60	-
Cherry Branch Sand				**Mortar Sand + Kaolinite**			
Depth (ft)	Slope (m_0)	Intercept (b_0)	R^2	Depth (ft)	Slope (m_0)	Intercept (b_0)	R^2
0.5	-0.059	37.23	0.93	0.5	-0.023	13.71	-
1.0	-0.062	37.89	0.78	1.0	-0.023	16.56	-
1.5	-0.067	41.08	0.78	1.5	-0.025	19.26	-
2.0	-0.064	41.49	0.81	2.0	-0.036	27.12	-
2.5	-0.069	44.88	0.89				

When plotted with depth, the regression coefficients provide the relationship between pile insertion characteristics and soil type as shown in Figure 5.4 and Figure 5.5.

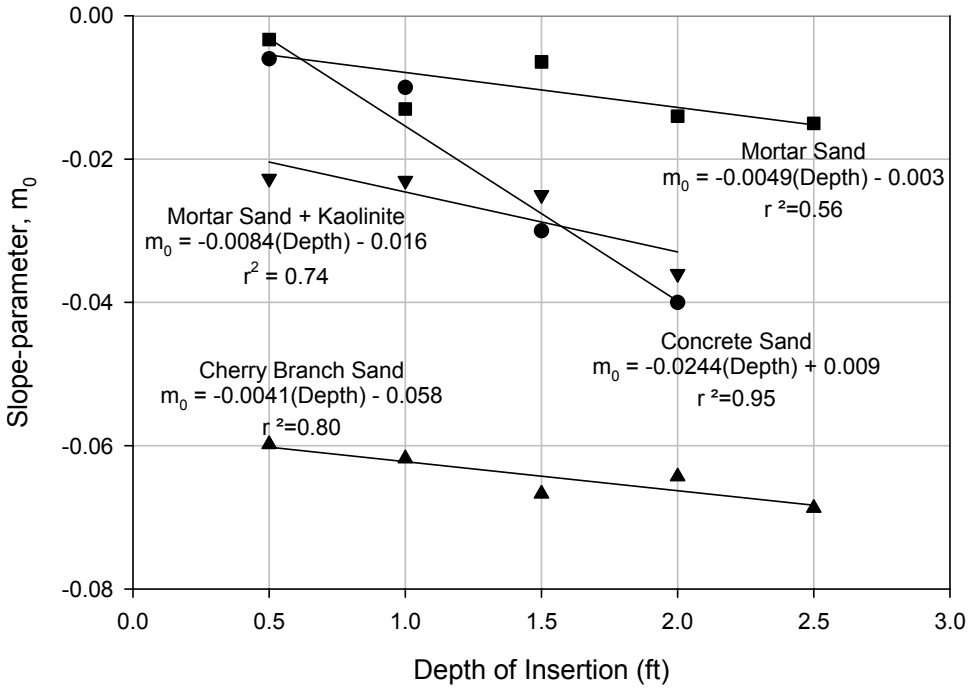

Figure 5.4 Slope-parameter Variation with Depth for Each Soil Type

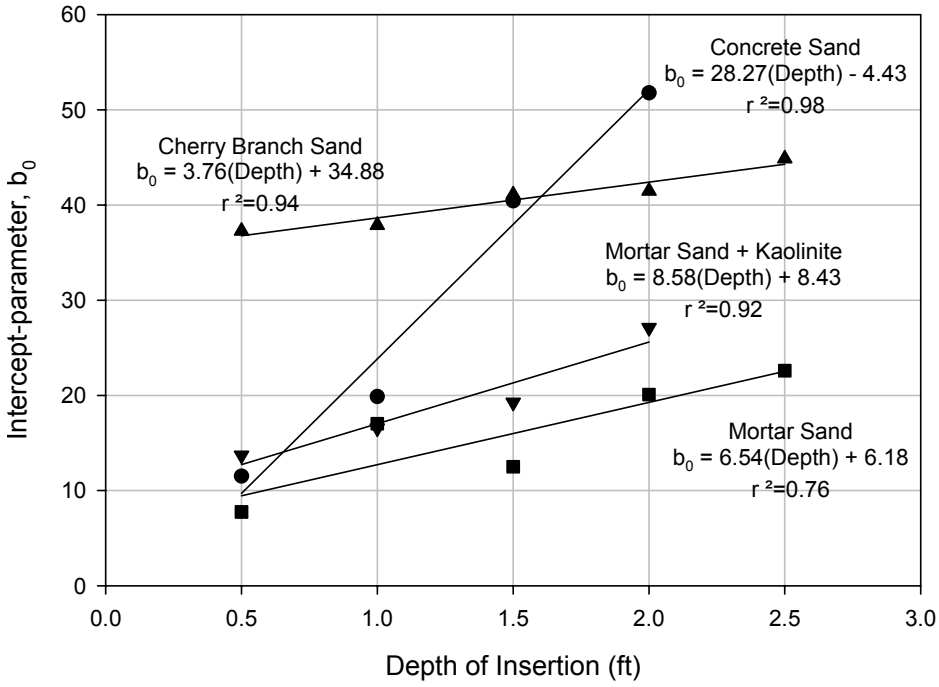

Figure 5.5 Intercept-parameter Variation with Depth for Each Soil Type

From Figure 5.3 it is shown that pile volume flow rate (Q_p) is related to Q_w and V_j by the following general equation:

$$Q_p = \frac{Q_w}{m_0(V_j) + b_0} \qquad \text{Eq. 5. 3}$$

where: Q_p = pile volume flowrate (ft^3/min)
Q_w = water volume flowrate (ft^3/min)
V_j = jet nozzle velocity (ft/min)
m_0 = depth dependent slope parameter $(ft/min)^{-1}$
b_0 = depth dependent intercept parameter

The slope (m_0) and intercept (b_0) parameters are dependent upon the pile insertion depth and the soil stratum properties as shown in Figures 5.4 and 5.5. Therefore, Equation 5.3 can be written as:

$$Q_p = \frac{Q_w}{(m_1(\text{Depth}) + b_1)(V_j) + (m_2(\text{Depth}) + b_2)} \qquad \text{Eq. 5. 4}$$

where: Q_p = pile volume flowrate (ft^3/min)
Q_w = water volume flowrate (ft^3/min)
V_j = jet nozzle velocity (ft/min)
m_1 = depth dependent slope parameter for specified soil type
b_1 = depth dependent intercept parameter for specified soil type
m_2 = depth dependent slope parameter for specified soil type
b_2 = depth dependent intercept parameter for specified soil type
and: $m_0 = m_1(\text{Depth}) + b_1$ (*Depth in feet*)
$b_0 = m_2(\text{Depth}) + b_2$ (*Depth in feet*)

The slope and intercept parameters for the various soil types used in the testing program are shown in Table 5.3. From these parameters, a correlation between the grain size distribution properties and the jetting characteristics can be obtained. Figures 5.6 through 5.9 display the slope and intercept values as a function of grain size distribution properties of the three natural occurring sands used in laboratory testing (i.e. Concrete, Mortar and Cherry Branch Sand). The slope and intercept values are not presented in this

figure for the Mortar Sand + Kaolinite mixture due to the extreme dissimilarities between the smaller fraction of soil particles of this synthetic material with those of the natural occurring sands. The addition of kaolinite (10% by weight) to the Mortar Sand resulted in grain size distribution characteristics and permeability characteristics that are not comparable to other sands used in the testing program (see Table 3.1 and 3.3).

Table 5.3 Slope and Intercept Parameters for Laboratory Soil Types

		Concrete Sand	Mortar Sand	Cherry Branch Sand	Mortar Sand + Kaolinite
$m_0 \rightarrow$	m_1	-0.0244	-0.0049	-0.0041	-0.0084
	b_1	0.009	-0.003	-0.058	-0.016
$b_0 \rightarrow$	m_2	28.27	6.54	3.76	8.58
	b_2	-4.43	6.18	34.88	8.43

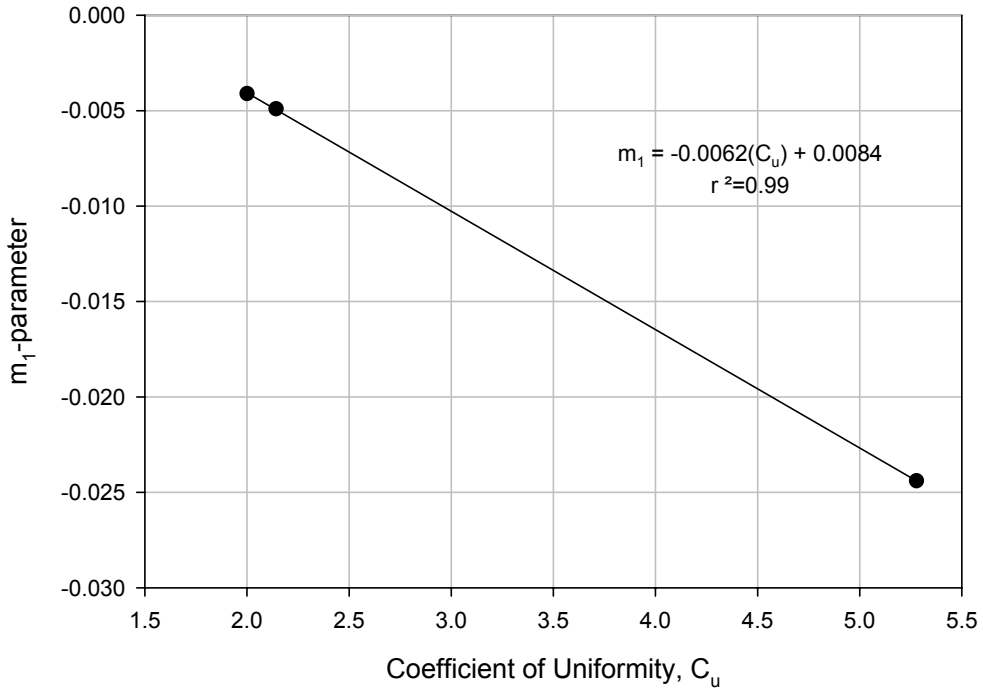

Figure 5.6 Slope-parameter, m_1, Due to Uniformity Coefficient (Natural Sands)

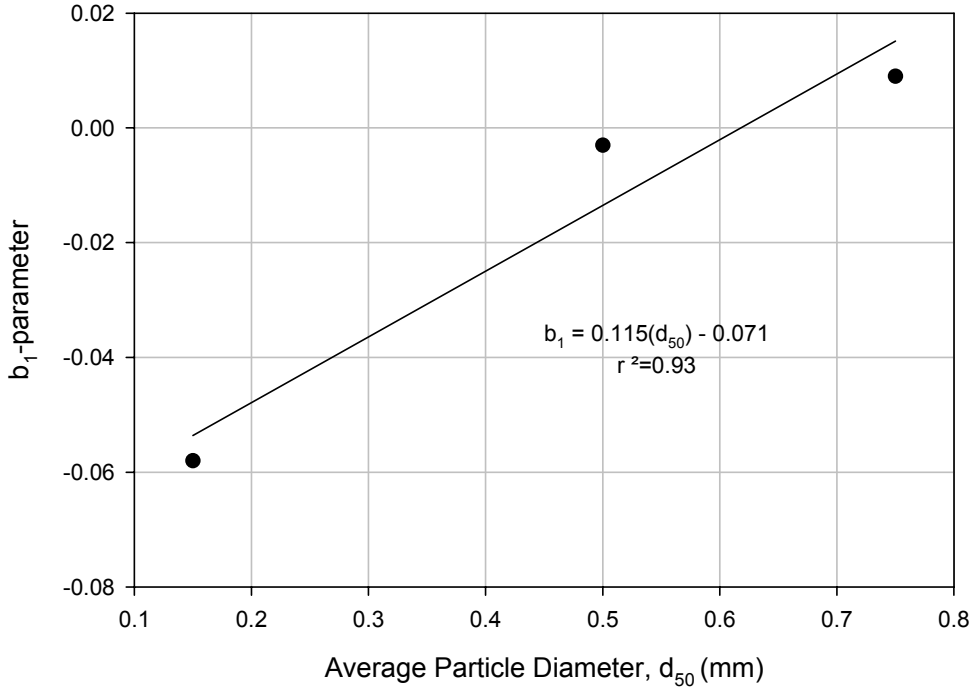

Figure 5.7 Intercept-parameter, b_1, Due to Average Particle Diameter (Natural Sands)

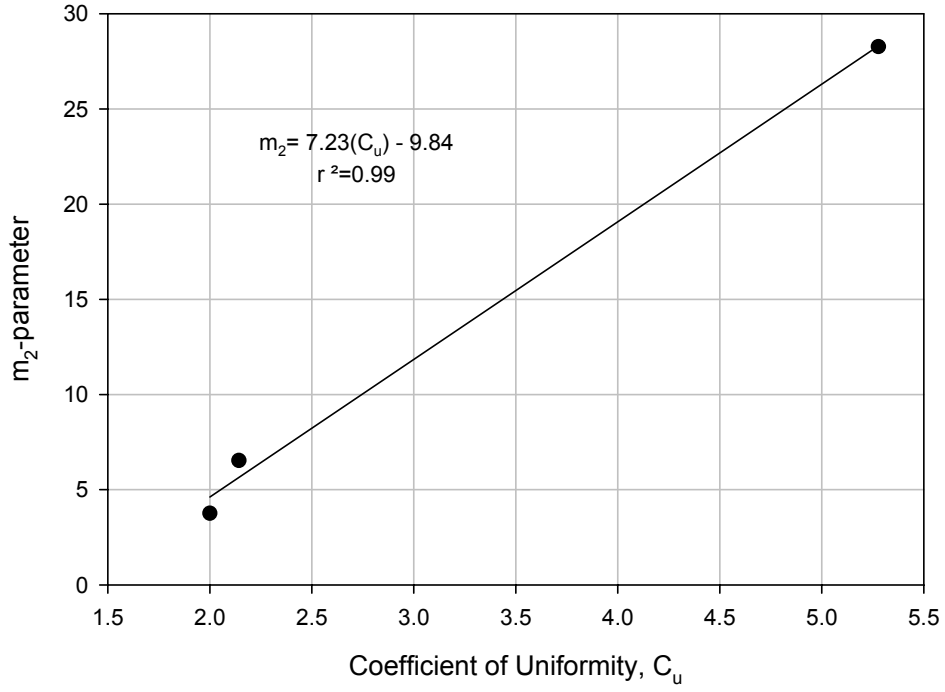

Figure 5.8 Slope-parameter, m_2, Due to Coefficient of Uniformity (Natural Sands)

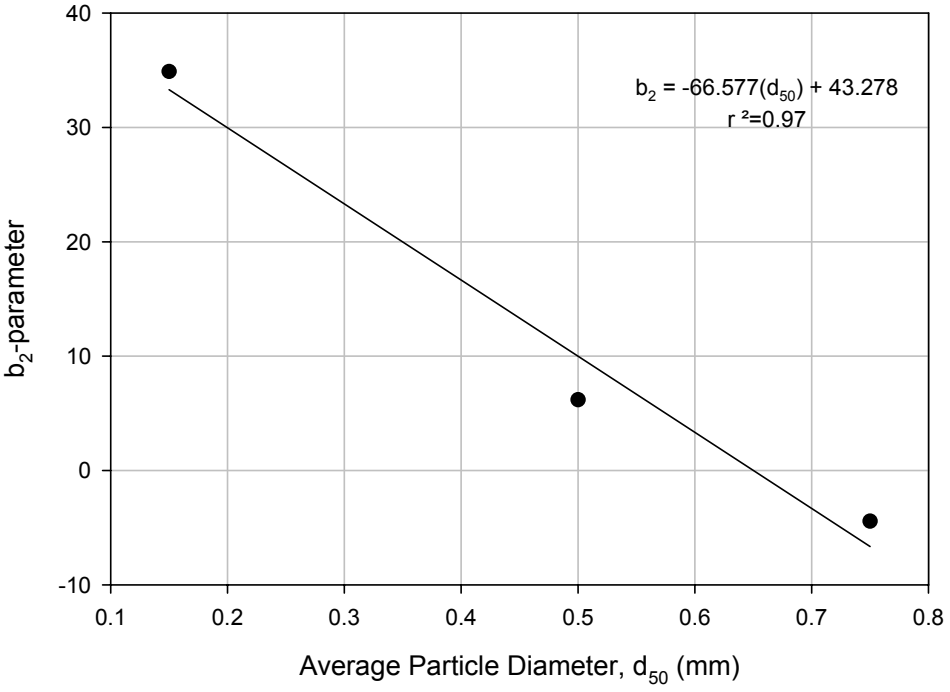

Figure 5.9 Intercept-parameter, b_2, Due to Average Particle Diameter (Natural Sands)

Figures 5.6 through 5.9 display the dependency of the pile insertion rate on the grain size distribution of the material in which jetting is implemented. The average particle diameter, d_{50}, is a general size parameter providing a reference to the complete grain size distribution curve, whereas, the coefficient of uniformity, C_u, provides a reference of the variation in particle size along the grain size distribution curve. Since the pile insertion rate depends on the ability of the return water to effectively transport soil particles from beneath the pile tip to the ground surface, the GSD curves significantly affect the insertion rates for given jetting parameters. The following examples reinforce this point:

For a depth of 2 feet within two soil stratums, the slope-parameters (m_1, b_1, m_2, and b_2) are determined based on the GSD properties from Figures 5.6-5.9. Assume: $Q_w = 2.667$ ft^3/min and $V_j = 500$ ft/min.

A) For equal average particle diameters;
Soil A – $d_{50} = 0.5$mm, $C_u = 4$
Soil B – $d_{50} = 0.5$mm, $C_u = 2$

Since: $m_0 = m_1(\text{Depth}) + b_1$ and $b_0 = m_2(\text{Depth}) + b_2$, equation 5.3 yields;

$$Q_{pA} = \frac{Q_w}{V_j(-0.046) + 52.77} \quad \text{and} \quad Q_{pB} = \frac{Q_w}{V_j(-0.022) + 23.85}$$

$$\text{Thus,} \quad \frac{Q_{pB}}{Q_{pA}} = \frac{29.77}{12.85} = 2.32$$

$$\text{So,} \quad Q_{pB} = 2.32(Q_{pA})$$

B) For equal Coefficients of Uniformity and Coefficients of Curvature;
Soil A – $d_{50} = 0.5$mm, $C_u = 2$
Soil B – $d_{50} = 0.25$mm, $C_u = 2$

Since: $m_0 = m_1(\text{Depth}) + b_1$ and $b_0 = m_2(\text{Depth}) + b_2$, equation 5.3 yields;

$$Q_{pA} = \frac{Q_w}{V_j(0.005) + 19.23} \quad \text{and} \quad Q_{pB} = \frac{Q_w}{V_j(-0.050) + 35.87}$$

$$\text{Thus,} \quad \frac{Q_{pB}}{Q_{pA}} = \frac{21.73}{10.87} = 1.99$$

$$\text{So,} \; Q_{pB} \approx 2(Q_{pA})$$

The previous examples provide some interesting points. In Example A, two soils with equal average particle sizes and varying coefficients of uniformity were considered. Since Soil A has a larger C_u it is expected that the GSD curve for Soil A is more well-graded than for Soil B. As a result, a larger fraction of soil particles greater than d_{50} are present in Soil A as compared to Soil B. (This assumption is made for a general comparison between two hypothetical GSD curves to develop a point. It should be realized that a full GSD evaluation should be conducted to determine all characteristics between jetted pile insertions and grain size distribution.) Therefore, at equal depths of insertion, it is realized that Soil B consisting of a more uniform gradation and d_{50} = 0.5 mm will have a higher Q_p than a more well-graded particle distribution with the same d_{50}. The average particle size effect on Q_p for equal jetting parameters and depth is also developed in Example B. Soils A & B have equal C_u with different d_{50} values (0.5mm and 0.25mm respectively). Since the GSD curves are assumed to have the same shape, it is expected that piles jetted into Soil B would have higher Q_p when compared with Q_p at equal depths and jetting parameters in Soil A. Therefore, it is realized that efficient pile jetting is accomplished after determining the grain size distribution characteristics and implementing fundamental concepts of soil particle transport.

5.1.2 Insertion Depth Characteristics

From Figure 5.2 it is shown that pile insertion rate (IR) is dependent on both Q_w, V_j, and the depth of the pile tip in the soil profile. The maximum depth at which a pile

may be installed due to jetting is also a function of these jetting parameters. Since Q_p depends on both jetting parameters, normalizing Q_w with Q_p takes into account V_j required to achieve the final depth of insertion (D_{final}) for a given Q_w for the test data acquired in the laboratory (Figure 5.10). To achieve greater insertion depths for a given Q_w, the Q_w/Q_p ratio must be minimized which only occurs by increasing V_j.

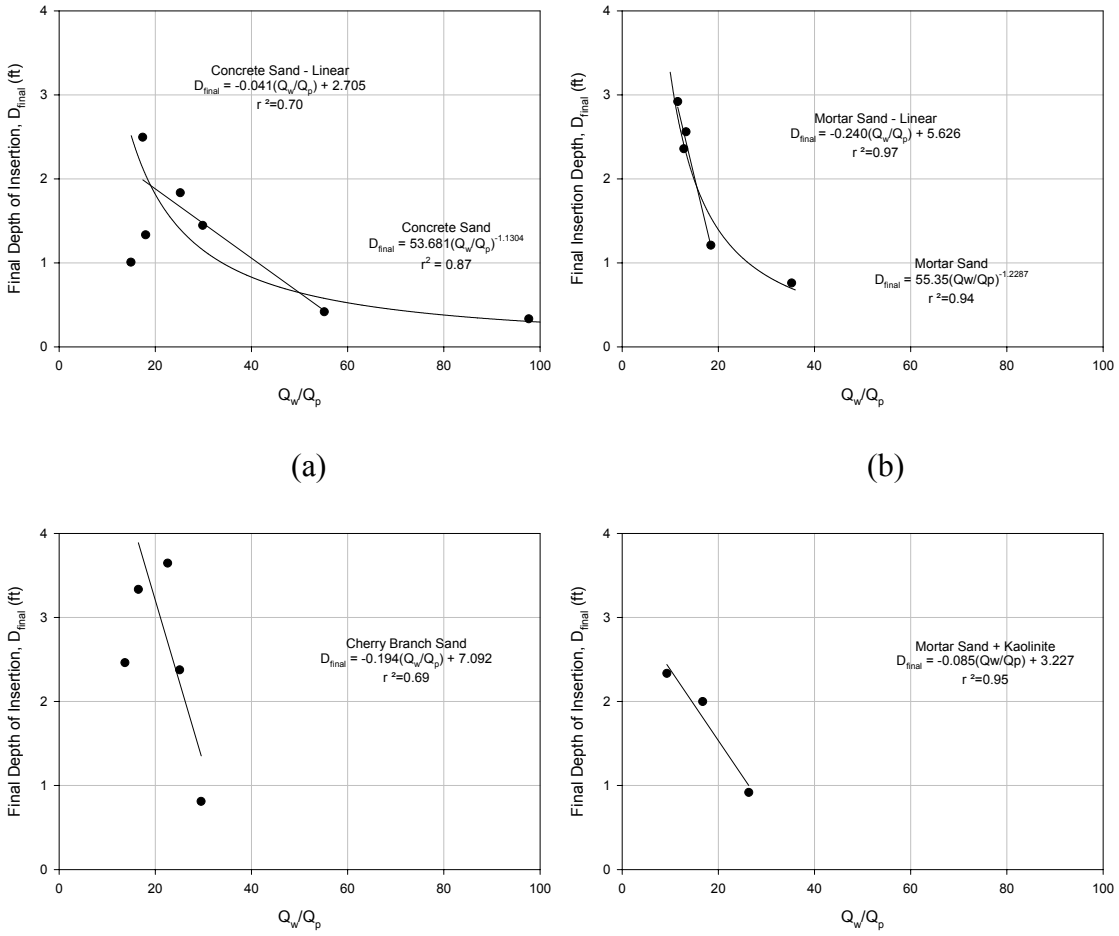

Figure 5.10 Final Depth of Insertion Due to Laboratory Jetting Parameters

In order to compare the final insertion depths with Q_w and V_j between the soil types, it is necessary to analyze the initial linear portions of the curves for the Concrete, Mortar, and Cherry Branch Sands. From Figure 5.10, the linear portions of the curves

represent effective jetting insertions. Beyond this portion of the data, combinations of Q_w and V_j have insufficient erosion capability to remove required quantities of soil to cause a bearing capacity failure and transport of particles to the specimen surface. Therefore, Q_w/Q_p values tend towards infinity as Q_p approaches zero or insertion refusal. Comparison of the regression parameters for the initial portion of the curves for the natural sand types provides the relationship between the installation depth parameters and the soil properties as shown in Figures 5.11 & 5.12.

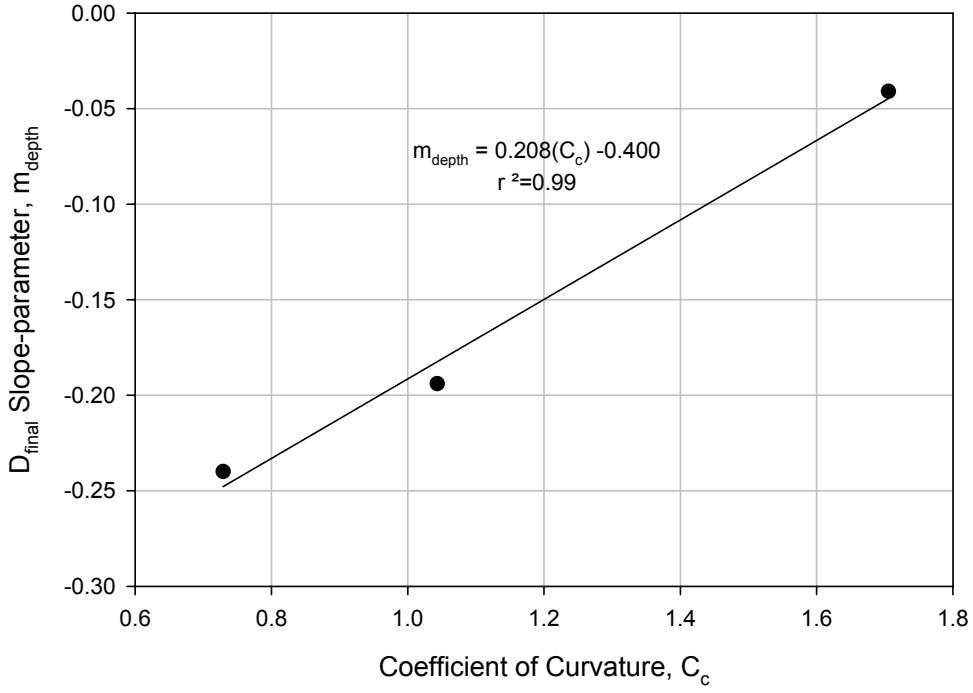

Figure 5.11 Depth Slope-parameter Relationship with C_c

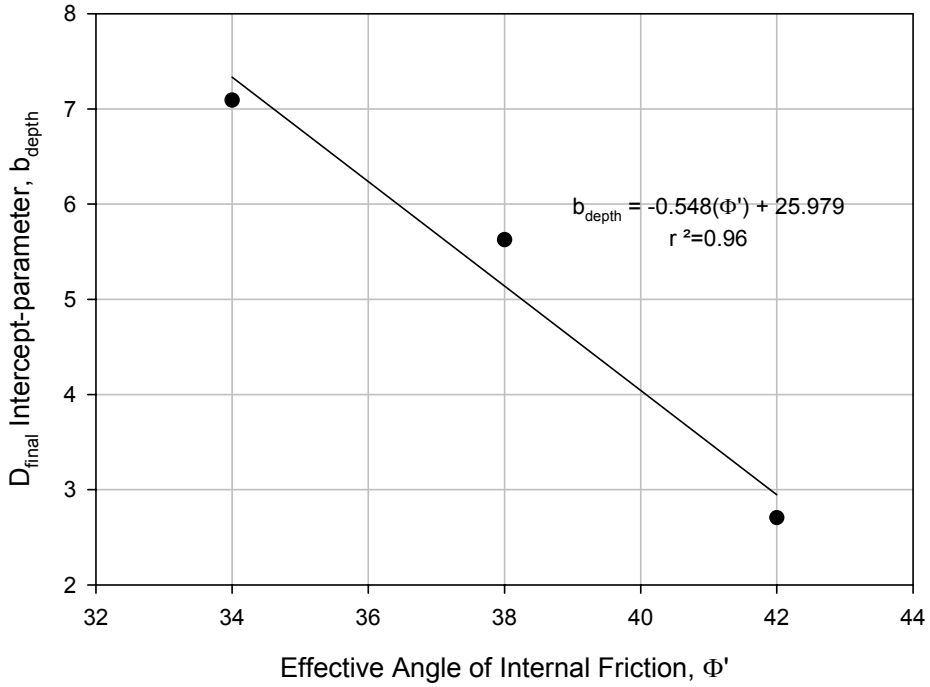

Figure 5.12 Depth Intercept-parameter Relationship with Φ'

Section 5.1.2 provides the relationship between soil material properties, pile insertion rate, and jetting parameters for jetted pile installations. From Figures 5.10 through 5.12, the relationship between the jetting parameters, soil properties, and final depth of insertion is developed. The grain size distribution characteristics influence the final depths of insertion and pile insertion rate for each soil type. The tip bearing capacity for each soil type is dependent on the effective angle of internal friction and effective stress. The grain-size distribution properties contribute to the effective angle of internal friction. The effective angle of internal friction for a well graded soil is expected to be greater than for a uniform graded soil at equal relative densities. Concrete Sand used in the laboratory jetting program is classified as the most well-graded soil based on GSD characteristics (C_c and C_u) as compared to the Mortar Sand and Cherry Branch

Sand. By direct shear testing of each material at similar relative densities, Figure 3.2 displays the Concrete Sand as exhibiting the highest effective angle of internal friction. Therefore, as piles jetted in Concrete Sand move deeper into the soil stratum, increased values of the jetting parameters must be applied to erode and transport greater quantities of soil, therefore, providing continual insertion. The increase in required eroded area is due to increase in bearing capacity with depth. Therefore, regression parameters for final depth of insertion (D_{final}) presented in Figures 5.11 & 5.12 are dependent on the GSD characteristics which determine the engineering properties of soils.

5.1.3 Insertion Characteristics with 10% Kaolinite Clay Fraction

Insertion characteristics with the addition of 10 % kaolinite clay (% by weight) to Mortar Sand were investigated. Comparing the regression parameters from the 100% Mortar Sand with the 90-10 Mortar Sand-Kaolinite mixture yields the following relationships shown in Figure 5.13 and 5.14.

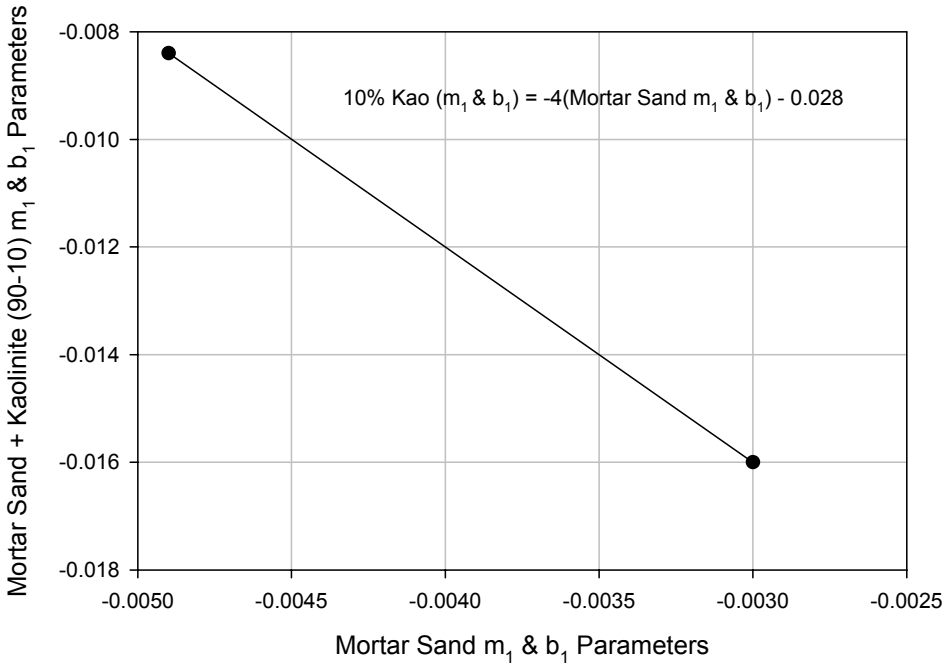

Figure 5.13 Variation of Insertion Parameters (m_1 & b_1) with the Addition of 10% Kaolinite

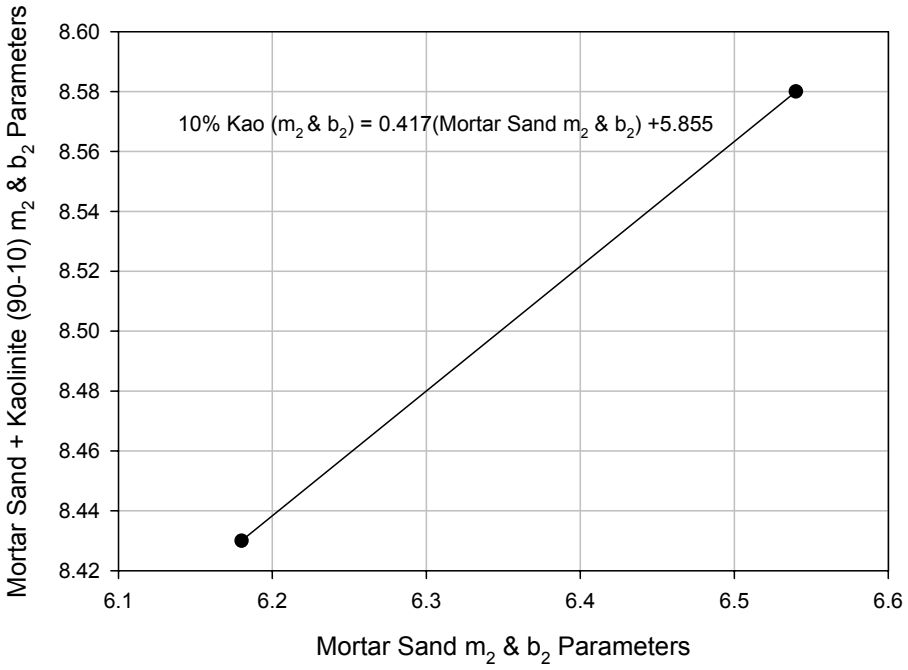

Figure 5.14 Variation of Insertion Parameters (m_2 & b_2) with the Addition of 10% Kaolinite

From Figures 5.13 and 5.14, the regression parameters for the addition of 10% Kaolinite to natural Mortar Sand can be determined from the following equations.

For m_1 and b_1 parameters,

(m_1 or b_1) 10% Kaolinite = -4(Mortar Sand m_1 or b_1) -0.028 Eq. 5. 5

For m_2 and b_2 parameters,

(m_2 or b_2) 10% Kaolinite = 0.417(Mortar Sand m_2 or b_2) + 5.86 Eq. 5. 6

The activity of Kaolinite Clay given by Skempton (1953) and Mitchell (1976) ranges from 0.3 to 0.5. Therefore, kaolinite is deemed an inactive clay with a Plasticity Index for the 90-10 mixture for the lab specimen of 4 from the following equation: (assuming an average Activity of 0.4 for Kaolinite Clay)

$$A = \left(\frac{PI}{\text{clay fraction}} \right) \qquad \text{Eq. 5. 7}$$

where: A = activity of clay mineral
PI = Plasticity Index
clay fraction = percentage of sample less than 2 μm

Since the kaolinite is an inactive clay mineral and the narrow range of plasticity for the 90-10 mixture, it is assumed that the addition of 10% Kaolinite to the Mortar Sand in the laboratory specimens reduces permeability and affects the grain size distribution. The increase in percentage of small soil particles as compared to the natural Mortar Sand would seem to allow greater depths of penetration and greater insertion rates for the 90-10 mixture than that of the natural Mortar Sand. This is justified in Figures 5.15 and 5.16. For example, for Q_w of 1.337 ft^3/min (0.038 m^3/min) and V_j of 490 ft/min (149 m/min), the final depth of insertion in the Mortar Sand at six minutes is approximately

1.25 ft (0.38 m), whereas, the final depth of insertion in the 90-10 mixture at six minutes of jetting is approximately 2.4 ft (0.73 m). Therefore, for equal jetting parameters, the final depth of insertion and insertion rate is greater in soil profiles with larger percentages of fine particles. However, the ability of jetting to install piles through plastic clay profiles is not provided in this report. It is postulated that successful jetting in plastic clay profiles would stem from the ability of water jets to cut large chunks of the clay matrix from around the pile and transport these chunks of the matrix to the ground surface. These larger chunks of soil would require greater jet velocities and water flow rates as compared to the required jetting parameters for un-cemented sand profiles where the individual grains can be dispersed easily.

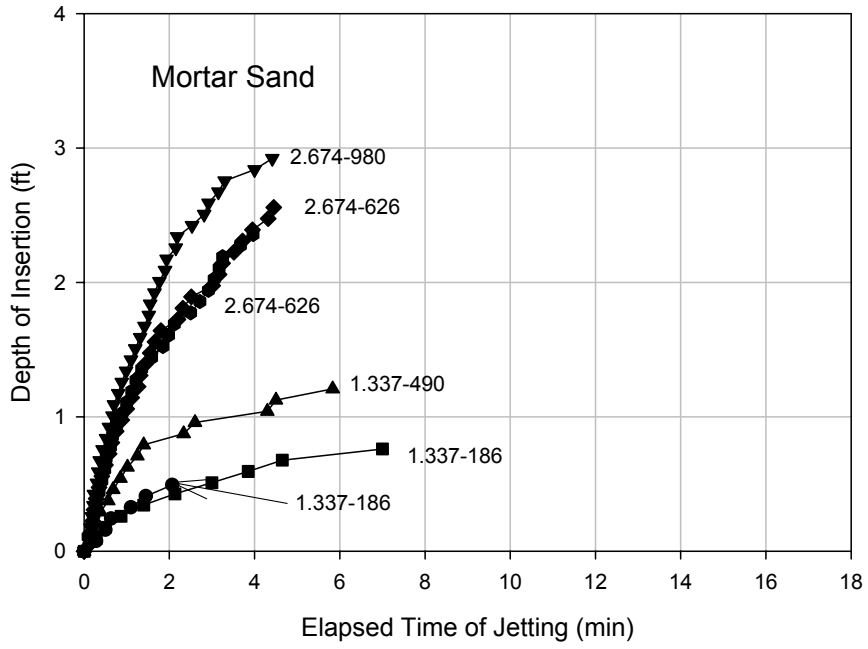

Figure 5.15 Depth of Insertion as a Function of Time for Various Water Flowrate and Jet Nozzle Velocity.

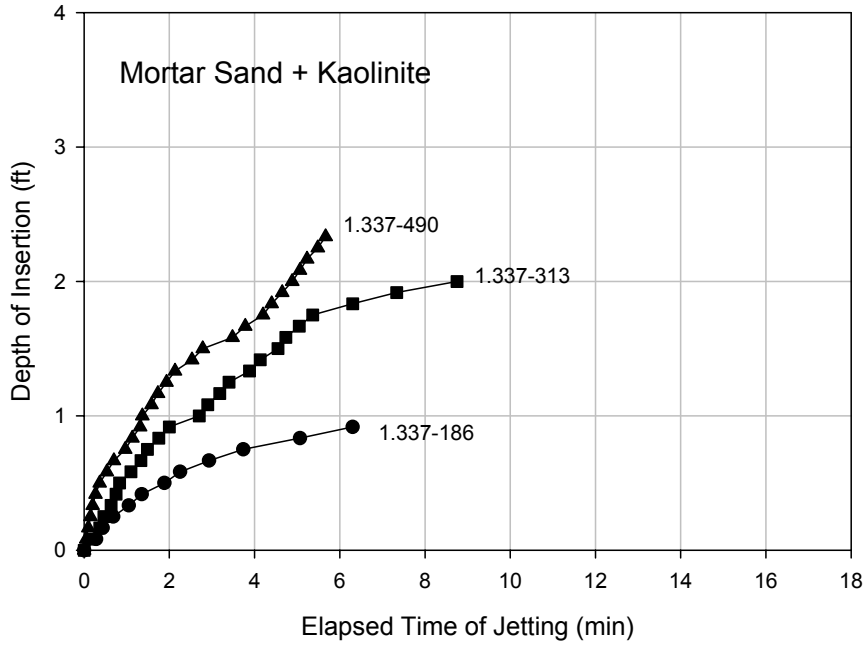

Figure 5.16 Depth of Insertion as a Function of Time for Various Water Flowrate and Jet Nozzle Velocity.

5.1.4 Insertion Characteristics – Angled Jets

As a form of practice modification, 45º angled jet nozzles were implemented into the jetting system to determine jet nozzle orientation effects on pile insertion characteristics. These tests were conducted in Mortar Sand specimens to compare the final depth of insertion and the insertion rates of the two jet nozzle orientations. The insertion characteristics for the angled jets are shown in Figure 5.17.

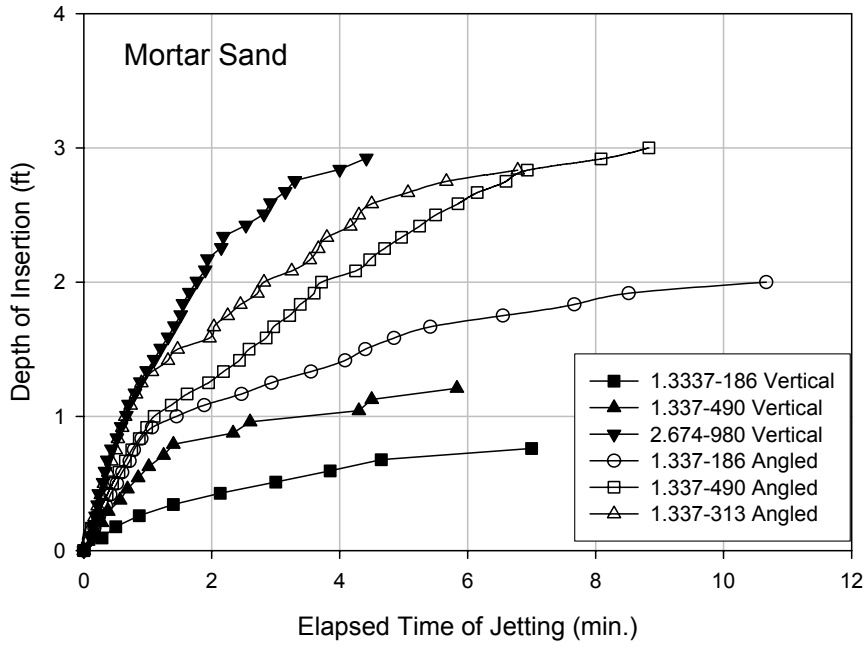

Figure 5.17 Depth of Insertion with Time for Various Water Flowrate and Jet Nozzle Velocity. (Angled and Vertical Jets)

Comparing insertion properties for equal jetting parameters in Mortar Sand in Figure 5.17, the angled jetting system provides greater depth of insertion and insertion rate capabilities. For example, for Q_w of 1.337 ft^3/min (0.038 m^3/min) and V_j of 490 ft/min (149 m/min), the vertical jets provide a depth of insertion at six minutes of 1.25 ft (0.38 m), whereas the angled jetting system provides a depth of insertion at six minutes of 2.75 ft (0.84 m). The angled jetting system allows for greater insertion depths and greater insertion rates for equal jetting parameters in a given soil type. Orienting the jet stream directly under the pile tip provides direct contact to the bearing soils by the jet water. Whereas, in vertically oriented jetting, the jet water flows parallel to the pile length. The jet stream erodes soil under the pile only after contact with soil directly beneath the jet and rebounding in all directions around the jet. The erosion efficiency of

the angled jets is greater due to the concentration of each water jet stream directly beneath the pile tip. The water jet streams effectively disperse all bearing soil particles beneath the pile tip. Insertion refusal for the angled jet system is therefore contributed to equilibrium of pile skin friction and buoyant weight of pile at the refusal depth.

5.1.5 Insertion Characteristics Summary

From the previous sections, it was shown that the insertion characteristics for a jetted pile depend on the water flowrate as well as the jet nozzle velocity for a given soil type. An important goal of the laboratory research was to conduct several jetting tests in different soil types and establish the relationships between the jetting parameters and jetted pile insertion properties. Figures 5.1 and 5.10 display important properties of pile insertion with variation of the jetting parameters. The behavior of jetted pile insertions in Mortar Sand with the addition of Kaolinite clay was also evaluated. Increased amounts of non-plastic fine particles in a soil profile seemed to increase allowable final depths of insertion and increase insertion rate for equal jetting parameters in similar soils with fewer fines. As a method of practice modification, angled jets were implemented into the jetting program to determine the affects of the jet nozzle orientation on the insertion properties of jetted piles. It is has been shown that orienting the jets 45º beneath the pile tip increases the final insertion depth and insertion rate for equal jetting parameters in a given soil profile.

The variation in pile insertion characteristics must also be attributed to the soil material properties. It is seen from Figures 5.1 and 5.10 that jetted piles in Concrete Sand behave significantly different than jetted piles in Cherry Branch Sand for equal jetting parameters. It is also recognized that physical and engineering properties of these soil

types vary greatly. In order to develop a model predicting the pile insertion characteristics, the regression parameters will be correlated to specific characteristics of the GSD curves. Therefore, like all geotechnical applications, thorough knowledge of underlying soils is critical in assuring an effective jetting program.

5.2 Debris Zone Characteristics

The debris zone characteristics rely on several variables. These include; water flow rate (Q_w), jet nozzle velocity (V_j), and penetration depth. However, it must be realized that penetration depth depends on both Q_w and V_j. Therefore, for a given insertion depth, there are many combinations of Q_w and V_j possible to achieve that depth. A key factor that must be recognized is the insertion rate and refusal depth variation due to changes in the jetting parameters. In order to determine the effects of pile insertion rate (IR) on the debris zone, full depth jetting tests as well as depth controlled tests were conducted. The depth control tests were used to compare the effects of insertion rate variation for a range of jetting parameters at a given depth.

5.2.1 Debris Volume Analysis – Full Tests

Upon termination of jetting, debris volumes (V_{debris}) were determined based on final survey of the specimen surface. These volumes were determined for each full test to establish the relationship between the total volume of pile jetted into the specimen and the quantity of material exiting the jetting annulus. The volume of pile jetted into the specimen was determined by multiplying the pile area (A_p) by the length of pile jetted from an initial datum reading. For each jetted pile insertion, the debris volume increased linearly with increasing jetted pile volume. In other words, for a given diameter pile, the

debris volume increases linearly with depth of insertion. This relationship held true for each soil type tested in the laboratory jetting program. As the pile moves further into the soil profile it is expected that debris volume exiting the annulus increases linearly with depth. These relationships are plotted with best-fit lines through the data for each soil type in Figure 5.18.

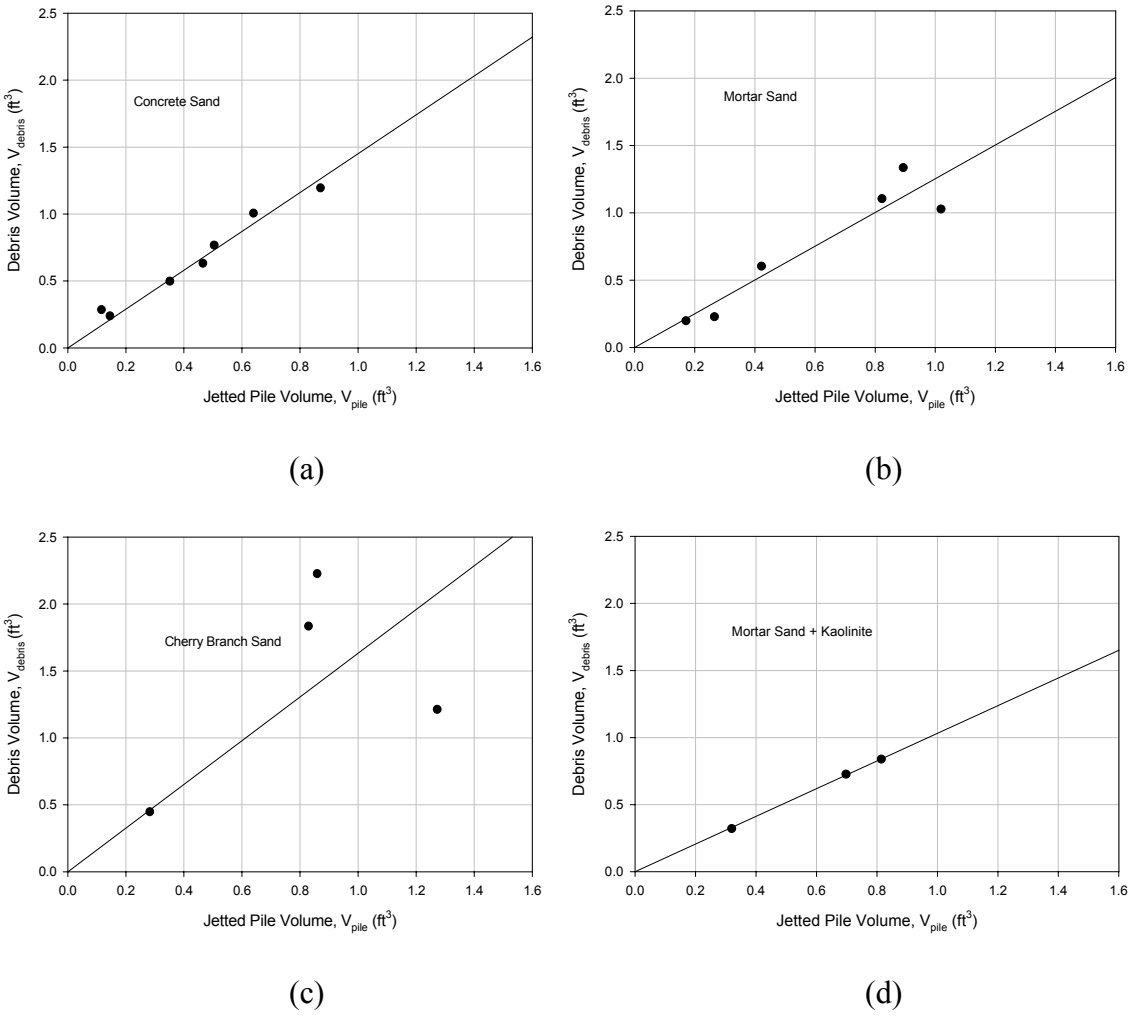

Figure 5.18 Debris Volume with Increase in Jetted Pile Volume

5.2.2 Debris Area Analysis – Full Depth Tests

Upon termination of jetting, debris areas (A_{debris}) were determined based on final survey of the specimen surface using the reference beam described in Chapter 4. These areas were determined for each full test to establish the relationship between the total volume of pile jetted into the specimen and the distribution of material from the annulus on the specimen surface. The debris areas calculated for each full depth test followed similar distribution with jetted pile volume as the debris volume quantities. The debris areas increased linearly with depth (increasing jetted pile volume) as shown in Figure 5.20.

(a) (b)

Figure 5.19 Comparison of Debris Areas in Concrete Sand at Various Insertion Depths

Figure 5.19 a & b displays the debris area distributions for a jetted pile in Concrete Sand to a depth of approximately 36 inches (0.91 m) and 14 inches (0.36 m) respectively. The variation in extent of the debris zone can easily be discerned from the two figures. The pile jetted to a greater depth within the soil profile (approx. 36 inches in Figure 5.19a) yields larger debris area and volume as compared to the same pile jetted to a lesser depth (approx. 16 inches in Figure 5.19b). This characteristic held true for all soil types tested

within the experimental program. However, it should be stated that the measuring system used in the experimental program was precise to 0.039 inches (1mm). Therefore, soil particles smaller than this value could not be distinguished. It is realized that smaller particles would travel further than the debris zones shown in Figure 5.19. However, due to the boundary constraints of the jetting setup, these extents were not determined.

The debris areas (A_{debris}) for each full depth test conducted on the various sand types are shown in Figure 5.20 with the exception of the Cherry Branch Sand.

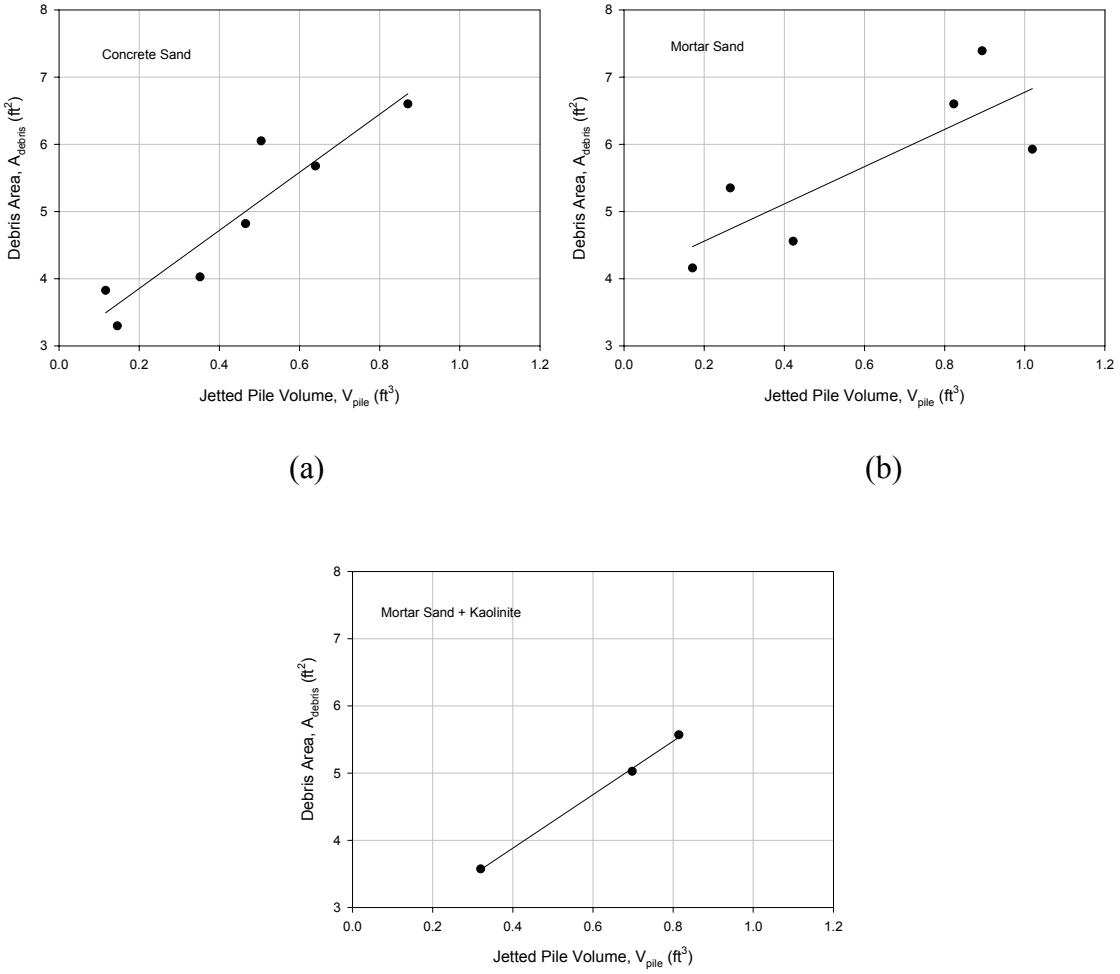

(a) (b)

(c)

Figure 5.20 Debris Area with Increase in Jetted Pile Volume

The ability to attain greater depths of insertion with lower values of Q_w and V_j for the Cherry Branch Sand as compared to the "larger" sand types has been presented. However, insertion rates for the Cherry Branch tests were lower at greater depths due to the low required jetting parameters as compared to high required jetting parameters needed to reach the same depth for the larger sand types. Therefore, greater quantities of water and larger time intervals were required for jetting piles in Cherry Branch Sand to refusal. Due to these characteristics, and the smaller size particles of the Cherry Branch Sand, debris areas could not be determined because of transport of soil particles over the specimen boundaries. The smaller particles were lifted from the jetting annulus and displaced over the boundaries by increasing volumes of water. The Cherry Branch Sand particles were easily transported great distances with the low jet nozzle velocities due to the relatively small size. This point is illustrated in Figure 5.21.

Figure 5.21 Immeasurable Debris Area Distribution for Cherry Branch Sand

5.2.3 Debris Zone Analysis - 45º Angled Jets – Full Tests

The debris zones associated with implementation of angled jets in pile jetting systems demonstrate similar attributes when compared to debris zones produced by jetting with vertical nozzle systems. For equal jetting parameters, the insertion rate and final depth of insertion for piles jetted with 45º angled jets are greater as compared to vertical jet nozzle insertions. When comparing the pile insertion depth with the debris zone characteristics, Figures 5.22 and 5.23 demonstrate that angled jets have negligible effect on the debris zone quantities from the vertical jet nozzle orientations. Therefore, it is believed that employing angled jets into jetting systems will benefit insertion characteristics and have little effect on the debris zone when compared to equal depth insertions with vertical jet orientations.

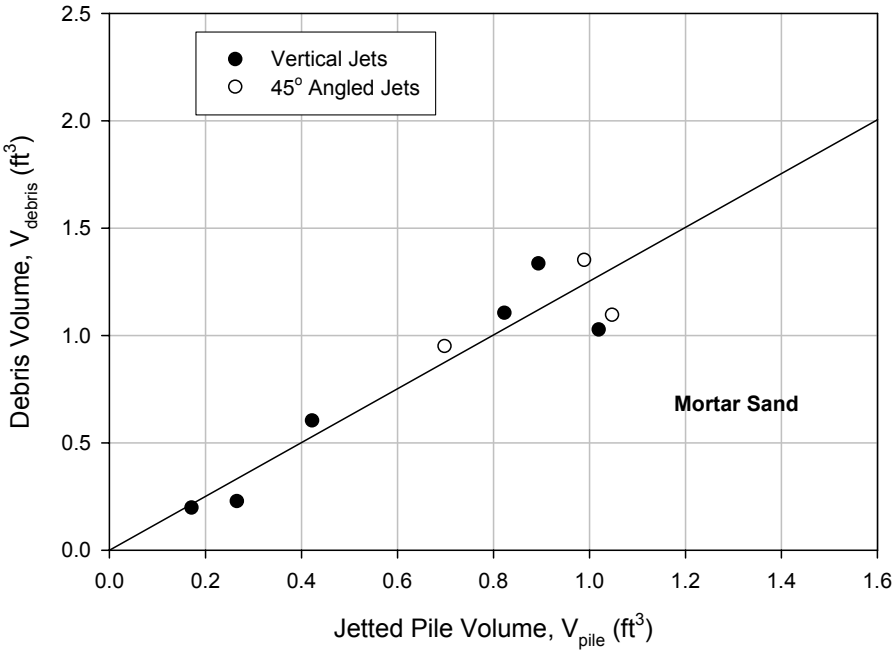

Figure 5.22 Comparison of Debris Zone Volumes Due to Various Nozzle Orientations

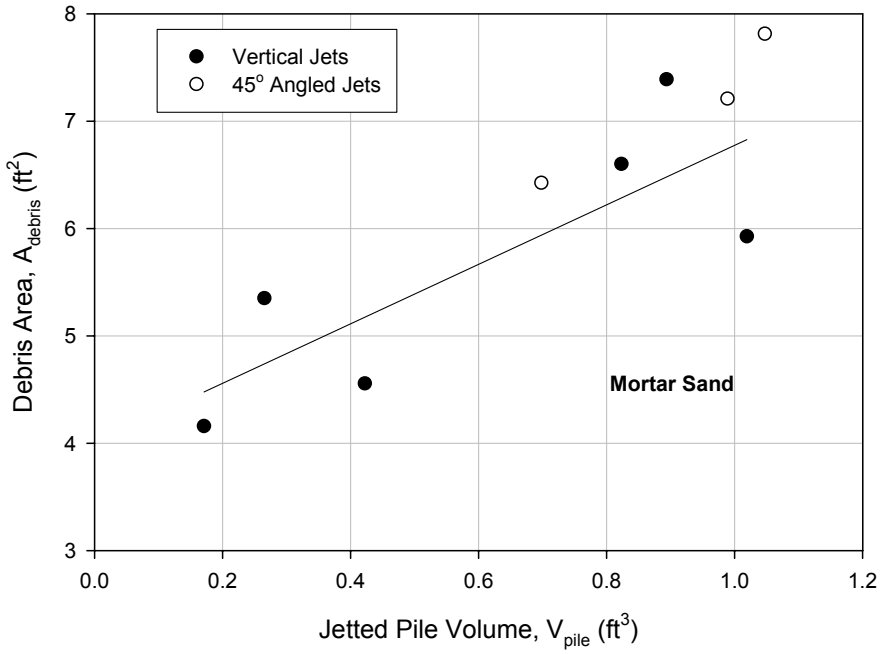

Figure 5.23 Comparison of Debris Zone Areas Due to Various Nozzle Orientations

5.2.4 Debris Zone Evaluation – Depth Control Tests

The relationship between final insertion depth and debris volume was developed in section 5.2.1. The debris volumes obtained from the full-depth tests are for a specified Q_w, V_j, and final depth of insertion based on these jetting parameters. However, from those tests, it is impossible to compare debris volumes and jetting parameters for equal depths of insertion. It was shown previously that the jetting parameters have a considerable effect on pile insertion rate for a given depth increment. In order to establish a relationship between debris zone and jetting parameters for a given insertion depth, "depth-controlled" tests were conducted. The test specimens were prepared consistently with full-depth test specimens presented earlier. A depth-control test consists of installing the test pile to a given depth with a variety of jetting parameters.

The cutoff depth was determined based on the insertion depth limit of tests conducted with the smallest values of Q_w and V_j. For all soil types, this cutoff depth was determined as one foot (0.30 m) of jetted pile in the profile. A series of tests were conducted in each soil type by increasing the water flowrate and jet nozzle velocity between tests. Upon initiation of jetting, the piles penetrated the specimen surface at various rates depending on the jetting parameters. Upon reaching the cutoff depth, jetting was stopped and the debris zone quantities were determined.

Depth-control tests were conducted primarily to determine the optimum jetting parameters for installing a pile in a given soil type. Optimum jetting parameters are defined as a combination of water flow rate and jet nozzle velocity allowing adequate pile insertion rate while generating the minimum debris volume and minimum debris area. For example, for a given soil type, it is desired that a pile be installed a given percentage of the total length by jetting. There are many combinations of Q_w and V_j that will sufficiently install the pile to the required depth. However, due to the insertion rate characteristics of the jetting parameter combinations, there will exist an optimum Q_w and V_j, that will minimize surface impacts. Impact minimization is a key responsibility of the research conducted in this experimental program while ensuring acceptable pile installation rates. The depth-control tests conducted in this program are used to develop a model for pile installations by extrapolating results of model testing to full-scale jetted pile installations. The tests provide a comparison between the jetting parameters and the associated debris zone characteristics of the various soil types at equal depths of pile insertion.

5.2.4.1 Debris Zone Analysis – Depth Control Tests

It was shown previously that for a given water flow rate, increases in jet nozzle velocity produce higher insertion rates at a given depth. With this point in mind, less water is needed to jet a given pile to a certain depth than required for an installation with a lower jet nozzle velocity. It may be inferred from Figure 5.24 and 5.27 that the total volume of water (V_{wtotal}) along with Q_w/Q_p at a given depth has a distinct effect on the debris volume (V_{debris}) and debris area (A_{debris}) surrounding jetted pile installations. Since Q_p depends on both jetting parameters, normalizing Q_w with Q_p takes into account V_j required to achieve the insertion depth. Therefore, to achieve greater insertion rates for a given Q_w at a specified depth, the Q_w/Q_p ratio must be minimized resulting in higher required values of V_j. In Figure 5.24, debris volume is normalized with total volume of water to provide a comparison between the jetting parameters and time required to jet a pile to the cutoff depth. For each data point in Figures 5.24 & 5.27 the total volume of water is dependent on pile insertion rate due to Q_w and V_j as seen in Figure 5.2.

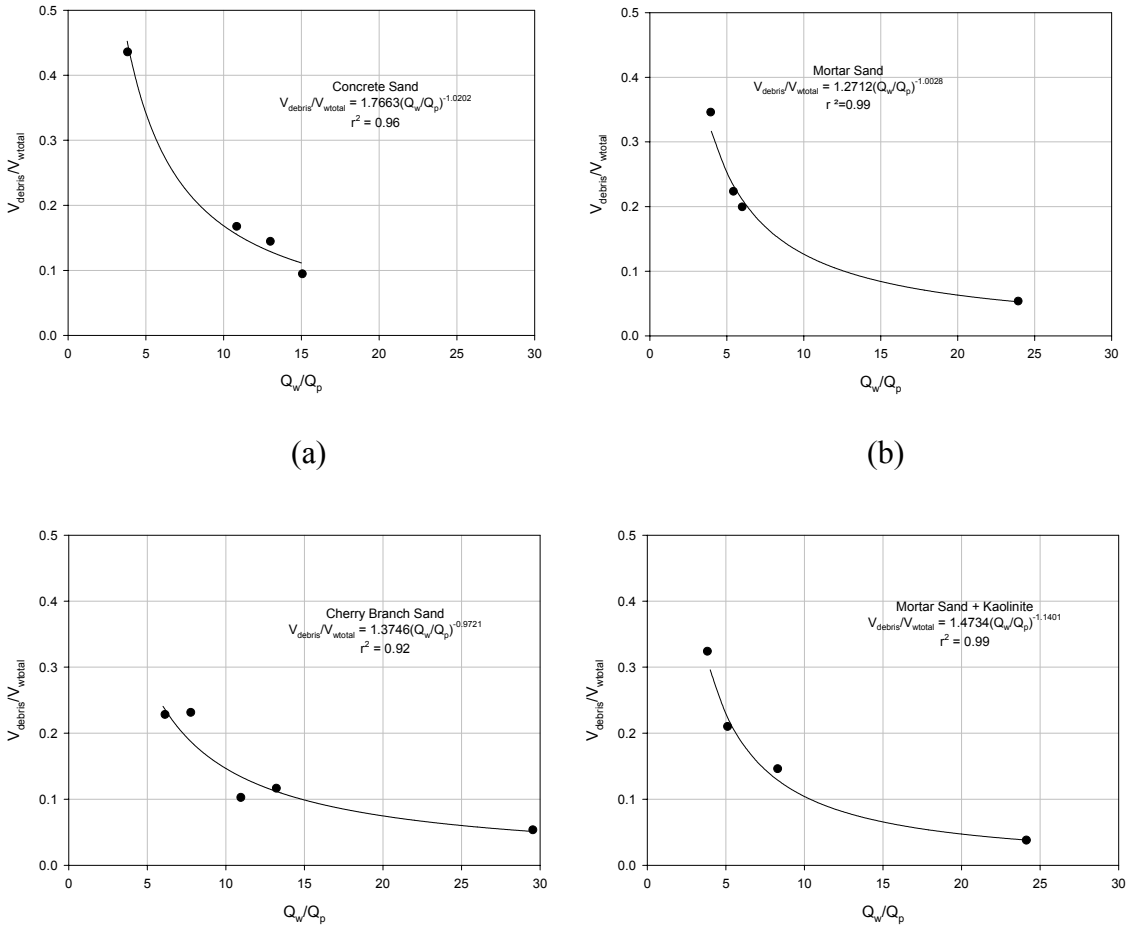

Figure 5.24 Correlations between Pile Insertion Rate and Debris Volume (Depth = 1.0 ft)

The debris volume for each soil type can be expressed by the following equation:

$$V_{debris} = V_{wtotal} \times a_{volume} \left(\frac{Q_w}{Q_p} \right)^{b_{volume}} \qquad \text{Eq. 5. 8}$$

where: V_{debris} = debris volume (L^3)
V_{wtotal} = total volume of jetted water (L^3)
a_{volume} = GSD dependent volume parameter
b_{volume} = d_{50} dependent volume parameter
Q_w = water volume flowrate (L^3/min)
Q_p = pile volume flowrate (L^3/min)

Comparing the regression parameters from Figure 5.24 for the natural soils, Figures 5.25 & 5.26 provide the dependency of debris volume characteristics on GSD and jetting parameters for given tests. The curves presented in Figure 5.24 demonstrate the variability in debris volume characteristics of soils due to variation in jetting parameters. Therefore, the debris volume quantities are affected by the pile insertion rate through the soil stratum. Variations between particle size and gradation curve characteristics of the different soils contribute to dissimilar debris zone quantities when similar jetting parameters are invoked for pile jetting.

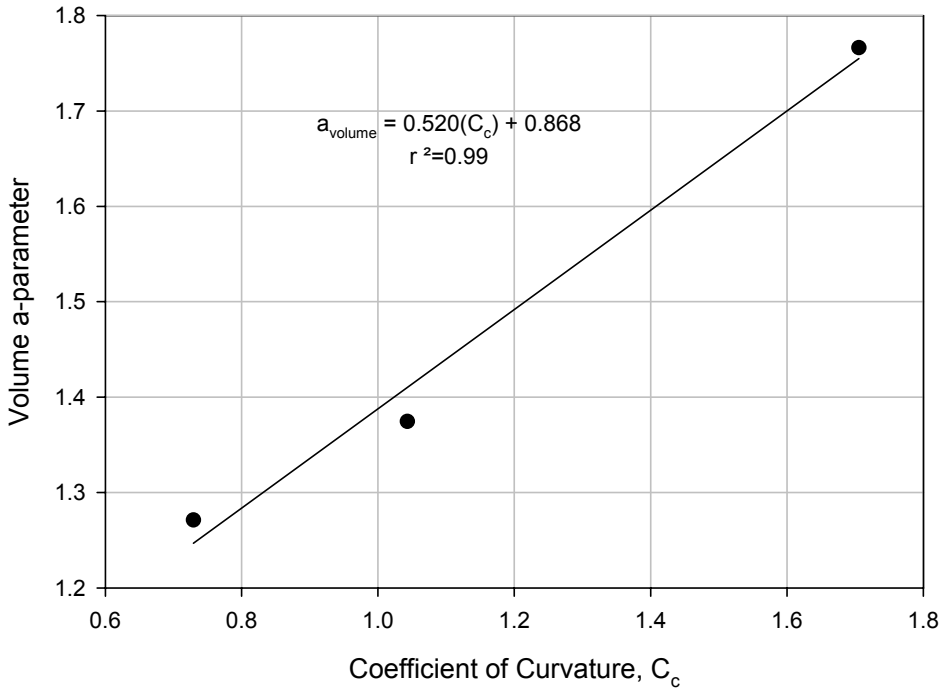

Figure 5.25 Volume a-parameter due to C_c

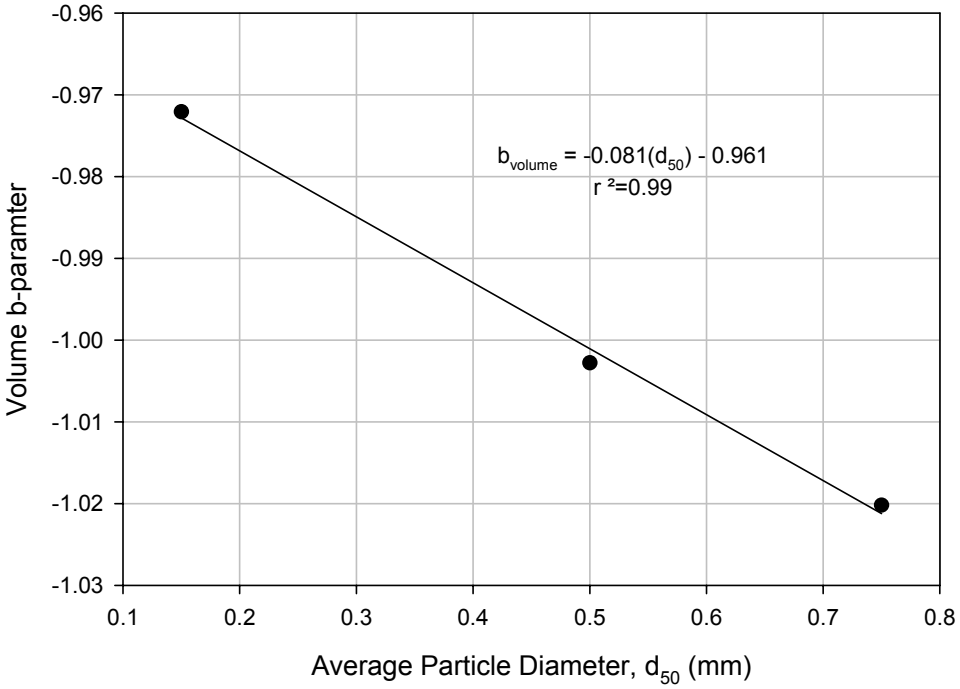

Figure 5.26 Volume b-parameter due to d_{50}

The debris area stemming from a jetted pile installation depends on the jetting parameters affect on the pile insertion rate and the total volume of water required to insert the pile. In Figure 5.27, the debris area is multiplied by the pile diameter (D_p) and normalized with the total volume of water. This normalization was used to develop the relationship between the pile diameter and the total volume of water necessary to jet the pile to the cutoff depth.

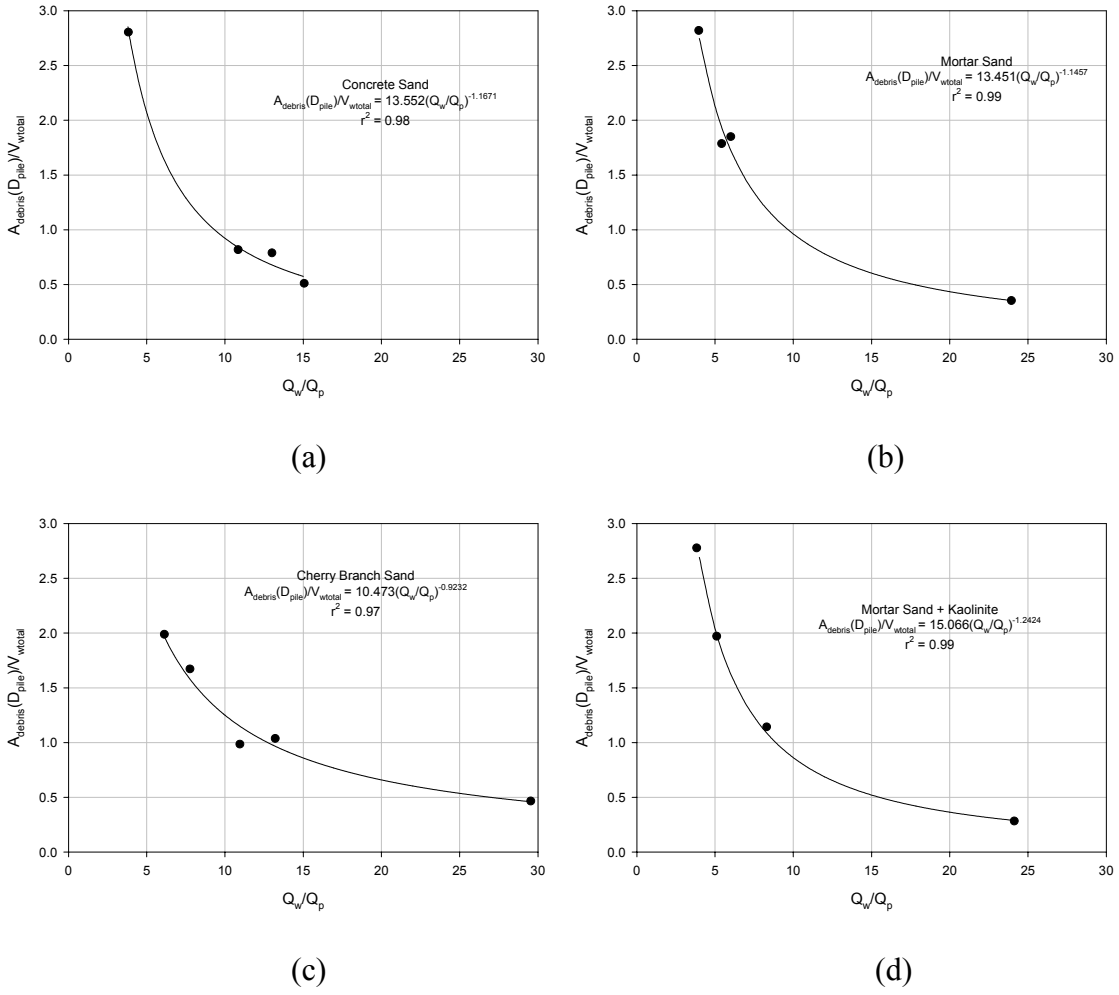

Figure 5.27 Correlations between Pile Insertion Rate and Debris Area (Depth = 1.0 ft)

The debris area for each soil type can be expressed by the following equation:

$$A_{debris} = \left(\frac{V_{wtotal}}{D_{pile}}\right) \times a_{area} \left(\frac{Q_w}{Q_p}\right)^{b_{area}} \qquad \text{Eq. 5. 9}$$

where: A_{debris} = debris area (L^2)
V_{wtotal} = total volume of jetted water (L^3)
D_{pile} = pile diameter (L)
a_{area} = GSD dependent area parameter
b_{area} = d_{50} dependent area parameter
Q_w = water volume flowrate (L^3/min)
Q_p = pile volume flowrate (L^3/min)

Comparing the regression parameters from Figure 5.27 for the natural soils, Figures 5.28 & 5.29 provide the dependency of debris area on GSD characteristics and jetting parameters. The curves presented in Figure 5.27 demonstrate the variability in debris area characteristics between the soils due to the effect of the jetting. The debris areas are affected by the pile insertion rate through the soil stratum. Variations in particle size and gradation curves of the different soils contribute to dissimilar debris areas when similar jetting parameters are implemented for pile jetting.

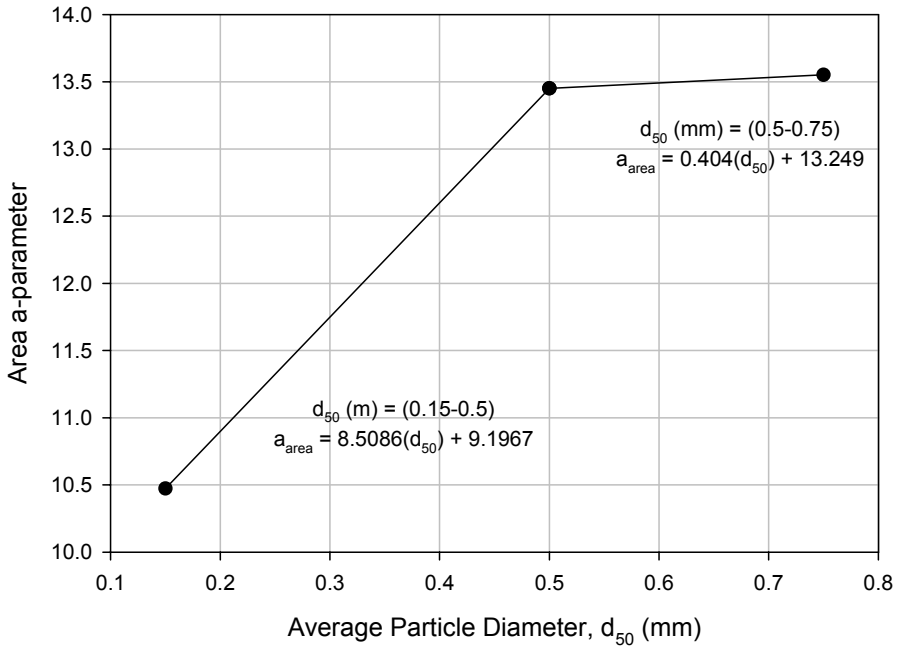

Figure 5.28 Area a-parameter with d_{50}

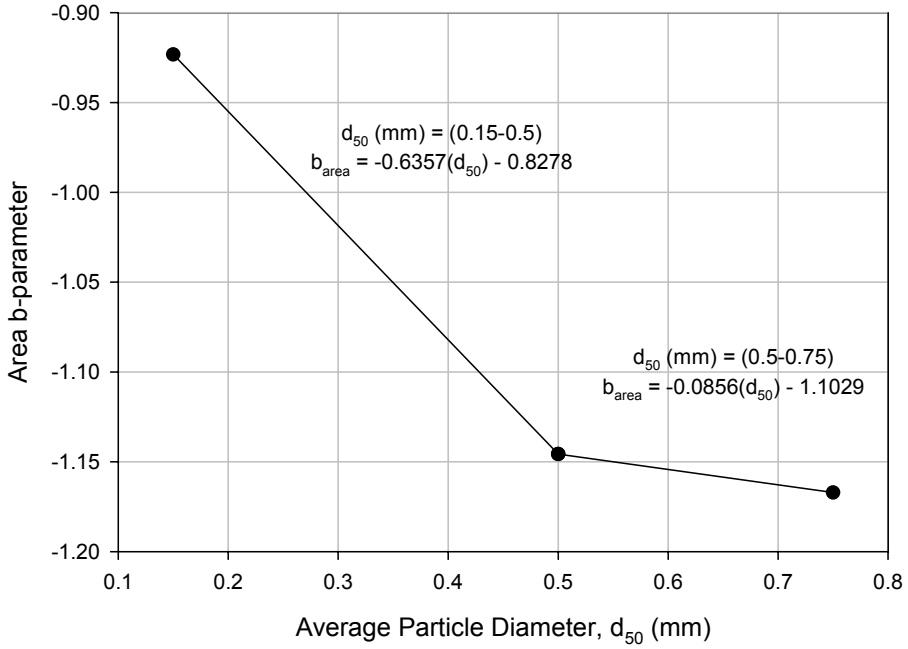

Figure 5.29 Area b-parameter with d_{50}

5.2.5 Summary of Debris Zone Analysis

The relationships between pile insertion depth and debris zone quantities (V_{debris} and A_{debris}) were developed in the previous sections (5.2.1 and 5.2.2). The debris volume transported from the jetting annulus increases with the depth of the pile insertion as shown in Figures 5.18. The debris area in which soil particles removed from the jetting annulus are displaced around the specimen surface also increases with the depth of pile insertion (Figure 5.20). However, since refusal depths for jetted piles varied with changes in jetting parameters, comparisons of the debris zone characteristics with pile insertion rates for given depths could not be presented from the full-depth tests. Therefore, a series of depth-control tests were undertaken to provide insight on varying jetting parameters for piles installed at equal depths in the different soil profiles.

The depth–controlled tests provide useful information on the debris zone characteristics due to the jetting parameters. It is shown in Figures 5.24 & 5.27 that comparison between Q_p and V_{wtotal} follows a power relationship dependent upon Q_w and V_j. For a given Q_w, higher V_j produces higher Q_p at a specific depth, requiring a lower V_{wtotal} than tests with lower V_j at the same depth and Q_w. For a given Q_w, increased V_j (thus increased Q_p) requires less V_{wtotal}. Therefore, V_{debris} and A_{debris} at a specified depth decrease with decreased V_{wtotal}. Since Q_p is dependent on Q_w and V_j, for a given depth, the minimum Q_w and highest V_j will produce minimum debris zone effects. Thus, the minimum Q_w and highest V_j enabling the pile to penetrate to the design depth are the optimum jetting parameters.

CHAPTER 6 - MODEL DEVELOPMENT

The primary goal of this research was to quantify the zone of disturbance due to pile installations using jetting applications. After conducting several laboratory tests and data analysis, the influence on surface disturbance due to the jetting parameters and soil type was quantified. The experimental program undertaken in this research allows for development of a universal model for large-scale jetted pile installations. The model encompasses both pile insertion rate and debris zone attributes. To provide a relationship between jetted pile characteristics and jetting parameters, it is necessary to model the laboratory pile insertions with dimensionless parameters. This method of dimensional analysis is founded on the Buckingham Pi Theorem. The Buckingham Pi Theorem provides a functional relationship between all dimensionless parameters (pi terms) applicable to the problem. Dimensional analysis provides a systematic approach to determine the effects on test results by variation of original variables in the problem. This method of analysis was implemented to provide an understanding of jetting parameter effects in jetted pile insertions.

6.1 Pile Insertion Rate – Vertical Jets

The effects of jetting parameters on pile insertion rates (IR) with depth were not provided in previous literature on pile jetting. In this study, water flowrate and jet nozzle velocity were seen to have significant effects on pile insertion characteristics. The jetting parameters effect on IR also varied among the four soil types evaluated in the laboratory experimental program. These relationships were developed in the previous chapter.

.

To develop a universal model for jetted pile installations, dimensional analysis allows the user freedom of employing various pile dimensions, soil types, and jetting system configurations. The model presented herein is based on a series of laboratory tests conducted on an eight inch (200 mm) diameter, eight feet (2.44 m) long circular concrete pile. The jetting water flowrates (Q_w) used in the laboratory testing program were normalized with pile volume insertion rates (Q_p). The relationship between jet nozzle velocity (V_j) and Q_w are linearly related and thus dually influence Q_p. Therefore, the model must encompass the ability to vary both Q_w and V_j for jetted pile installations.

Due to the various shapes, sizes, and material types of foundation piles, dimensionless parameters are provided normalizing pile bearing pressure (q_{app}) with vertical effective stress (q_{app}/σ'_v). The vertical effective stress increases linearly with depth and buoyant unit weight of soil yielding increases in tip and side bearing resistance in uniform sand profiles. The effects of increasing capacity, with depth, on the insertion rates and refusal depths of jetted piles have been demonstrated. The bearing pressure of a pile decreases with depth in a saturated soil profile due to the buoyant unit weight of pile in the stratum. Bearing capacity increase, coupled with decreasing bearing pressure reduces the efficiency of jetting with depth. The q_{app}/σ'_v ratio decreases with depth due to the maximum bearing pressure at the ground surface and minimum vertical effective stress at that point. Therefore, for constant jetting parameters, pile insertion rates near the ground surface will be at a maximum due to the elevated pile bearing pressure and minimal bearing resistance. This attribute is confirmed in the q_{app}/σ'_v distribution with depth for a saturated soil profile given in Figure 6.1. Since all tests in this experimental

program were conducted at equal relative densities, the insertion rate comparisons between soil types are justified at given values of q_{app}/σ'_v.

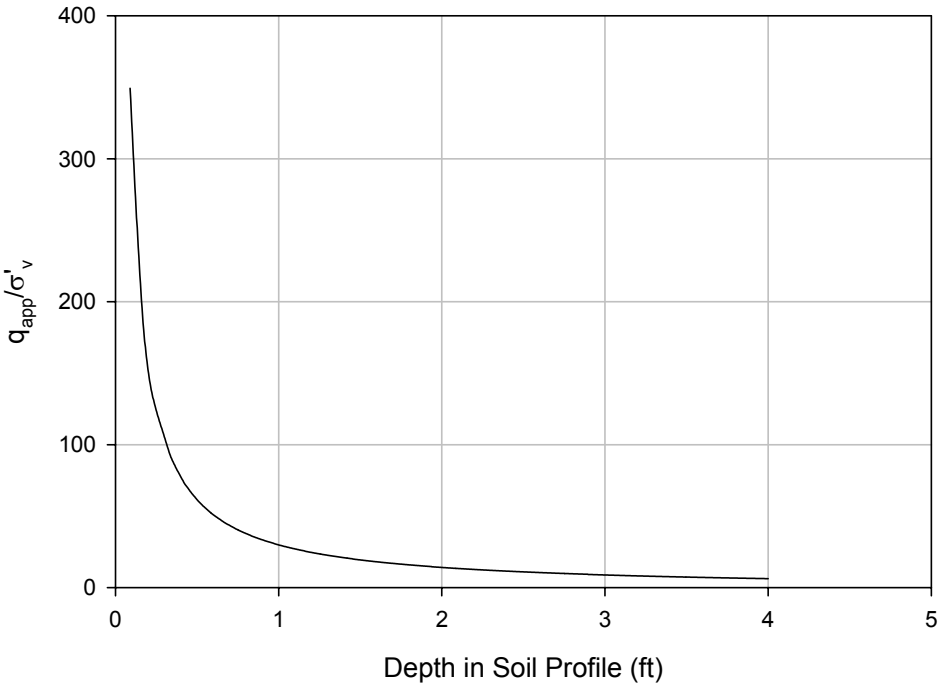

Figure 6.1 Relationship between Bearing Pressure and Vertical Effective Stress with Increasing Depth in a Saturated Soil Profile

For all soil types evaluated in the laboratory testing program, Q_w/Q_p ratios were plotted as a function of V_j at equal values of q_{app}/σ'_v providing relationships between various soil properties and insertion rate characteristics. Figures 6.2-6.4 provide these insertion relationships for the laboratory soil types.

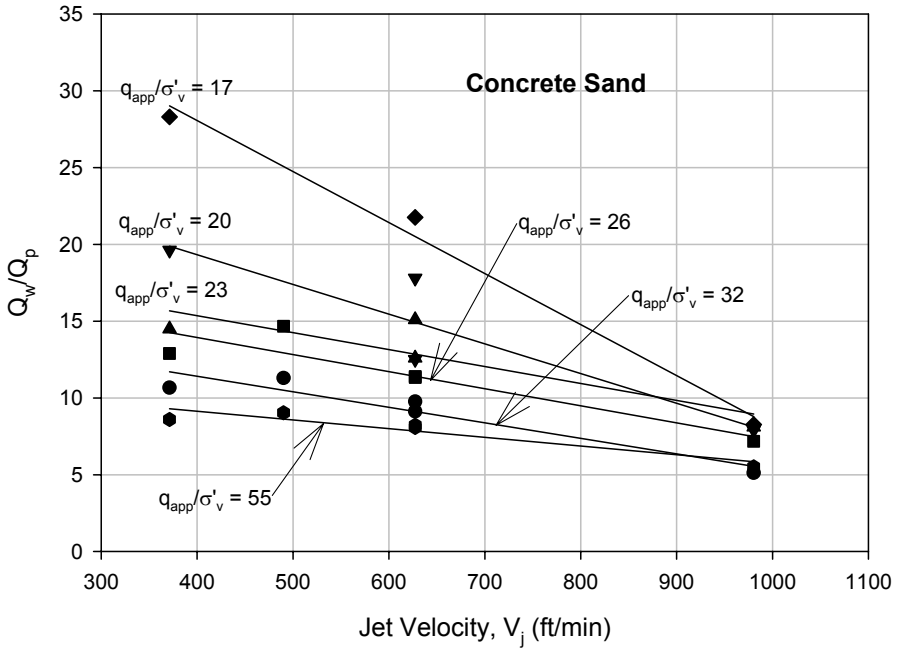

Figure 6.2 Q_w/Q_p Relation with V_j at Increments of q_{app}/σ'_v

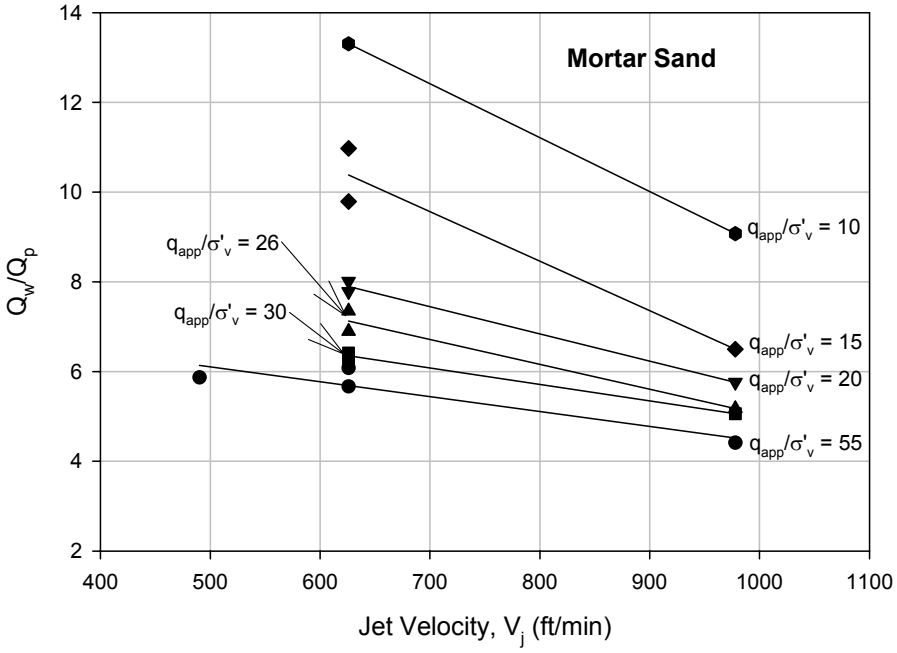

Figure 6.3 Q_w/Q_p Relation with V_j at Increments of q_{app}/σ'_v

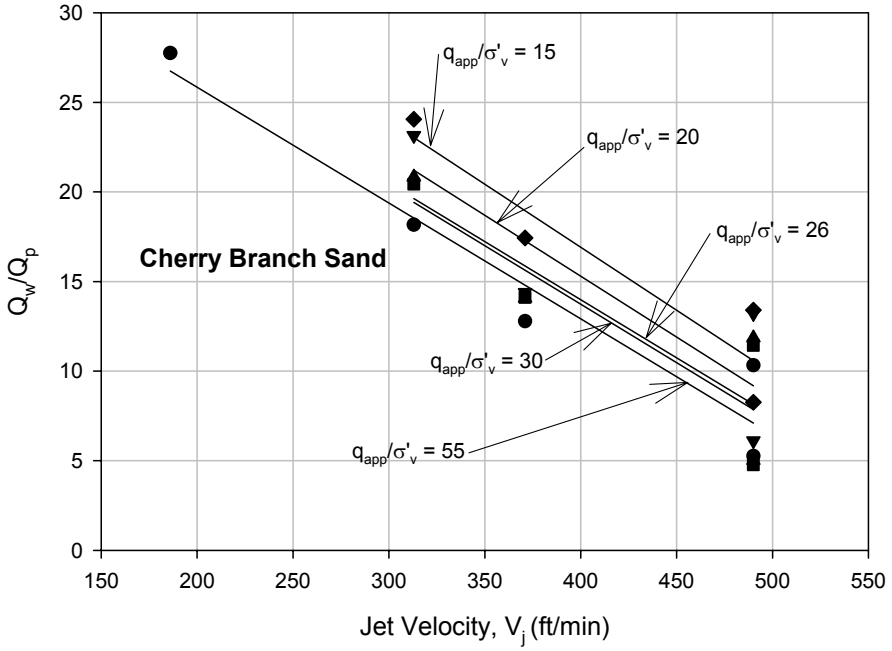

Figure 6.4 Q_w/Q_p Relation with V_j at Increments of q_{app}/σ'_v

It should be noticed from Figures 6.2-6.4 that for each soil tested in the jetting program, there exists a linear relationship between Q_p and the jetting parameters with q_{app}/σ'_v. Q_p decreases with decreasing q_{app}/σ'_v (increasing depth) for constant jetting parameters contributing to an increase in Q_w/Q_p with decreasing q_{app}/σ'_v. These Q_w/Q_p ratios were determined at q_{app}/σ'_v providing relationships between insertion characteristics and the jetting parameters for each soil type. For each soil type displayed in Figures 6.2-6.4, the pile volume flow rate is linearly dependent on Q_w and V_j for a given q_{app}/σ'_v increment. The relationships are defined by a specific slope and intercept of the regression line through all the data points for a given q_{app}/σ'_v increment. The regression properties relating Q_p at depth for given Q_w and Vj for all soil types are given in Table 6.1.

Table 6.1 Regression Coefficients for all Soil Types in Figures 6.2-6.4

Concrete Sand				Mortar Sand			
q_{app}/σ'_v	Slope (m_0)	Intercept (b_0)	R^2	q_{app}/σ'_v	Slope (m_0)	Intercept (b_0)	R^2
55	-0.0057	11.3948	0.87	55	-0.0033	7.7672	0.86
32	-0.0101	15.4363	0.90	30	-0.0037	8.6516	0.99
23	-0.0110	19.7600	0.76	26	-0.0055	10.5922	0.96
20	-0.0194	27.0658	0.83	20	-0.0061	11.6891	0.99
17	-0.0332	41.3506	0.99	15	-0.0110	17.2859	0.93
				10	-0.0120	20.8291	-

Cherry Branch Sand			
q_{app}/σ'_v	Slope (m_0)	Intercept (b_0)	R^2
55	-0.0646	38.7200	0.94
30	-0.0653	39.8741	0.80
26	-0.0649	39.9465	0.79
20	-0.0679	42.4747	0.74
15	-0.0703	45.0480	0.82

From Figures 6.2-6.4, pile volume flow rate (Q_p) is related to Q_w and V_j by the following general equation:

$$Q_p = \frac{Q_w}{m_0(V_j) + b_0} \qquad \text{Eq. 6. 1}$$

where: Q_p = pile volume flowrate (L^3/T)
Q_w = water volume flowrate (L^3/T)
V_j = jet nozzle velocity (L/T)
m_0 = q_{app}/σ'_v dependent slope parameter $(L/T)^{-1}$
b_0 = q_{app}/σ'_v dependent intercept parameter

Plotting the regression coefficients with q_{app}/σ'_v, the insertion rate properties of a jetted pile with any dimensions can be determined for comparable soil types tested in the laboratory experimental program. These relationships are shown in Figures 6.5-6.10.

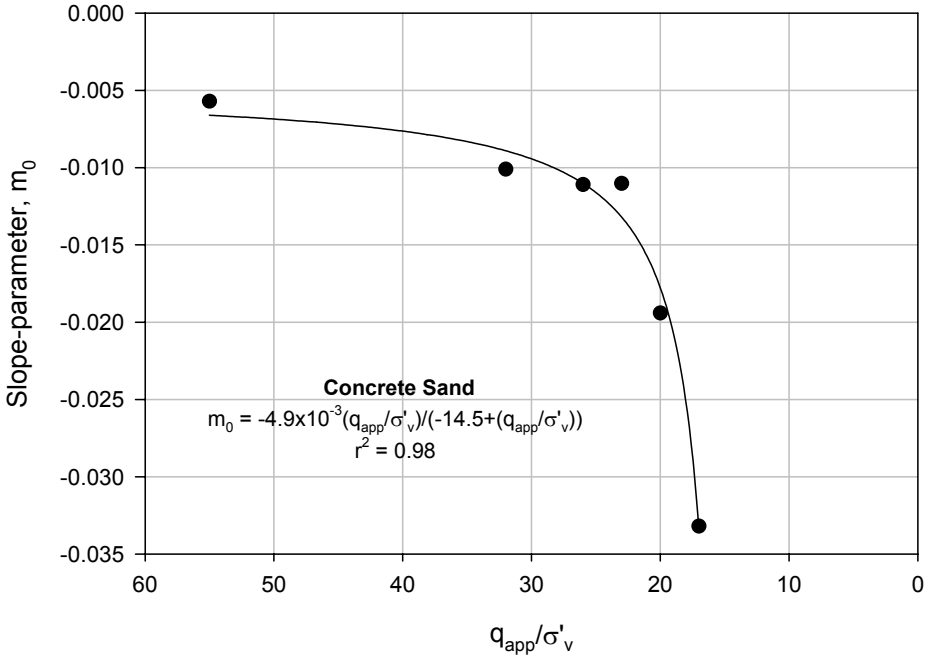

Figure 6.5 Slope-parameter, m_0 due to q_{app}/σ'_v (Concrete Sand)

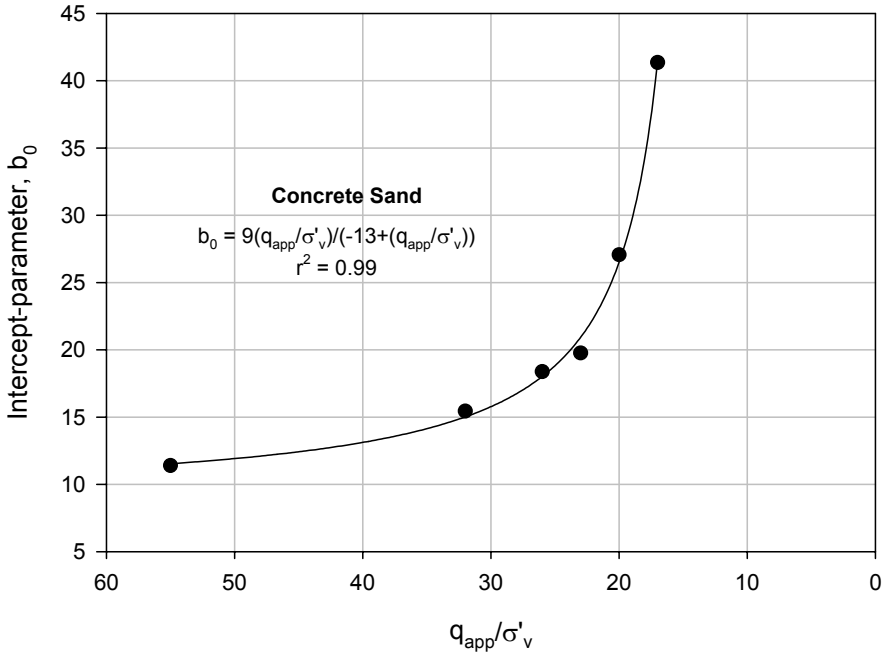

Figure 6.6 Intercept-parameter, b_0 due to q_{app}/σ'_v (Concrete Sand)

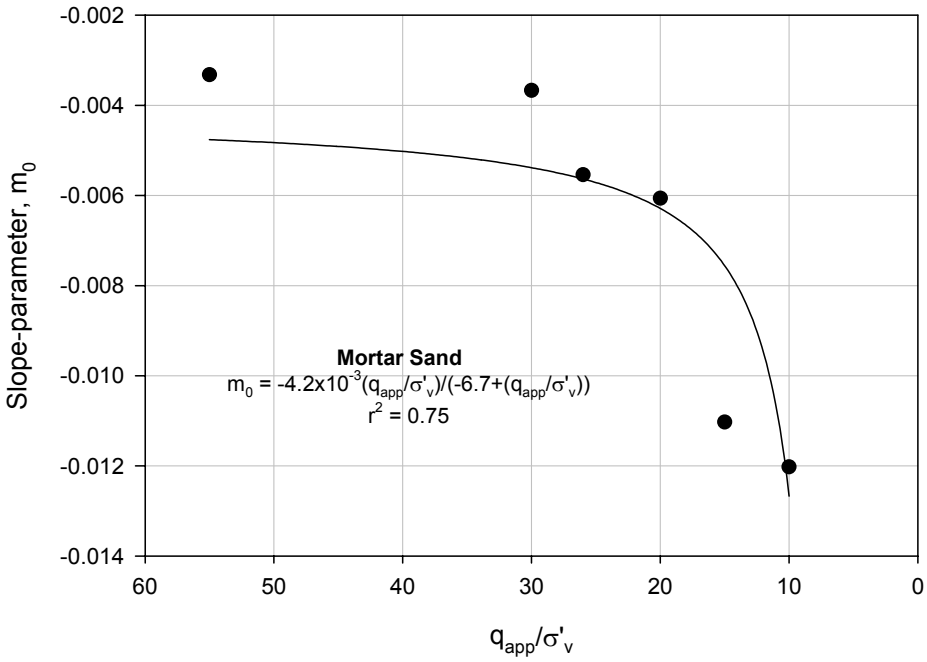

Figure 6.7 Slope-parameter, m_0 due to q_{app}/σ'_v (Mortar Sand)

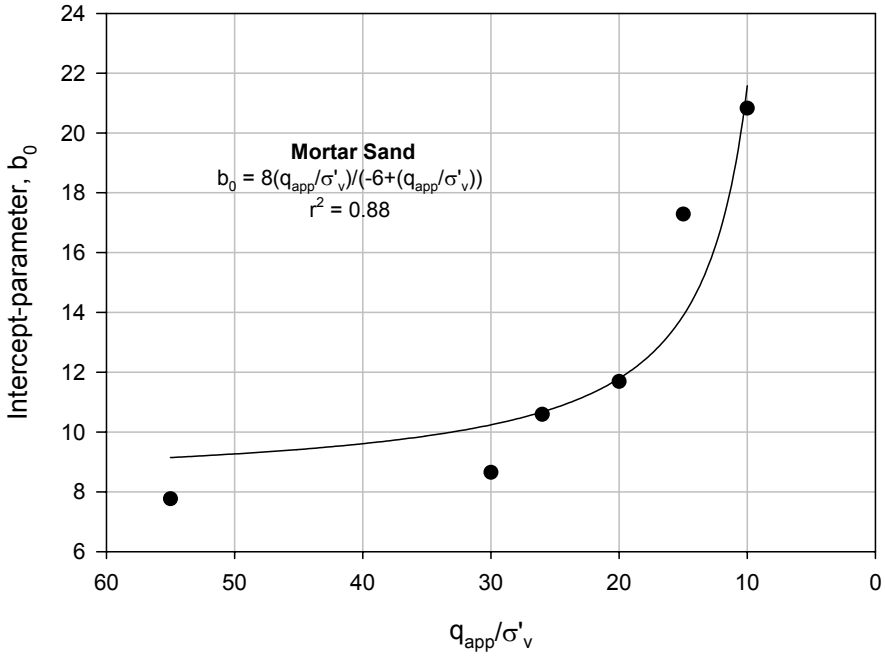

Figure 6.8 Intercept-parameter, b_0 due to q_{app}/σ'_v (Mortar Sand)

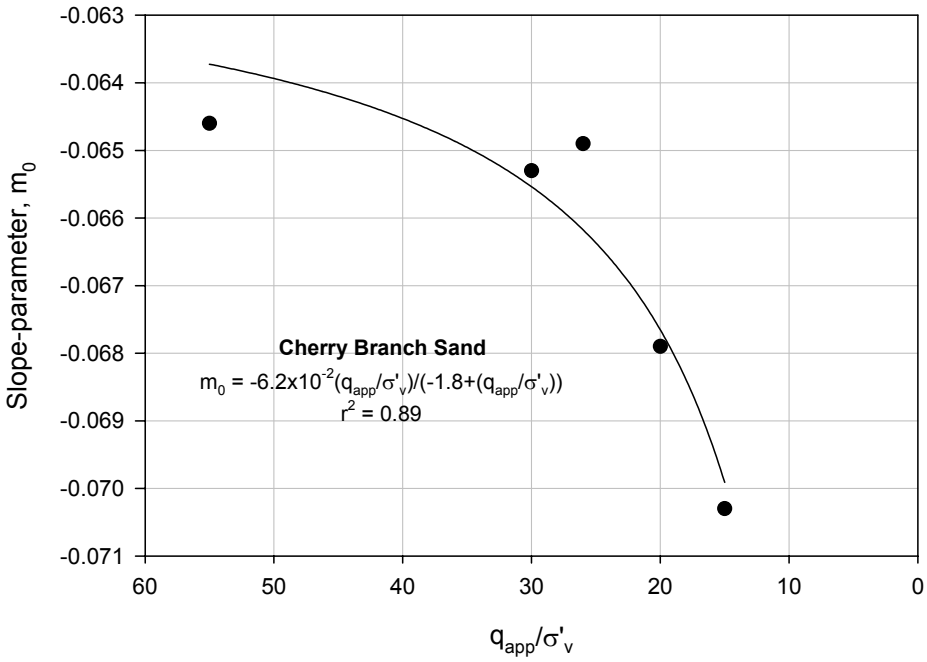

Figure 6.9 Slope-parameter, m_0 due to q_{app}/σ'_v (Cherry Branch Sand)

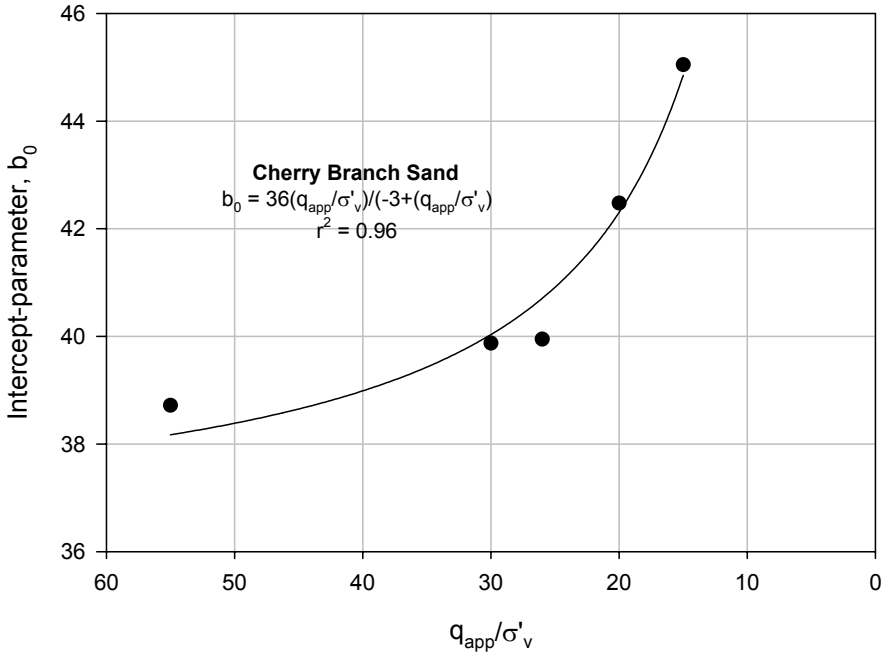

Figure 6.10 Intercept-parameter, b_0 due to q_{app}/σ'_v (Cherry Branch Sand)

As shown in Figures 6.5-6.10, the regression parameters for Q_w/Q_p due to V_j are not continuously linear with q_{app}/σ'_v. This is due to the distribution of q_{app}/σ'_v with depth as seen in Figure 6.1. The slope (m_0) and intercept (b_0) parameters are governed by the pile insertion characteristics. The pile insertion characteristics are intern governed by the q_{app}/σ'_v ratio and jetting parameters for a given soil type. Since the q_{app}/σ'_v variation with depth is nonlinear as presented in Figure 6.1, the pile insertion properties from the ground surface (higher q_{app}/σ'_v) to greater depths (lower q_{app}/σ'_v) are not expected to be linear with constant jetting parameters. Near the ground surface, insertion rates are high upon initiation of jetting due to the small required erosion area to cause bearing capacity failure and short transport distance of soil particles from beneath the pile tip to the specimen surface. Also, when the water jets are near the ground surface, the effective area of disturbed soil encompasses the entire perimeter of the pile, eliminating all side friction. The maximum bearing pressure at this point coupled with minimum bearing capacity and side friction produce high insertion rates in the upper profile. The high insertion rates consistent with this process occur at q_{app}/σ'_v ratios from infinity to approximately 30 for the soils tested in this research. As pile insertion depth increases, tip bearing capacity and side friction increase. Therefore, greater quantities of soil must be removed from the pile tip and the perimeter of the pile to allow insertion. The increase in required soil erosion coincides with increased time intervals yielding slower pile insertion rates. The decreasing insertion rates consistent with this process occur at q_{app}/σ'_v ratios from approximately 30 to 15 for the soils tested in this research. Therefore, the sudden change in the insertion properties as seen in Figures 6.5-6.10 at these q_{app}/σ'_v values seem reasonable. With these characteristics in mind, hyperbolic

functions were used to develop the relationships between pile insertion characteristics and soil properties for the range of q_{app}/σ'_v reached in the laboratory jetting experimentation. These relationships are modeled with a single rectangular, two-parameter hyperbolic function of the form:

$$m_0 = \frac{a\left(\frac{q_{app}}{\sigma'_v}\right)}{b + \left(\frac{q_{app}}{\sigma'_v}\right)} \qquad \text{Eq. 6. 2}$$

where: m_0 = depth dependent slope parameter for specified soil type
q_{app}/σ'_v = bearing pressure-effective stress ratio
a = hyperbolic regression slope-parameter
b = hyperbolic regression slope-parameter

$$b_0 = \frac{c\left(\frac{q_{app}}{\sigma'_v}\right)}{d + \left(\frac{q_{app}}{\sigma'_v}\right)} \qquad \text{Eq. 6. 3}$$

where: b_0 = depth dependent slope parameter for specified soil type
q_{app}/σ'_v = bearing pressure-effective stress ratio
c = hyperbolic regression intercept-parameter
d = hyperbolic regression intercept-parameter

For these soil types, the pile volume flowrate due to the jetting parameters at any depth increment can be described by the following equation:

$$Q_p = \frac{Q_w}{\frac{a\left(\frac{q_{app}}{\sigma'_v}\right)}{b + \left(\frac{q_{app}}{\sigma'_v}\right)}(V_j) + \frac{c\left(\frac{q_{app}}{\sigma'_v}\right)}{d + \left(\frac{q_{app}}{\sigma'_v}\right)}} \qquad \text{Eq. 6. 4}$$

where: Q_p = pile volume flowrate (L^3/T)
Q_w = water volume flowrate (L^3/T)
V_j = jet nozzle velocity (L/T)
q_{app}/σ'_v = bearing pressure-effective stress ratio
a = hyperbolic regression slope-parameter
b = hyperbolic regression slope-parameter
c = hyperbolic regression intercept-parameter
d = hyperbolic regression intercept-parameter

In order to develop a universal model for jetted pile installations in natural soils, the dependency of the slope and intercept factors on the soil properties were developed. As seen previously in Figures 6.5-6.10, these slope and intercept factors vary with soil type and q_{app}/σ'_v ratio. The slope and intercept parameters for m_0 and b_0 were compared between all soil types for equal ranges of q_{app}/σ'_v to establish design charts for the proposed model.

Figures 6.11 through 6.14 provide the relationship between m_0 and b_0 hyperbolic regression parameters with soil properties for the soil types presented.

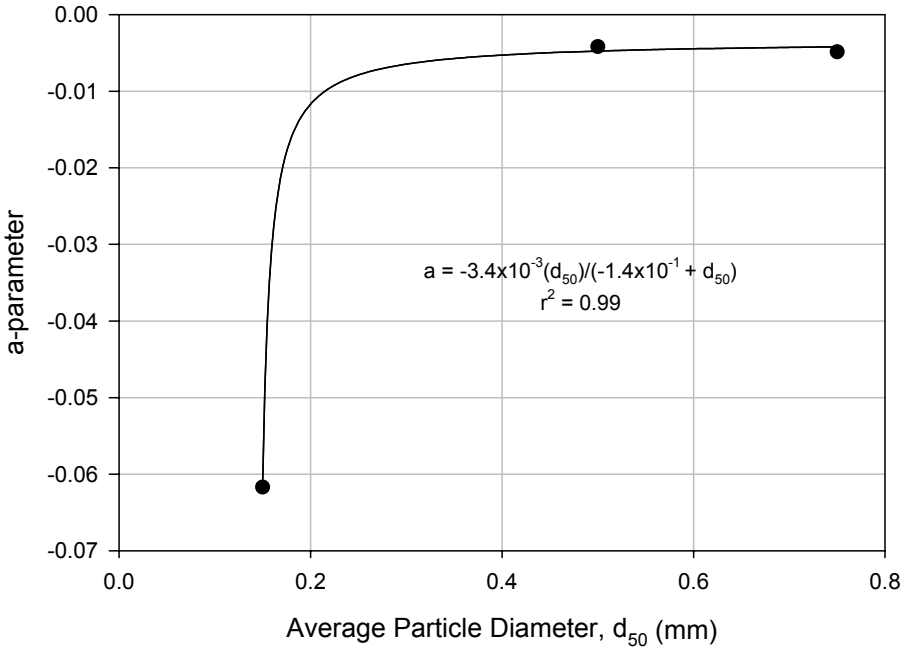

Figure 6.11 m_0 (a-parameter) relation to d_{50}

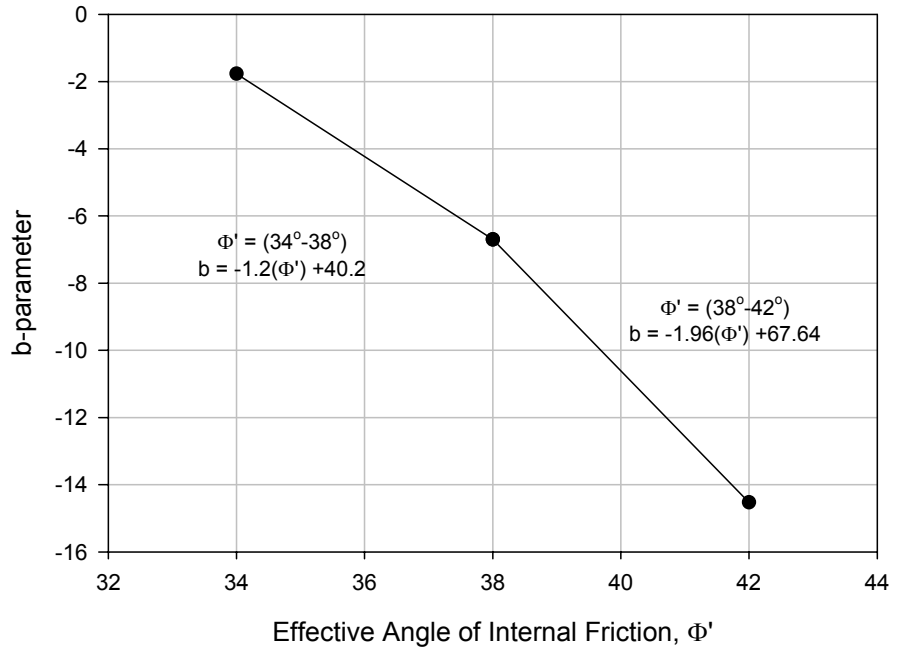

Figure 6.12 m_0 (b-parameter) relation to Φ'

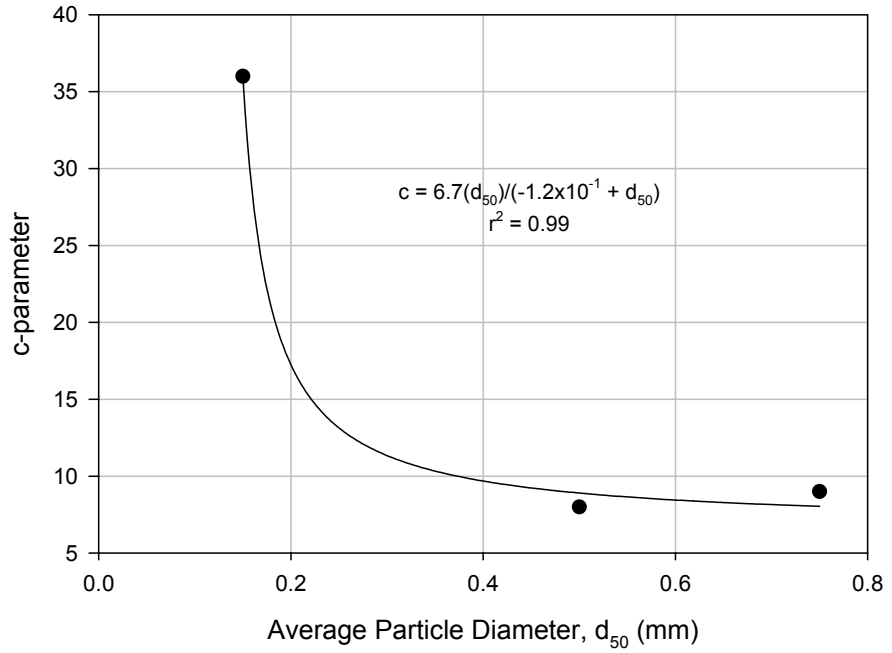

Figure 6.13 b_0 (c-parameter) relation to d_{50}

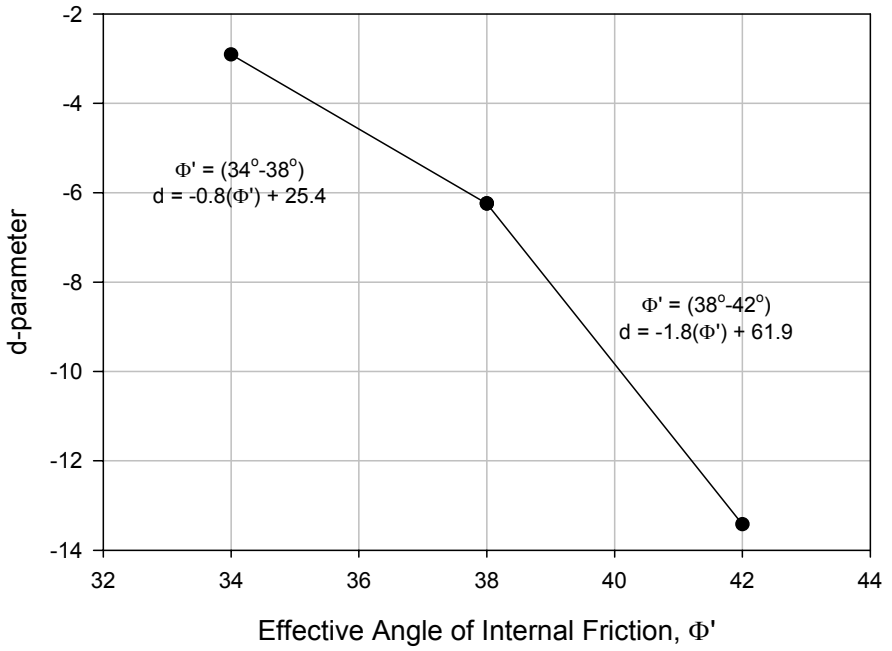

Figure 6.14 b_0 (d-parameter) relation to Φ'

In order to determine Q_p for any value of q_{app}/σ'_v (depth due to given pile dimensions) one must use Figures 6.11 through 6.14 to establish the relationship between soil properties and the jetting parameters invoked. Therefore, the following equations are suggested to determine insertion rates of jetted piles at given depths.

$$a = \frac{-3.4\times10^{-3}\left(d_{50}\right)}{-1.4\times10^{-1}+d_{50}} \qquad \text{Eq. 6. 5}$$

where: a = hyperbolic regression slope-parameter
d_{50} = average particle diameter (mm) *(inches to mm multiply by 25.4)*

For $34^o < \Phi' < 38^o$

$$b = -1.2\left(\varphi'\right)+40.22 \qquad \text{Eq. 6. 6}$$

For $38^o < \Phi' < 42^o$

$$b = -2\left(\varphi'\right)+67.6 \qquad \text{Eq. 6. 7}$$

where: b= hyperbolic regression slope-parameter
Φ' = effective angle of internal friction

$$c = \frac{6.7\left(d_{50}\right)}{-1.2\times10^{-1}+d_{50}} \qquad \text{Eq. 6. 8}$$

where: c = hyperbolic regression intercept-parameter
d_{50} = average particle diameter (mm) *(inches to mm multiply by 25.4)*

For $34^o < \Phi' < 38^o$

$$d = -0.8\left(\phi'\right)+25.4 \qquad \text{Eq. 6. 9}$$

For $38^{o} < \Phi' < 42^{o}$

$$d = -1.8(\phi') + 61.9 \qquad \text{Eq. 6. 10}$$

where: d = hyperbolic regression intercept-parameter
Φ' = effective angle of internal friction

These equations and parameters are based on the soils used in the laboratory experimental program. Therefore, actual insertion characteristics for soils outside of the q_{app}/σ'_v range and GSD parameter boundaries for the proposed equations may vary.

6.2 Pile Insertion Depth

The pile insertion depth due to a set of jetting parameters may also be estimated with the proposed model. The pile insertion depth may be back-calculated from the q_{app}/σ'_v ratio at the final insertion point for the final Q_w/Q_p ratio obtained from equation 6.1. Since the final depth of insertion depends on a specific Q_w and V_j for a given dimensioned pile, Figure 6.15 provides the relation between the jetting parameters and final q_{app}/σ'_v ratio for the given soil types.

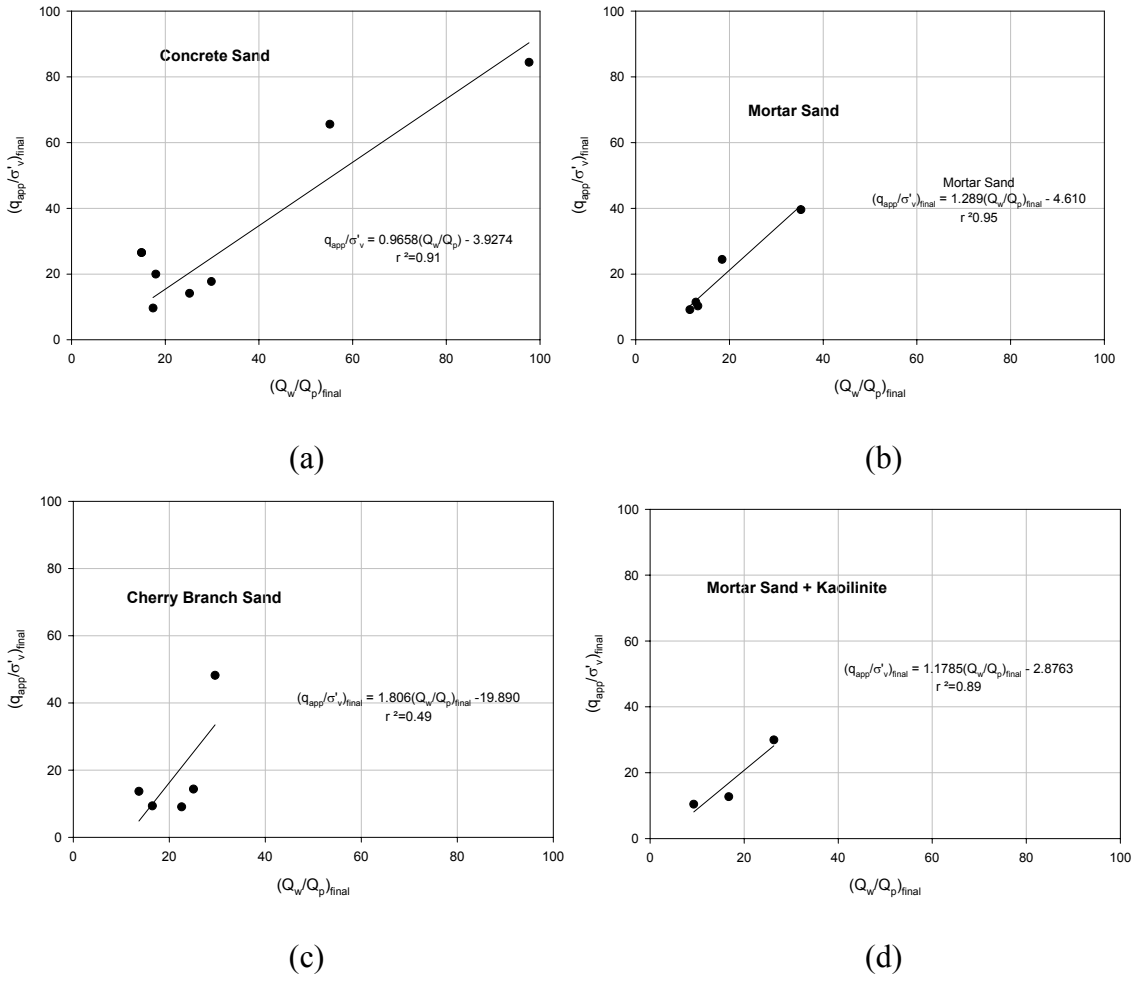

Figure 6.15 Final q_{app}/σ'_v due to Jetting Parameters

Plotting the regression parameters of the natural soils in Figure 6.15 with d_{50} (mm), provides a relationship between the jetting parameters and $(q_{app}/\sigma'_v)_{final}$ (Figure 6.16 & 6.17).

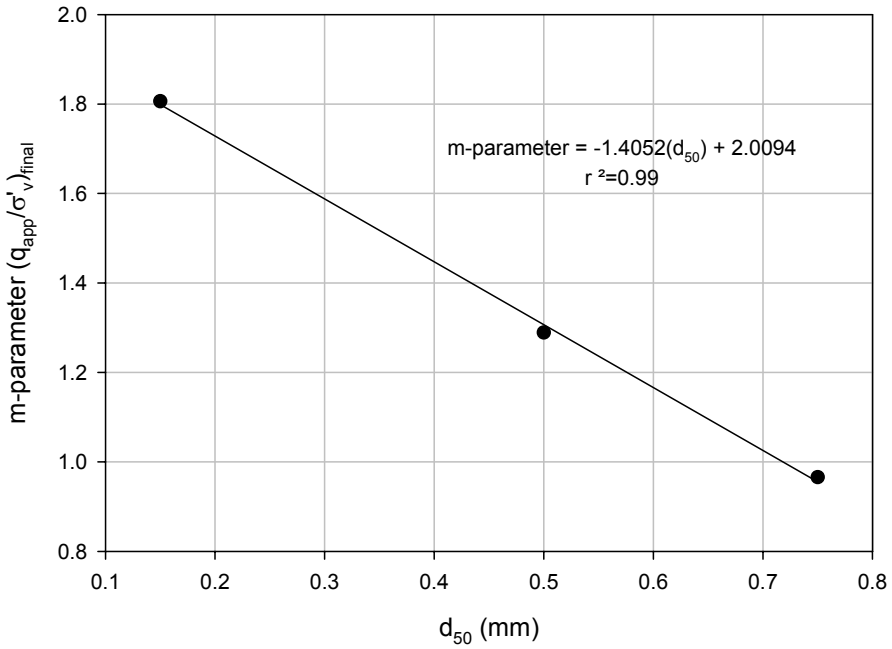

Figure 6.16 Slope-parameter for $(q_{app}/\sigma'_v)_{final}$ dependency on d_{50}

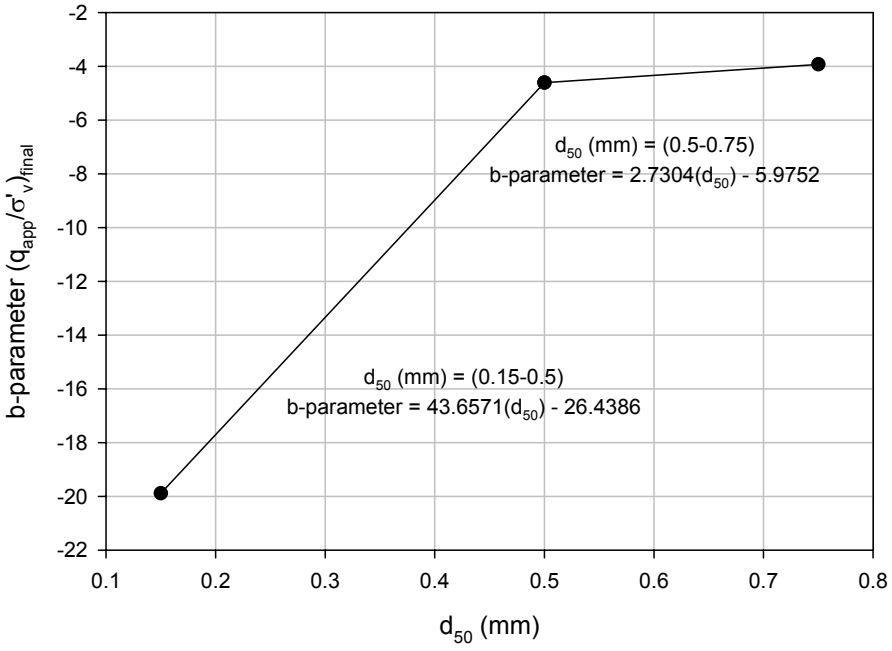

Figure 6.17 Intercept-parameter for $(q_{app}/\sigma'_v)_{final}$ dependency on d_{50}

Therefore, the following equation is presented to determine the $(q_{app}/\sigma'_v)_{final}$ relation with the jetting parameters for the various soil types.

$$\left(\frac{q_{app}}{\sigma'_v}\right)_{final} = m\left(\frac{Q_w}{Q_p}\right)_{final} + b \qquad \text{Eq. 6. 11}$$

where:

$$m = -1.4052(d_{50}) + 2.0094 \quad \textit{(d_{50} in mm)} \qquad \text{Eq. 6. 12}$$

For $d_{50} < 0.5$ mm, (*inches to mm multiply by 25.4*)

$$b = 43.651(d_{50}) - 26.4386 \qquad \text{Eq. 6. 13}$$

For $d_{50} > 0.5$ mm, (*inches to mm multiply by 25.4*)

$$b = 2.7304(d_{50}) - 5.9752 \qquad \text{Eq. 6. 14}$$

6.3 Debris Zone Modeling

From Section 5.2.3 it was shown that the debris volume (V_{debris}) and debris area (A_{debris}) follow power relationships with the total volume of water (V_{wtotal}) and jetting parameters required to achieve the final depth of insertion for jetted piles. The following equations provide the relationship between jetting parameters and debris zone disturbance for the various soil types.

$$V_{debris} = V_{wtotal} a_{volume} \left(\frac{Q_w}{Q_p}\right)^{b_{volume}} \qquad \text{Eq. 6. 15}$$

where: V_{debris} = total volume of soil material transported to ground surface (L^3)
V_{wtotal} = total volume of water required to jet a pile to a given depth with available jetting parameters (L^3)
a_{volume} = parameter based on C_c
b_{volume} = parameter based on d_{50}

and

$$a_{volume} = 0.520(C_c) + 0.868 \qquad \text{Eq. 6. 16}$$

$$b_{volume} = -0.081(d_{50}) - 0.961 \quad (d_{50} \text{ in mm}) \qquad \text{Eq. 6. 17}$$

(*inches to mm multiply by 25.4*)

$$A_{debris} = \left(\frac{V_{wtotal}}{D_{pile}}\right) a_{area} \left(\frac{Q_w}{Q_p}\right)^{b_{area}} \qquad \text{Eq. 6. 18}$$

where: A_{debris} = debris distribution on ground surface from jetted pile installation (L^2)
V_{wtotal} = total volume of water required to jet a pile to a given depth with available jetting parameters (L^3)
D_{pile} = diameter of jetted pile (L)
a_{area} = parameter based on d_{50}
b_{area} = parameter based on C_c

and

For $d_{50} < 0.5$ mm (*inches to mm multiply by 25.4*)

$$a_{area} = 8.5086(d_{50}) + 9.1967 \quad (d_{50} \text{ in mm}) \qquad \text{Eq. 6. 19}$$

$$b_{area} = -0.6357(d_{50}) - 0.8279 \quad (d_{50} \text{ in mm}) \qquad \text{Eq. 6. 20}$$

For $d_{50} > 0.5$ mm (*inches to mm multiply by 25.4*)

$$a_{area} = 0.404(d_{50}) + 13.249 \quad (d_{50} \text{ in mm}) \qquad \text{Eq. 6. 21}$$

$$b_{area} = -0.085(d_{50}) - 1.1029 \quad (d_{50} \text{ in mm}) \qquad \text{Eq. 6. 22}$$

6.4 Validation of Proposed Model with Laboratory Tests

Implementation of the proposed empirical model to the actual laboratory data was undertaken for validation purposes. This was to ensure that equations developed from data analysis were accurately coded in the model spreadsheet. This validation was conducted for both insertion characteristics and debris zone quantities.

6.4.1 Insertion Rate Validation

The model is developed on the principle of pile insertion rate at depth for given jetting parameters and subsurface characteristics. Therefore, for each test conducted in the testing program, the pile insertion rate at the final depth of insertion was determined due to the given jetting parameters. Using equation 6.1, Q_p was determined for the $(q_{app}/\sigma'_v)_{final}$ ratio based on the jetting parameters and soil type. The pile insertion rate (IR) was then determined by dividing Q_p by the pile area. Figure 6.18 presents the line of 100% agreement between the actual pile insertion rates from laboratory tests (IR_{lab}) and the estimated pile insertion rates (IR_{model}) from implementation of the empirical model.

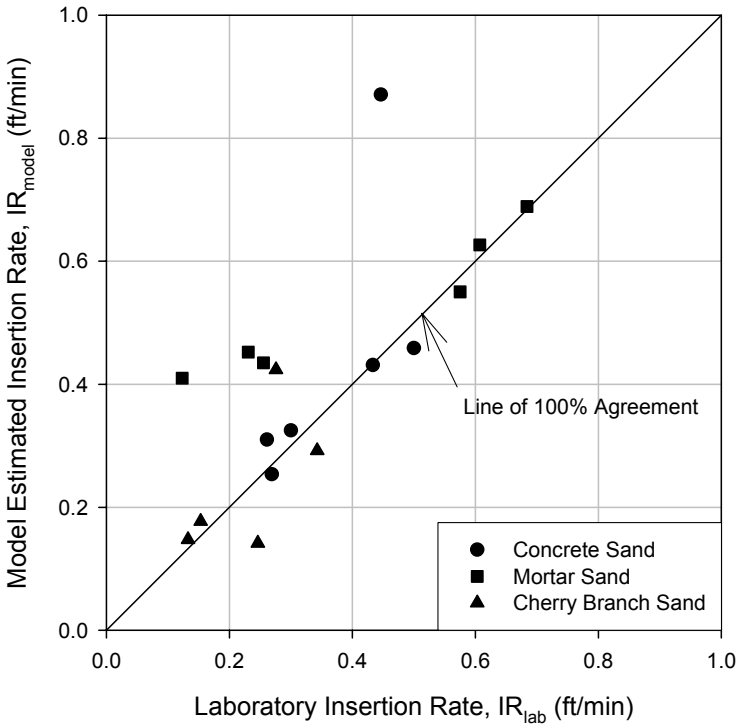

Figure 6.18 Insertion Rate Validation of Proposed Model

The proposed model provides a relatively accurate estimation of insertion rates for laboratory testing. Some scatter exists between the model and actual values due to the

regression of test parameters involving several tests. Overall, the model should provide accurate estimations of insertion rates for jet-driven piles within the range of q_{app}/σ'_v achieved in laboratory testing. However, applying the model to soils with GSD properties very different than those in which the model is based may yield inaccurate estimations.

6.4.2 Debris Zone Characteristics Validation

For each test conducted in the testing program, the debris zone characteristics at the final depth of insertion were determined due to the given jetting parameters. Using equations 6.15 and 6.18, the debris zone volume (V_{debris}) and debris zone area (A_{debris}) were estimated based on the final depth of insertion of actual laboratory tests. These estimated values were then compared to the actual values of debris zone quantities for the given soil types. Figure 6.19 & 6.20 present the line of 100% agreement between the actual debris zone quantities from laboratory tests (V_{lab} and A_{lab}) and the estimated debris zone quantities (V_{model} and A_{model}) from implementation of the empirical model.

NOTE: Boundary effects encountered in the Cherry Branch Sand full-depth tests produced immeasurable debris area properties.

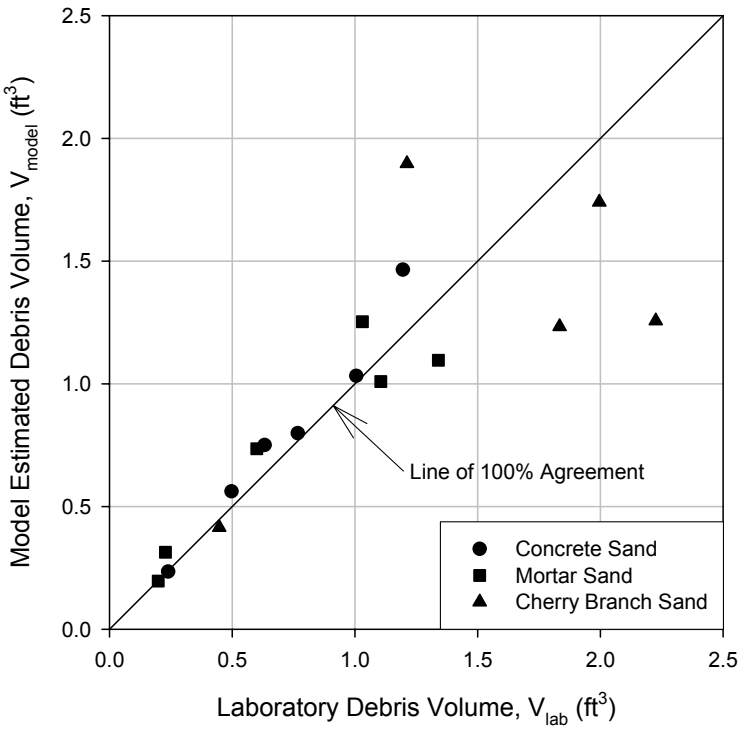

Figure 6.19 Debris Volume Validation of Proposed Model

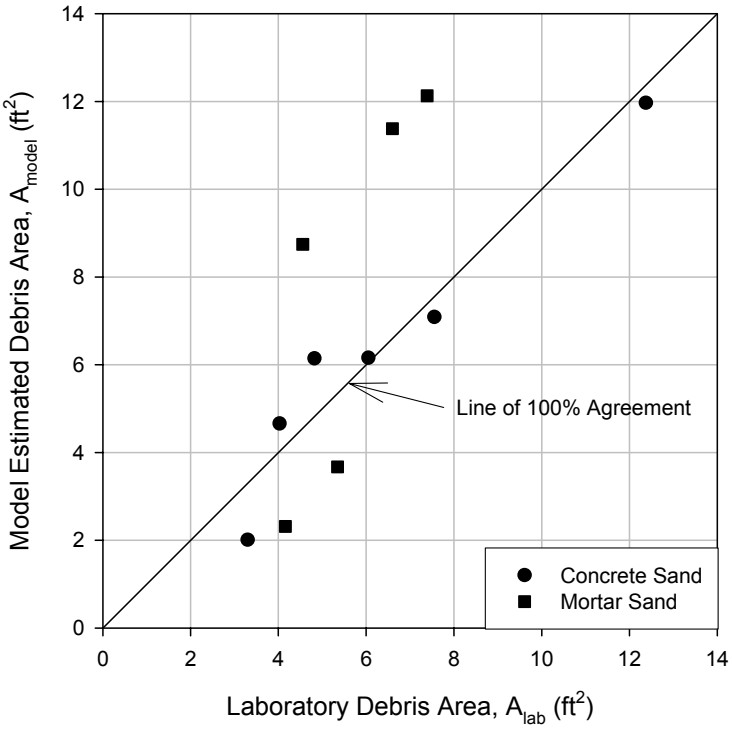

Figure 6.20 Debris Area Validation of Proposed Model

The proposed model also provides a relatively accurate estimation of debris zone characteristics for laboratory testing. Some scatter exists between the model and actual values due to the regression of test parameters involving several tests. Overall, the model should provide accurate estimations of debris zone characteristics for jet-driven piles within the range of q_{app}/σ'_v achieved in laboratory testing. However, applying the model to soils with GSD properties very different than those in which the model is based may yield inaccurate estimations.

6.5 Jetting Parameter Optimization for Impact Minimization

The following example illustrates the importance of using the optimum jetting parameters to minimize the debris zone characteristics in full-scale pile jetting

applications. The proposed model has been implemented to provide estimations of these debris zone characteristics based on variations in the jetting system. Equations 6.1 through 6.22 were used to determine the characteristics of the following jetted pile installations. The pile and soil characteristics are given in Table 6.2.

Table 6.2 Soil and Pile Properties for Jetting Example

Soil Index Properties	
D_{60} (mm)	0.60
D_{30} (mm)	0.35
D_{10} (mm)	0.28
D_{50} (mm)	0.50
Unit Weight of Soil, γ_{soil} (pcf)	100
Effective Angle of Internal Friction, (Φ')	38
C_u	2.14
C_c	0.73
Pile Properties	
Pile Length (ft)	40
Ground Water Table Depth (ft)	0
Unit Weight of Concrete, γ_{conc} (pcf)	150
Unit Weight of Water, γ_{water}(pcf)	62.4
Pile Area, A_p (ft^2)	3.141593
Pile Diameter, D_p (ft)	2

The analysis has been conducted for the final depth of installation of 9 feet (2.74m). Three different flow rates were inputted into the model with jet nozzles of 3 inches, 2.5 inches, and 2.0 inches (76mm, 64mm, and 51mm). The following output table displays the estimations of insertion rate and debris zone quantities from model implementation.

Table 6.3 Output Table of Pile Insertion Characteristics

Depth (ft)	q_{app}/σ'_v	Flowrate, Q_w (gpm)	Jet Nozzle Velocity, V_j (ft/min)	Jet Nozzle Dia. (each) (inch)	Pile Insertion Rate, IR (ft/min)	Total Volume of Water, V_{wtotal} (ft^3)	Debris Volume, V_{debris} (ft^3)	Debris Area, A_{debris} (ft^2)
9	14	100	136	3.0	0.38	314.35	33.24	133.98
9	14	100	196	2.5	0.40	302.88	33.25	134.70
9	14	100	306	2.0	0.43	281.76	33.25	136.12
9	14	200	272	3.0	0.83	288.28	33.25	135.67
9	14	200	392	2.5	0.91	265.33	33.25	137.32
9	14	200	613	2.0	1.08	223.09	33.26	140.83
9	14	300	409	3.0	1.38	262.18	33.25	137.56
9	14	300	588	2.5	1.58	227.77	33.26	140.40
9	14	300	919	2.0	2.20	164.42	33.28	147.21

CONVERSIONS:
gallons/min to m^3/min multiply by 0.0038
gallons/min to ft^3/min multiply by 0.1337
ft/min to m/min divide by 3.281
inch to mm multiply by 25.4
ft^3 to m^3 multiply by 0.0283
ft^2 to m^2 multiply by 0.093

The following figures present results demonstrating the ability to optimize jetting parameters resulting in minimal surface disturbance surrounding jetted pile installations.

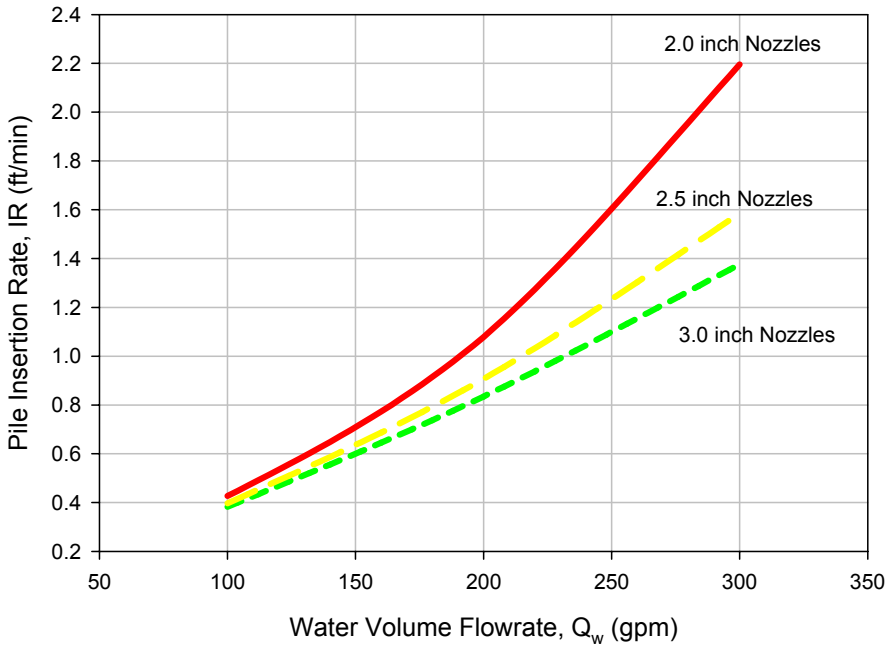

Figure 6.21 Optimal Jetting Parameters for Pile Insertion Rate

Figure 6.21 demonstrates the effect of increasing V_j, by decreasing the jet nozzle diameter with equal Q_w. For example, at Q_w = 200 gpm (0.75 m^3/min), decreasing the nozzle diameter from 3 inches (76 mm) to 2 inches (51 mm) increases the pile insertion rate from approximately 0.8 ft/min (0.244 m/min) to 1.1 ft/min (0.335 m/min). Therefore, for equal Q_w, the pile insertion rate increases with higher V_j.

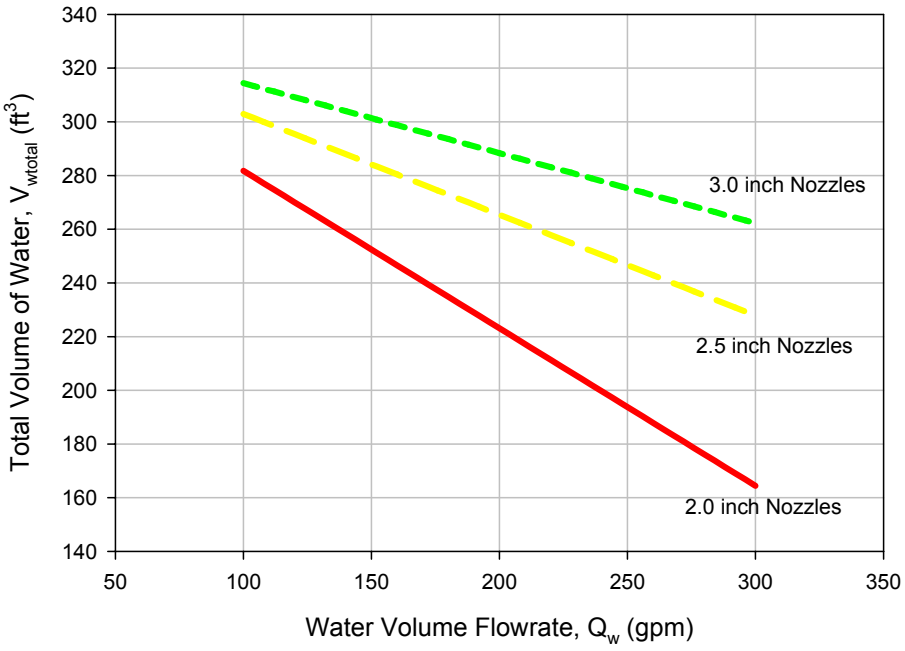

Figure 6.22 Optimal Jetting Parameters for Minimizing V_{wtotal}

Figure 6.22 demonstrates the effect of increasing V_j for a given Q_w on the total volume of water required to jet the given pile to the desired depth. For Q_w = 200 gpm (0.75m^3/min), the reduction in V_{wtotal} from using a 3 inch (76mm) diameter nozzle to a 2 inch (51mm) diameter nozzle is approximately 70 gallons (0.265 m^3). Therefore, the increased insertion rate (as seen in Figure 6.21) due to an increase in V_j, decreases the required V_{wtotal} and the Q_w/Q_p ratio. The relationship between pile insertion rate and debris zone properties are shown in Figures 6.23 and 6.24.

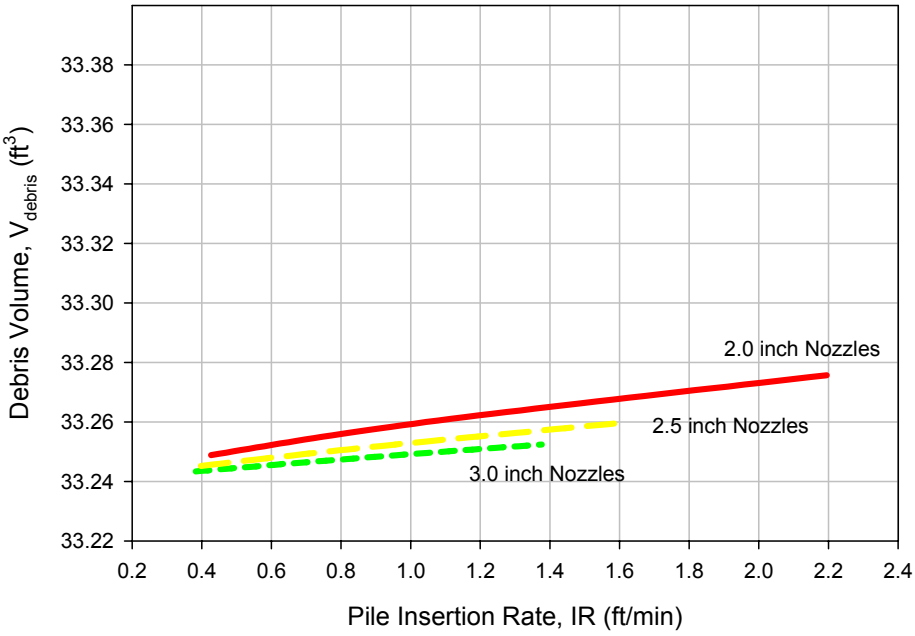

Figure 6.23 Optimization of Jetting Parameters for V_{debris}

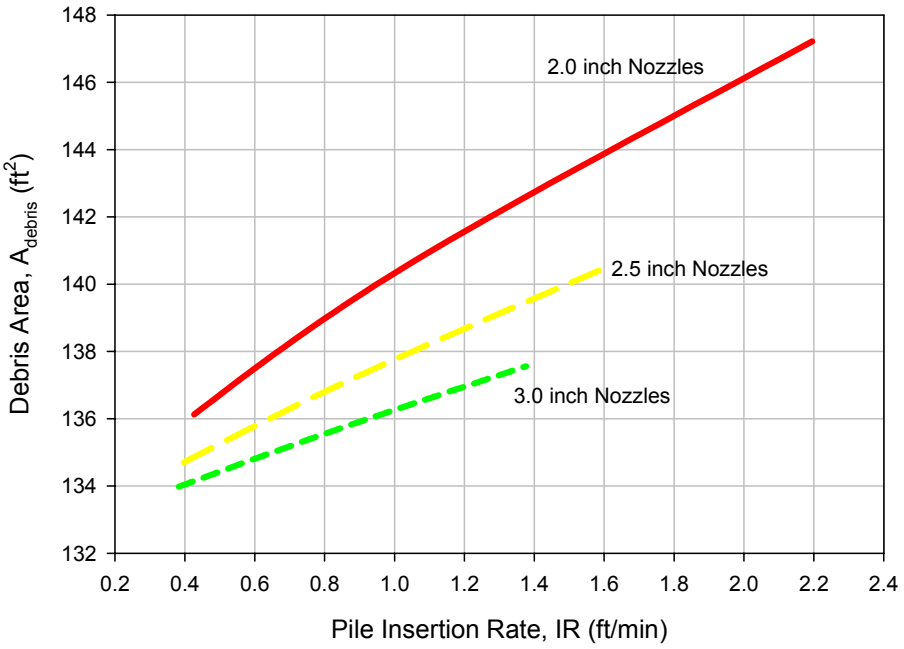

Figure 6.24 Optimization of Jetting Parameters for A_{debris}

Figures 6.23 and 6.24 provide the relationship between debris zone volume and debris zone area due to increasing insertion rate for given jet nozzle diameters. For example, for the 2.0 inch (51mm) diameter nozzles, increased pile insertion rates are obtained by increasing Q_w. As mentioned earlier, this increase in insertion rate decreases V_{wtotal} and Q_w/Q_p. However, an important concept should be realized from Figures 6.23 and 6.24. Entering Figure 6.23 or 6.24 at the highest insertion rate for the 3.0 inch (76 mm) diameter nozzle (approximately IR = 1.4 ft/min (0.427m/min)), V_{debris} and A_{debris} are approximately 33.25 ft^3 (0.942m^3) and 138 ft^2 (12.774 m^2) respectively. The water volume flowrate (Q_w) at these points are 300 gpm (1.136 m^3/min). Looking at the same figures for the 2.0 inch (51mm) diameter nozzles at an insertion rate of approximately 2.2 ft/min (0.671 m/min), V_{debris} and A_{debris} are approximately 33.27 ft^3 (0.942 m^3) and 147 ft^2 (13.65 m^2) respectively. The water volume flowrate at these points are 300 gpm (1.136 m^3/min). The pile jetted into the soil stratum at a lower insertion rate produces less debris zone disturbance than the pile jetted at a higher insertion rate. However, the debris zone volumes are not greatly affected by variation in jetting parameters for the given insertion depth and pile dimensions. The increase in debris area with increased insertion rate is due to the velocity of jet water stemming from the pile annulus during jetting. The increase in jet nozzle velocity reduces the V_{wtotal}, but intern increases the exit water velocity from the jet annulus. This displaces the debris zone material farther from the pile center generating an increase in A_{debris}.

6.6 Proposed Practice and Design Approach

In order to estimate jetted pile insertion properties for q_{app}/σ'_v greater than 15 and the effects of the installation on the debris zone surrounding the installed pile, the following design method is provided.

1. Conduct a routine subsurface investigation to determine GSD curves.
2. Determine pile insertion rate parameters based on GSD (Equations 6.5-6.10).
3. Determine final depth of insertion parameters based on GSD (Equations 6.12-6.14).
4. Determine debris zone volume parameters (Equations 6.16 & 6.17) and debris area parameters (Equations 6.19-6.22) based on GSD.
5. Determine jetting pump capacities with various nozzle diameters from pump backpressure logs.
6. For a given pile type, length, and diameter, determine q_{app}/σ'_v ratios at various depths within the soil profile.
7. With Q_w and V_j for a given jetting system, determine Q_p (Equation 6.4) at various depth increments, constrained by the final depth of insertion (Equation 6.11) for given Q_w and V_j.
8. Determine the volume of water required at each depth increment to insert the pile with given jetting parameters.
9. Determine V_{wtotal} needed to insert the given pile and the total Q_w/Q_p ratio for the given jetting parameters.
10. Determine V_{debris} and A_{debris} from Equations 6.15 and 6.18 for the given jetting parameters.

11. From steps 7 and 9 determine the necessary jetting parameters to allow optimal pile insertion rate and debris zone properties for variations in the jetting system.

The previous model was developed as a tool for geotechnical engineers to estimate the debris zone properties due to variations in jetting systems and soil conditions. This model was developed from a series of laboratory tests with the three sand types at relative densities of 50-70 % discussed in the model development section of this chapter. It is important to realize that variations in soil profiles from the material tested in the laboratory may exhibit different pile installation and debris zone characteristics.

CHAPTER 7 - SUMMARY AND CONCLUSIONS

The literature review presented the state of practice of pile jetting with guidelines available for installation of various pile sizes into subsurface profiles. However, the literature provided no information on the debris zone characteristics or pile insertion rates of piles installed using water jetting. The present research consisted of jetting model piles into various soil profiles through implementation of a laboratory experimental program. This program allowed the researchers to determine the effects of jetting parameters on pile insertion, pile refusal depth, and debris zone characteristics. From the extensive laboratory testing program, a universal model for predicting the properties of jetted pile installations has been presented. An investigation into the mechanics of jetted piles was conducted within a fabricated plexi-glass specimen box. This enabled the researchers to view the mechanics of pile installations in jetting applications. Based on the experimental laboratory program, the following conclusions are advanced:

1. Installation of piles due to the application of water jetting stems from the simultaneous erosion of soils beneath the pile tip and transport of these soil particles to the ground surface. The pile advances only after a sufficient area of soil has been eroded to cause a tip bearing capacity failure and the reduction of side friction from the liquefied jetting annulus.
2. Optimization of water flowrate (Q_w) and jet nozzle velocity (V_j) for a given soil profile provides minimal debris zone characteristics and insertion rate predictions for jetted installations.

3. The rate of insertion and the maximum attainable depth of insertion were greater for uniform sand than well-graded sand for equal jetting parameters and similar average particle sizes (d_{50}).
4. Comparison of jetted piles in two uniform sand profiles provided variations in the jetting installation characteristics due to the average size of sand particles in the profile. Jetting in a sand profile with a small average particle diameter (d_{50} = 0.15 mm) provided greater depths of insertion (approximately 170% greater) and insertion rates (approximately 18% faster) as compared to a sand profile with greater average particle diameter (d_{50} = 0.5 mm) and comparable GSD shape parameters (C_u approximately 2, C_c approximately 0.8).
5. For equal jetting parameters, the extent of the debris zone for sands with smaller average particle sizes (d_{50} = 0.15 mm) were approximately 100% further from the pile center than sands with larger average particle size (d_{50} = 0.5 mm).
6. The proposed model estimates jetted pile installation characteristics for q_{app}/σ'_v ratios greater than 15. Full-scale jetted pile installations will be conducted to establish the jetting installation model for installations to q_{app}/σ'_v ratios less than 15 (greater depth).

CHAPTER 8 - RECOMMENDATIONS FOR FUTURE RESEARCH

Based on the results of research presented in this report, the following recommendations for future research are advanced.

1. Full-scale jetting should be conducted at q_{app}/σ'_v ratios beyond the range attained in this experimental program. These tests should be conducted in profiles exhibiting more natural characteristics and with jetting systems applicable to full-scale jetted pile installations. An extension to this model should be developed for deeper jetted pile installations than provided in this research.
2. Explore the effects of subsurface profiles consisting of clays with various plasticity characteristics (LL, PI, and activity) on the insertion and debris zone properties of jetted pile installations.
3. Full-scale jetted pile installations should be conducted in soil profiles with average particle diameters (d_{50}) varying from those tested in the laboratory experimental program. This will provide a better understanding of the functional shape of regressed jetting parameters with soil properties. This may allow the development of a more general model encompassing greater variations in soil profiles in which jetting may be employed.
4. Determine the efficiency and availability of using angled jets in full-scale pile jetting applications.

REFERENCE

Adamus, P.R., L.T. Stockwell, E.J. Clairain, M.E. Morrow, L.P. Rozas, and R.D. Smith (1991) "Wetland Evaluation Technique (WET)" Volume 1: Literature Review and Evaluation Rationale, Environmental Laboratory, Report No. WRP-DE-2, Waterways Experiment Station, Vicksburg, MS.

Allen, J.R.L. (1985) Principles of Physical Sedimentology, George Allen & Unwin Publishers Ltd., London.

ASTM D 422 Test Method for Particle-Size Analysis of Soils, ASTM, Vol. 4.08, Soil and Rock; Dimension Stone; Geosynthetics.

ASTM D 854 Test Method for Specific Gravity of Soils, ASTM, Vol. 4.08, Soil and Rock; Dimension Stone; Geosynthetics.

ASTM D 3080 Test Method for Direct Shear Test of Soils Under Consolidated Drained Conditions, ASTM, Vol. 4.08, Soil and Rock; Dimension Stone; Geosynthetics.

ASTM D 4253 Test Methods for Maximum Index Density and Unit Weight of Soils Using a Vibratory Table, ASTM, Vol. 4.08, Soil and Rock; Dimension Stone; Geosynthetics.

ASTM D 4254 Test Methods for Minimum Index Density and Unit Weight of Soils and Calculation of Relative Density, ASTM, Vol. 4.08, Soil and Rock; Dimension Stone; Geosynthetics.

Federal Regulations 40446 (August 14, 1991) "Proposed Revisions to the Federal Manual for Delineating Wetlands.

Gunaratne, M., R.A. Hameed, C. Kuo, S. Putcha, and D.V. Reddy (1999) Investigation of the Effects of Pile Jetting and Preforming, Research Report No. 772, Florida Department of Transportation, in cooperation with Federal Highway Administration.

Holtz, R.D., and W.D. Kovacs (1981) An Introduction to Geotechnical Engineering, Prentice-Hall, Inc., New Jersey.

Matlin, A. (1983) Wide Flange, Concrete Sheet Pile Warves, Proceedings of ASCE Specialty Conference, Ports, 1983, New Orleans, LA., Mar 21-23, 389-401.

McGregor, T.H. (1963) T-shaped Concrete Sheet Piles Renew Deteriorated Bulkhead. Engineering News-Record, January 3, 20-21.

Mitchell, J.K. (1976) Fundamentals of Soil Behavior, John Wiley & Sons, Inc., New York, 422 pp.

Munson, B.R., T.H. Okiishi, and D.F. Young (1998) Fundamentals of Fluid Mechanics, Third Edition, John Wiley & Sons, Inc., Canada.

North Carolina Department of Transportation Soils and Foundations Design reference Manual, Version 2001.

Open University Oceanography Course Team (1999)

Shestopal, A.O. (1959) Jetting of Pipes, Piles, and Sheet Piles. Hydroproject Institute, Moscow, U.S.S.R.

Skempton, A.W., (1953) The Colloidal Activity of Clays, Proceedings of the Third International Conference on Soil Mechanics and Foundation Engineering, Vol I, pp 57-61.

Tsinker, G.P. (1988) Pile Jetting, Journal of Geotechnical Engineering, ASCE, Vol. 144, No. 3 March 1988, pp. 326-334.

APPENDIX

Characteristics of Laboratory Testing Medium

Index Density

Table A- 1 Maximum and Minimum Index Densities of Testing Material

Maximum and Minimum Index Density

Specimen	H1 (in.)	H2 (in.)	Avg. 1&2 (in.)	H3 (in.)	H4 (in.)	Avg. 3&4 (in.)	Avg. (in.)	Height of Sample (in.)	Volume (ft^3)	Weight (lbs.)	Density (lb./ft.^3)	Avg. max (pcf)
Mortar - 1	0.475	0.436	0.456	0.412	0.381	0.397	0.4260	5.190	0.0848	9.136	107.7	108.0
Mortar - 2	0.313	0.316	0.315	0.561	0.573	0.567	0.4408	5.175	0.0846	9.155	108.2	
Concrete - 1	0.268	0.266	0.267	0.617	0.613	0.615	0.4410	5.175	0.0846	9.713	114.8	114.8
Concrete - 2	0.426	0.476	0.451	0.329	0.289	0.309	0.3800	5.236	0.0856	9.821	114.8	
Cherry Branch	1.352	1.357	1.355	1.459	1.232	1.346	1.3500	4.740	0.0773	7.902	102.2	102.0

Specimen	Height of Sample (in.)	Specimen Diameter (in)	Specimen Area (in^2)	Specimen Volume (in^3)	Specimen Volume (ft^3)	Specimen Weight (lb)	Density (lb./ft.^3)	Avg. min (pcf)
Mortar - 1	6.098	5.996	28.2366	172.1871	0.0996	8.98	90.11966	90.1
Mortar - 2	6.098	5.996	28.2366	172.1871	0.0996	8.98	90.11966	
Concrete - 1	6.098	5.996	28.2366	172.1871	0.0996	9.38	94.13389	94.1
Concrete - 2	6.098	5.996	28.2366	172.1871	0.0996	9.38	94.13389	
Cherry Branch-1	6.09	5.99	28.1802	171.6172	0.0993	8.13	81.86033	82.0
Cherry Branch2	6.09	5.99	28.1802	171.6172	0.0993	8.16	82.16239	

Effective Angle of Internal Friction

Table A- 2 Direct Shear Test Data for Testing Material

Direct Shear Test Data

Mortar Sand		Concrete Sand		Cherry Branch Sand		Mortar Sand + Kaolinite	
Normal Stress (psf)	Shear Stress at Failure (psf)	Normal Stress (psf)	Shear Stress at Failure (psf)	Normal Stress (psf)	Shear Stress at Failure (psf)	Normal Stress (psf)	Shear Stress at Failure (psf)
277.5	244.6256747	277.5	366.9385121	277.5	265.0111476	504.5	407.7094579
504.5	428.0949308	504.5	611.5641868	504.5	428.0949308	277.5	183.469256
1008	835.8043886	1008	958.117226	1008	754.2624971	1008	550.4077681
2006	1549.29594	2006	1691.99425	2006	1304.670265	2006	1161.971955

Permeability

Table A- 3 Falling Head Permeability Data (Concrete Sand)

Sample Name: Concrete Sand
Date: 7/21/2003

rho=2.65

Vs (cm^3)	321.69
Vv (cm^3)	214.5877
e =	0.667064

Unit Weight Information

Measurement	Specimen Diameter (cm)	Specimen Length (cm)
1	7.214	13
2	7.264	13
3	7.264	13
Average	7.247333333	13

Specimen Area (cm^2) 41.25212782
Specimen Volume cm^3) 536.2776617

Weight of Dry Soil (lb):	2.0035
Dry Unit Weight (pcf):	104.9
Void Ratio:	0.667063513
Relative Density:	57

Pore Volume (cm^3) 214.5877

dstandpipe = 7.6cm
Area of Standpipe, a (cm^2) = 45.4

Beaker Tare gm 115.35

=QL/hAt Constant Head

=(2.3aL/At) log(h1/h2) Falling Head

Test No.	Cell Pressure (psi)	Head Pressure (psi)	Mass of Pore (gm)	Flow Volume (ft^3)	Time (s)	Q/At	h/L	h	k (cm/s)	h1 (cm)	h2 (cm)	k (cm/s)
1.00	10.00	11.00	315.89	200.54	54.00	0.09	5.41	70.34	0.0166	74.76	70.34	0.0161
2.00	10.00	11.00	320.66	205.31	61.30	0.08	5.41	70.34	0.0150	74.86	70.34	0.0145
3.00	10.00	11.00	323.39	208.04	65.90	0.08	5.41	70.34	0.0141	74.92	70.34	0.0137
4.00	10.00	11.00	312.72	197.37	69.70	0.07	5.41	70.34	0.0127	74.69	70.34	0.0123
5.00	10.00	11.00	237.75	122.40	36.00	0.08	5.41	70.34	0.0152	73.03	70.34	0.0149
6.00	10.00	11.00	314.37	199.02	83.00	0.06	5.41	70.34	0.0107	74.72	70.34	0.0104
7.00	10.00	11.00	314.85	199.50	105.80	0.05	5.41	70.34	0.0084	74.73	70.34	0.0082
8.00	10.00	11.00	314.06	198.71	128.20	0.04	5.41	70.34	0.0069	74.72	70.34	0.0067
9.00	10.00	11.00	314.36	199.01	157.60	0.03	5.41	70.34	0.0057	74.72	70.34	0.0055
10.00	10.00	11.00	319.63	204.28	190.65	0.03	5.41	70.34	0.0048	74.84	70.34	0.0046
11.00	10.00	11.00	315.28	199.93	180.20	0.03	5.41	70.34	0.0050	74.74	70.34	0.0048
12.00	10.00	11.00	315.33	199.98	210.80	0.02	5.41	70.34	0.0043	74.74	70.34	0.0041
13.00	10.00	11.00	312.90	197.55	178.30	0.03	5.41	70.34	0.0050	74.69	70.34	0.0048
14.00	10.00	11.00	312.10	196.75	197.00	0.02	5.41	70.34	0.0045	74.67	70.34	0.0043
15.00	10.00	11.00	311.80	196.45	215.00	0.02	5.41	70.34	0.0041	74.67	70.34	0.0040
16.00	10.00	11.00	310.20	194.85	215.00	0.02	5.41	70.34	0.0041	74.63	70.34	0.0039
17.00	10.00	11.00	285.20	169.85	213.00	0.02	5.41	70.34	0.0036	74.08	70.34	0.0035
18.00	10.00	11.00	212.20	96.85	126.00	0.02	5.41	70.34	0.0034	72.47	70.34	0.0034
									0.004658			0.004519 10^-2

97.03303

Table A- 4 Falling Head Permeability Data (Mortar Sand)

Sample Name: Mortar Sand
Date: 1/17/2003

rho=2.65

Vs (cm^3)	341.06
Vv (cm^3)	221.0902
e =	0.648263

Unit Weight Information

Measurement	Specimen Diameter (cm)	Specimen Length (cm)
1	7.2009	13.8
2	7.2009	13.8
3	7.20344	13.8
Average	7.201746667	13.8

Specimen Area (cm^2) 40.73479752
Specimen Volume cm^3) 562.1402058

Weight of Dry Soil (lb):	1.9925
Dry Unit Weight (pcf):	100.6
Void Ratio:	0.648263321
Relative Density:	62.7

Pore Volume (cm^3) 221.0902058

dstandpipe = 7.6cm
Area of Standpipe, a (cm^2) = 45.4

Beaker Tare gm 119.69

=QL/hAt Constant Head

=(2.3aL/At) log(h1/h2) Falling Head

Test No.	Cell Pressure (psi)	Head Pressure (psi)	Mass of Pore (gm)	Flow Volume (cm^3)	Time (s)	Q/At	h/L	h	k (cm/s)	h1 (cm)	h2 (cm)	k (cm/s)
1.00	5.00	7.50	338.38	218.69	79.00	0.07	12.74	175.85	0.01	180.66	175.85	0.01
2.00	5.00	6.00	341.38	221.69	87.81	0.06	5.10	70.34	0.01	75.22	70.34	0.01
3.00	5.00	6.00	341.92	222.23	91.60	0.06	5.10	70.34	0.01	75.23	70.34	0.01
4.00	5.00	6.00	342.32	222.63	89.70	0.06	5.10	70.34	0.01	75.24	70.34	0.01
5.00	5.00	6.00	341.32	221.63	90.75	0.06	5.10	70.34	0.01	75.22	70.34	0.01
6.00	5.00	6.00	295.62	175.93	66.72	0.06	5.10	70.34	0.01	74.21	70.34	0.01
7.00	10.00	11.00	339.77	220.08	54.00	0.08	5.10	70.34	0.02	75.19	70.34	0.02
8.00	10.00	11.00	342.11	222.42	54.06	0.09	5.10	70.34	0.02	75.24	70.34	0.02
9.00	10.00	11.00	338.21	218.52	63.10	0.09	5.10	70.34	0.02	75.15	70.34	0.02
10.00	10.00	11.00	338.20	218.51	63.70	0.08	5.10	70.34	0.02	75.15	70.34	0.02
11.00	10.00	11.00	338.80	219.11	64.00	0.08	5.10	70.34	0.02	75.16	70.34	0.02
12.00	10.00	11.00	335.58	215.89	65.46	0.08	5.10	70.34	0.02	75.09	70.34	0.02
13.00	10.00	11.00	336.99	217.30	66.47	0.08	5.10	70.34	0.02	75.12	70.34	0.02
14.00	10.00	11.00	335.06	215.37	64.20	0.08	5.10	70.34	0.02	75.08	70.34	0.02
									0.0163			0.0158 10^-2

% error
96.81967

Table A- 5 Falling Head Permeability Data (Cherry Branch Sand)

Sample Name: Cherry Branch
Date: 7/17/2003

rho=2.61

Vs (cm^3)	321.69
Vv (cm^3)	227.2152
e =	0.706317

Unit Weight Information

Measurement	Specimen Diameter (cm)	Specimen Length (cm)
1	7.186	13.5
2	7.2009	13.5
3	7.1984	13.5
Average	7.1951	13.5

Specimen Area (cm^2) 40.65984195
Specimen Volume cm^3) 548.9051684

Weight of Dry Soil (lb):	1.851
Dry Unit Weight (pcf):	95.4
Void Ratio:	0.706317157
Relative Density:	72

Pore Volume (cm^3) 227.2152

dstandpipe = 7.6cm
Area of Standpipe, a (cm^2) = 45.4

Beaker Tare gm 103.75

=QL/hAt (Constant Head) | =(2.3aL/At) log(h1/h2) (Falling Head)

Test No.	Cell Pressure (psi)	Head Pressure (psi)	Mass of Pore (gm)	Volume (cm^3)	Time (s)	Q/At	h/L	h	k (cm/s)	h1 (cm)	h2 (cm)	k (cm/s)
1.00	5.00	7.50	336.34	232.59	91.00	0.06	13.03	175.85	0.005	180.97	175.85	0.005
2.00	5.00	6.00	333.09	229.34	87.00	0.06	5.21	70.34	0.012	75.39	70.34	0.012
3.00	5.00	6.00	334.55	230.80	90.50	0.06	5.21	70.34	0.012	75.42	70.34	0.012
4.00	5.00	6.00	333.02	229.27	91.53	0.06	5.21	70.34	0.012	75.39	70.34	0.011
5.00	5.00	6.00	331.42	227.67	85.20	0.07	5.21	70.34	0.013	75.35	70.34	0.012
6.00	5.00	6.00	251.73	147.98	103.30	0.04	5.21	70.34	0.007	73.60	70.34	0.007
7.00	10.00	11.00	330.03	226.28	83.00	0.07	5.21	70.34	0.013	75.32	70.34	0.012
8.00	10.00	11.00	332.25	228.50	86.40	0.07	5.21	70.34	0.012	75.37	70.34	0.012
9.00	10.00	11.00	330.73	226.98	87.50	0.06	5.21	70.34	0.012	75.34	70.34	0.012
10.00	10.00	11.00	331.06	227.31	105.20	0.05	5.21	70.34	0.010	75.35	70.34	0.010
11.00	10.00	11.00	330.44	226.69	88.30	0.06	5.21	70.34	0.012	75.33	70.34	0.012
12.00	10.00	11.00	329.89	226.14	91.70	0.06	5.21	70.34	0.012	75.32	70.34	0.011
13.00	10.00	11.00	329.93	226.18	94.27	0.06	5.21	70.34	0.011	75.32	70.34	0.011
14.00	10.00	11.00	329.67	225.92	98.04	0.06	5.21	70.34	0.011	75.31	70.34	0.010
15.00	10.00	11.00	331.44	227.69	105.21	0.05	5.21	70.34	0.010	75.35	70.34	0.010
16.00	10.00	11.00	331.82	228.07	108.70	0.05	5.21	70.34	0.010	75.36	70.34	0.010
17.00	10.00	11.00	329.55	225.80	114.90	0.05	5.21	70.34	0.009	75.31	70.34	0.009
18.00	10.00	11.00	328.26	224.51	112.30	0.05	5.21	70.34	0.009	75.28	70.34	0.009
19.00	10.00	11.00	330.84	227.09	117.80	0.05	5.21	70.34	0.009	75.34	70.34	0.009
20.00	10.00	11.00	331.20	227.45	123.70	0.05	5.21	70.34	0.009	75.35	70.34	0.008
21.00	10.00	11.00	329.84	226.09	128.20	0.04	5.21	70.34	0.008	75.32	70.34	0.008
22.00	10.00	11.00	329.30	225.55	214.30	0.03	5.21	70.34	0.005	75.31	70.34	0.005
23.00	10.00	11.00	328.82	225.07	140.00	0.04	5.21	70.34	0.008	75.30	70.34	0.007
	10.00	11.00	252.94	149.19	99.00	0.04	5.21	70.34	0.007	73.62	70.34	0.007
									0.0084607			0.008173 10^-2

96.59906

Table A- 6 Falling Head Permeability Data (Mortar Sand + Kaolinite)

Sample Name: Kaolin + Sand
Date: 7/22/2003

ρ=2.65

Vs (cm^3)	340.11
Vv (cm^3)	189.4424
e =	0.557003

Unit Weight Information

Measurement	Specimen Diameter (cm)	Specimen Length (cm)
1	7.20344	13
2	7.2136	13
3	7.1982	13
Average	7.201746667	13

Specimen Area (cm^2) 40.73479752
Specimen Volume cm^3) 529.5523678

Weight of Dry Soil (lb):	
Dry Unit Weight (pcf):	
Void Ratio:	
Relative Density:	

Pore Volume (cm^3) 189.4424

dstandpipe = 7.6cm
Area of Standpipe, a (cm^2) = 45.4

Beaker Tare gm 101.02

=QL/hAt (Constant Head) | =(2.3aL/At) log(h1/h2) (Falling Head)

Test No.	Cell Pressure (psi)	Head Pressure (psi)	Mass of Pore (gm)	Volume (cm^3)	Time (s)	Q/At	h/L	h	k (cm/s)	h1 (cm)	h2 (cm)	k (cm/s)
1.00	10.00	11.00	340.44	239.42	1332.00	0.00	5.41	70.34	0.0008	75.61	70.34	0.0008
2.00	10.00	11.00	327.28	226.26	1424.00	0.00	5.41	70.34	0.0007	75.32	70.34	0.0007
3.00	10.00	11.00	331.60	230.58	1051.00	0.01	5.41	70.34	0.0010	75.42	70.34	0.0010
4.00	10.00	11.00	317.21	216.19	1078.00	0.00	5.41	70.34	0.0009	75.10	70.34	0.0009
									0.000860			0.000830 10^-3

Full-depth Test Data (Refusal Tests)

Table A- 7 Full Depth Tests Data (Concrete Sand)

Full Depth Tests - Concrete Sand

Test Description	Jet Velocity (ft/min)	Pile Dia. (in)	Ap (ft^2)	Dj (in)	Aj (ft^2)	Final Depth of Insertion (ft)	Ap/Aj	Q (ft^3/min)	Pile Volume(ft^3)	Time	Qw/Qp (Total)
5/29/2003 10DW8-.5	490	8	0.34906585	0.5	0.002727	1.0079	128	1.337	0.3518144	3.9333	14.94784
5/29/2003 20DW8-.8125	371	8	0.34906585	0.8125	0.007201	1.44	48	2.674	0.504358926	5.63	29.86669
5/29/2003 20DW8-.5	980	8	0.34906585	0.5	0.002727	2.49	128	2.674	0.870603213	5.67	17.40479
5/30/2003 20DW8-.625	627	8	0.34906585	0.625	0.004261	1.83	82	2.674	0.639954059	6.033333	25.20983
6/2/2003 10DW8-.625	314	8	0.34906585	0.625	0.004261	0.33	82	1.337	0.116366919	8.500	97.66092
6/3/2003 20DW8-.625	627	8	0.34906585	0.625	0.004261	1.33	82	2.674	0.465422297	3.133	18.002
6/25/03 10DW8-.625	314	8	0.34906585	0.625	0.004261	0.4167	82	1.337	0.14545574	6.000	55.1508

5/29/2003 10DW8-.5
490

Vj/Ir	Average Vj/IR	Depth (ft)	Average Depth (ft)	time (min)	Average Time (min)	qapp/σ'v	average qapp/σ'v	average qapp/ σ'v for model analysis	Qw/Qp
1881.09		0.09		0.35		307.56			
784.32	1332.70	0.17	0.13	0.48	0.42	160.02	233.79		12.01
1078.43		0.26		0.67		107.83			
784.32	931.37	0.34	0.30	0.80	0.73	81.14	94.49		9.38
1176.47		0.42		1.00		64.93			
1176.47	1176.47	0.51	0.47	1.20	1.10	54.03	59.48	55.06	9.04
2549.03		0.59		1.63		46.21			
1470.59	2009.81	0.67	0.63	1.88	1.76	40.32	43.26		10.64
2058.83		0.76		2.23		35.72			
1470.59	1764.71	0.84	0.80	2.48	2.36	32.04	33.88	32.26	11.30
5784.33		0.92		3.47		29.02			
2745.10	4264.72	1.01	0.97	3.93	3.70	26.50	27.76	27.76	14.67

5/29/2003 20DW8-.8125
371

Vj/Ir	Average Vj/IR	Depth (ft)	Average Depth (ft)	time (min)	Average Time (min)	qapp/σ'v	average qapp/σ'v	average qapp/ σ'v for model analysis	Qw/Qp
332.84		0.11		0.10		247.00			
519.78		0.19		0.22		140.77			
297.02	383.21	0.28	0.19	0.28	0.20	98.17	161.98		7.86
668.29		0.36		0.43		75.21			
148.51	408.40	0.44	0.40	0.47	0.45	60.85	68.03		8.55
594.04		0.53		0.60		51.03		55.94	8.60
445.53	519.78	0.61	0.57	0.70	0.65	43.88	47.45		8.74
891.06		0.69		0.90		38.44			
445.53	668.29	0.78	0.74	1.00	0.95	34.17	36.31		9.88
1262.33		0.86	0.82	1.28	1.14	30.73		32.45	10.67
445.53	853.93	0.94	0.90	1.38	1.33	27.89	29.31		11.31
2301.90		1.03		1.90		25.51		25.63	12.90
1113.82	1707.86	1.11	1.07	2.15	2.03	23.49	24.50	23.59	14.50
3415.72		1.19		2.92		21.75			
2227.64	2821.68	1.28	1.24	3.42	3.17	20.24	21.00	20.30	19.62
5866.12		1.36		4.73		18.91			
4009.76	4937.94	1.44	1.40	5.63	5.18	17.74	18.33	18.33	28.30

5/29/2003 20DW8-.5
980

Vj/Ir	Average Vj/IR	Depth (ft)	Average Depth (ft)	time (min)	Average Time (min)	qapp/σ'v	average qapp/σ'v	average qapp/ σ'v for model analysis	Qw/Qp
1477.24		0.08		0.12		354.03			
196.08	836.66	0.16	0.12	0.13	0.13	169.77	261.90		8.04
784.32		0.24		0.20		111.32			
588.24	686.28	0.33	0.29	0.25	0.23	82.63	96.98		6.03
588.24		0.41		0.30		65.57			
588.24	588.24	0.49	0.45	0.35	0.33	54.27	59.92	55.36	5.50
588.24		0.58		0.40		46.23			
1176.47	882.36	0.66	0.62	0.50	0.45	40.22	43.23		5.57
196.08		0.74		0.52		35.56			
196.08	196.08	0.83	0.79	0.53	0.53	31.83	33.69	32.06	5.12
2549.03		0.91		0.75		28.79			
3333.34	2941.18	0.99	0.95	1.03	0.89	26.26	27.52	26.39	7.17
1568.63		1.08		1.17		24.11			
392.16	980.39	1.16	1.12	1.20	1.18	22.28	23.20	23.20	8.10
588.24		1.24		1.25		20.69		20.00	7.90
1176.47	882.36	1.33	1.29	1.35	1.30	19.30	20.00		7.75
784.32		1.41		1.42		18.08			
3529.42	2156.87	1.49	1.45	1.72	1.57	16.99	17.53	17.03	8.26
6666.68		1.58		2.28		16.02			
392.16	3529.42	1.66	1.62	2.32	2.30	15.14	15.58		10.88
1960.79		1.74		2.48		14.35			
1176.47	1568.63	1.83	1.79	2.58	2.53	13.63	13.99		10.87
980.39		1.91		2.67		12.97			
1960.79	1470.59	1.99	1.95	2.83	2.75	12.37	12.67	12.39	10.79
7843.16		2.08		3.50		11.82			
8823.55	8333.35	2.16	2.12	4.25	3.88	11.31	11.56		14.01
1960.79		2.24		4.42		10.83			
11764.73	6862.76	2.33	2.29	5.42	4.92	10.39	10.61		16.48
1372.55		2.41		5.53		9.99			
1568.63	1470.59	2.49	2.45	5.67	5.60	9.60	9.79		17.49

Table A- 8 Full Depth Tests Data (Concrete Sand) – continued

5/30/2003 20DW8-.625									
627									
Vj/Ir	Average Vj/IR	Depth (ft)	Average Depth (ft)	time (min)	Average Time (min)	qapp/σ'v	average qapp/σ'v	average qapp/ σ'v for model analysis	Qw/Qp
1129.41		0.08		0.15		341.57			
376.47	752.94	0.17	0.13	0.20	0.18	170.04	255.81		10.72
627.45		0.25		0.28		112.87			
125.49	376.47	0.33	0.29	0.30	0.29	84.28	98.57		7.66
878.43		0.42		0.42		67.13			
1003.92	941.18	0.50	0.46	0.55	0.48	55.69	61.41	56.78	8.08
1003.92		0.58		0.68		47.52			
501.96	752.94	0.67	0.63	0.75	0.72	41.40	44.46		8.78
1003.92		0.75		0.88		36.63			
878.43	941.18	0.83	0.79	1.00	0.94	32.82	34.73	33.05	9.11
2258.83		0.92		1.30		29.70			
1756.87	2007.85	1.00	0.96	1.53	1.42	27.10	28.40	27.24	11.32
1756.87		1.08		1.77		24.90			
1254.90	1505.89	1.17	1.13	1.93	1.85	23.02	23.96	23.10	12.60
878.43		1.25		2.05		21.38			
878.43	878.43	1.33	1.29	2.17	2.11	19.95	20.67	20.01	12.50
10290.22		1.42		3.53		18.69			
9160.81	1631.38	1.50	1.46	4.75	4.14	17.57	18.13	17.61	21.76
2384.32		1.58		5.07		16.57			
2635.30	2509.81	1.67	1.63	5.42	5.24	15.67	16.12		24.71
3764.71		1.75		5.92		14.85			
878.43	2321.57	1.83	1.79	6.03	5.98	14.11	14.48		25.55

6/2/2003 10DW8-.625									
314									
Vj/Ir	Average Vj/IR	Depth (ft)	Average Depth (ft)	time (min)	Average Time (min)	qapp/σ'v	average qapp/σ'v	average qapp/ σ'v for model analysis	Qw/Qp
627.20		0.08		0.17		342.05			
9725.51	5176.36	0.17	0.13	2.75	1.46	170.31	256.18		44.67
8470.61		0.25		5.00		113.05			
13176.50	10823.55	0.33	0.29	8.50	6.75	84.42	98.74		88.63

6/3/2003 20DW8-.625									
627									
Vj/Ir	Average Vj/IR	Depth (ft)	Average Depth (ft)	time (min)	Average Time (min)	qapp/σ'v	average qapp/σ'v	average qapp/ σ'v for model analysis	Qw/Qp
878.40		0.08		0.12		341.15			
376.47	627.43	0.17	0.13	0.17	0.14	169.84	255.50		8.68
376.47		0.25		0.22		112.73			
878.43	627.45	0.33	0.29	0.33	0.28	84.18	98.45		7.22
627.45		0.42		0.42		67.05			
1129.41	878.43	0.50	0.46	0.57	0.49	55.62	61.33	56.71	8.22
376.47		0.58		0.62		47.47			
1380.40	878.43	0.67	0.63	0.80	0.71	41.35	44.41		8.68
627.45		0.75		0.88		36.59			
1882.36	1254.90	0.83	0.79	1.13	1.01	32.78	34.68	33.01	9.76
752.94		0.92		1.23		29.67			
2886.28	1819.61	1.00	0.96	1.62	1.43	27.07	28.37	27.20	11.39
3639.22		1.08		2.10		24.87			
1756.87	2698.05	1.17	1.13	2.33	2.22	22.99	23.93	23.07	15.09
4015.70		1.25		2.87		21.36			
2007.85	3011.77	1.33	1.29	3.13	3.00	19.93	20.64	20.64	17.79

6/25/03 10DW8-.625									
314									
Vj/Ir	Average Vj/IR	Depth (ft)	Average Depth (ft)	time (min)	Average Time (min)	qapp/σ'v	average qapp/σ'v	average qapp/ σ'v for model analysis	Qw/Qp
940.80		0.08		0.25		333.69			
2007.85		0.17		0.78		166.15			
4768.64	3388.24	0.25	0.21	2.05	1.42	110.29	138.22		52.08
4517.66		0.33		3.25		82.36			
10352.97	7435.31	0.42	0.38	6.00	4.63	65.60	73.98		94.47

Table A- 9 Full Depth Tests Data (Mortar Sand)

Full Depth Tests - Mortar Sand

4/17/2003 20DU8-.625
626

Vj/Ir	Average Vj/IR	Depth (ft)	Average Depth (ft)	time (min)	Average Time (min)	qapp/σ'v	average qapp/σ'v	average qapp/σ'v for model analysis	Qw/Qp
1611.64		0.06		0.15		517.98			
125.49		0.14		0.17		212.50			
250.98	662.70	0.23	0.14	0.20	0.17	133.23	287.90		9.28
250.98		0.31		0.23		96.81			
376.47	313.73	0.39	0.35	0.28	0.26	75.88	86.34		5.64
501.96		0.48		0.35		62.29			
501.96	501.96	0.56	0.52	0.42	0.38	52.76	57.52	53.58	5.67
627.45		0.64		0.50		45.70			
627.45	627.45	0.73	0.68	0.58	0.54	40.27	42.99		6.06
501.96		0.81		0.65		35.95			
752.94	627.45	0.89	0.85	0.75	0.70	32.45	34.20	30.99	6.29
1003.92		0.98		0.88		29.54			
878.43	941.18	1.06	1.02	1.00	0.94	27.09	28.31		7.08
878.43		1.14	1.10	1.12	1.06	25.00		26.04	7.35
1129.41	1003.92	1.23	1.18	1.27	1.19	23.19	24.09		7.69
376.47		1.31		1.32		21.61			
878.43	627.45	1.39	1.35	1.43	1.38	20.22	20.92	20.28	7.78
878.43		1.48		1.55		18.99			
878.43	878.43	1.56	1.52	1.67	1.61	17.89	18.44		8.10
1003.92		1.64		1.80		16.90			
3011.77	2007.85	1.73	1.68	2.20	2.00	16.01	16.46		9.08
878.43		1.81		2.32		15.20		15.22	9.79
1505.89	1192.16	1.89	1.85	2.52	2.42	14.46	14.83		9.98
3764.71		1.98		3.02		13.78			
1129.41	2447.06	2.06	2.02	3.17	3.09	13.16	13.47		11.71
627.45		2.14		3.25		12.59			
2007.85	1317.65	2.23	2.18	3.52	3.38	12.06	12.32		11.84
1505.89		2.31		3.72		11.57			
1756.87	1631.38	2.39	2.35	3.95	3.83	11.11	11.34		12.46
2760.79		2.48		4.32		10.68			
1003.92	1882.36	2.56	2.52	4.45	4.38	10.28	10.48	10.48	13.31

5/8/2003 20DU8-.625
626

Vj/Ir	Average Vj/IR	Depth (ft)	Average Depth (ft)	time (min)	Average Time (min)	qapp/σ'v	average qapp/σ'v	average qapp/σ'v for model analysis	Qw/Qp
534.48		0.11		0.09		283.96			
690.20	612.34	0.19	0.15	0.18	0.14	159.34	221.65		7.04
376.47		0.27		0.23		110.44			
376.47	376.47	0.36	0.32	0.28	0.26	84.33	97.39		6.25
501.96		0.44		0.35		68.09			
501.96	501.96	0.52	0.48	0.42	0.38	57.02	62.55		6.07
501.96		0.61		0.48		48.98		53.00	6.08
250.98	376.47	0.69	0.65	0.52	0.50	42.88	45.93		5.88
752.94		0.77		0.62		38.09			
376.47	564.71	0.86	0.82	0.67	0.64	34.23	36.16		6.01
752.94		0.94		0.77		31.06			
878.43	815.69	1.02	0.98	0.88	0.83	28.40	29.73	29.73	6.41
878.43		1.11		1.00		26.15			
878.43	878.43	1.19	1.11	1.12	1.00	24.20	25.18	26.25	6.90
752.94		1.27		1.22		22.52			
1003.92	878.43	1.36	1.32	1.35	1.28	21.04	21.78		7.45
1756.87		1.44	1.40	1.58	1.47	19.73		20.38	8.01
2007.85	1882.36	1.52	1.48	1.85	1.72	18.56	19.15		8.85
1003.92		1.61		1.98		17.52			
1003.92	1003.92	1.69	1.65	2.12	2.05	16.58	17.05		9.50
2886.28		1.77		2.50		15.72			
1631.38	2258.83	1.86	1.82	2.72	2.61	14.94	15.33	15.33	10.97
1505.89		1.94		2.92		14.23			
1003.92	1254.90	2.02	1.98	3.05	2.98	13.58	13.91		11.50
878.43		2.11		3.17		12.98			
627.45	752.94	2.19	2.15	3.25	3.21	12.43	12.71		11.41
3137.26		2.27		3.67		11.91			
2258.83	2698.05	2.36	2.32	3.97	3.82	11.44	11.68		12.59

4/15/2003 10DU8-.8125
186

Vj/Ir	Average Vj/IR	Depth (ft)	Average Depth (ft)	time (min)	Average Time (min)	qapp/σ'v	average qapp/σ'v	average qapp/σ'v for model analysis	Qw/Qp
560.55		0.09		0.28		332.07			
482.66		0.18		0.50		175.11			
816.80	649.73	0.26	0.22	0.87	0.68	118.57	146.84		11.96
1188.08		0.34		1.40		89.44			
1633.60	1410.84	0.43	0.39	2.13	1.77	71.67	80.55		17.55
1930.62		0.51		3.00		59.71			22.51
1893.50	1912.06	0.59	0.55	3.85	3.43	51.10	55.40		23.76
1782.11		0.68		4.65		44.61			
5234.96	3508.54	0.76	0.72	7.00	5.83	39.54	42.08		31.04

Table A- 10 Full Depth Tests Data (Mortar Sand) – continued

4/11/2003 10DU8-.8125									
186									
Vj/Ir	Average Vj/IR	Depth (ft)	Average Depth (ft)	time (min)	Average Time (min)	qapp/σ'v	average qapp/σ'v	average qapp/σ'v for model analysis	Qw/Qp
691.02		0.08		0.28		386.54			
482.66	586.84	0.16	0.12	0.50	0.39	183.72	285.13		12.74
297.02		0.24		0.63		120.13			
1039.57	668.29	0.33	0.28	1.10	0.87	89.04	104.59		11.67
779.67		0.41		1.45		70.61			
1373.71	1076.69	0.49	0.45	2.07	1.76	58.41	64.51		16.06

4/15/2003 20DU8-.8125	Incremental Test								
372									
Vj/Ir	Average Vj/IR	Depth (ft)	Average Depth (ft)	time (min)	Average Time (min)	qapp/σ'v	average qapp/σ'v	average qapp/σ'v for model analysis	Qw/Qp
1113.82		0.83		0.08		35.95			
891.06	1002.44	0.92	0.88	0.45	0.27	32.53	34.24		2.33
594.04		1.00		0.58		29.68			
742.55	668.29	1.08	1.04	0.75	0.67	27.27	28.48		4.89
742.55		1.17		0.92		25.21			
1113.82	928.18	1.25	1.21	1.17	1.04	23.42	24.32		6.59
1336.59		1.33		1.47		21.86			
965.31	1150.95	1.42	1.38	1.68	1.58	20.47	21.16		8.75
594.04		1.50		1.82		19.25			
1559.35	1076.69	1.58	1.54	2.17	1.99	18.15	18.70		9.87
1262.33		1.67		2.45		17.16			
965.31	1113.82	1.75	1.71	2.67	2.56	16.26	16.71		11.44
742.55		1.83		2.83		15.45			
3341.46	2042.01	1.92	1.88	3.58	3.21	14.71	15.08		13.07
2079.13		2.00		4.05		14.03			
2227.64	2153.39	2.08	2.04	4.55	4.30	13.40	13.71		16.09
1039.57		2.17		4.78		12.82			
1559.35	1299.46	2.25	2.21	5.13	4.96	12.29	12.56		17.15
1707.86		2.33		5.52		11.79			
4158.26	2933.06	2.42	2.38	6.45	5.98	11.33	11.56		19.25

4/16/2003 10DU8-.5									
490									
Vj/Ir	Average Vj/IR	Depth (ft)	Average Depth (ft)	time (min)	Average Time (min)	qapp/σ'v	average qapp/σ'v	average qapp/σ'v for model analysis	Qw/Qp
782.26		0.13		0.20		249.84			
490.20	636.23	0.21	0.17	0.28	0.24	149.40	199.62		5.54
588.24		0.29		0.38		106.30			
1078.43	833.34	0.38	0.33	0.57	0.48	82.33	94.31		5.45
686.28		0.46		0.68		67.08			
980.39	833.34	0.54	0.50	0.85	0.77	56.51	61.79	56.50	5.87
980.39		0.63		1.02		48.76			
1372.55	1176.47	0.71	0.67	1.25	1.13	42.83	45.80		6.51
882.36		0.79		1.40		38.16			
5490.21	3186.28	0.88	0.83	2.33	1.87	34.37	36.26		8.58
1568.63		0.96		2.60		31.24			
10000.02	5784.33	1.04	1.00	4.30	3.45	28.61	29.92	29.92	13.21
1176.47		1.13		4.50		26.37			
7843.16	4509.81	1.21	1.69	5.83	7.32	24.44	25.40	26.47	16.60

4/16/2003 20DU8-.5	Incremental Test								
980									
Vj/Ir	Average Vj/IR	Depth (ft)	Average Depth (ft)	time (min)	Average Time (min)	qapp/σ'v	average qapp/σ'v	average qapp/σ'v for model analysis	Qw/Qp
132.93		1.48		0.20		19.73			
784.32	458.62	1.56	1.52	0.27	0.23	18.58	19.16		1.18
196.08		1.64		0.28		17.56			
2549.03	1372.55	1.73	1.68	0.50	0.39	16.63	17.09		1.78
784.32		1.81		0.57		15.79			
1764.71	1274.51	1.89	1.85	0.72	0.64	15.02	15.41		2.65
784.32		1.98		0.78		14.32			
1176.47	980.39	2.06	2.02	0.88	0.83	13.67	14.00		3.16
392.16		2.14		0.92		13.08			
1764.71	1078.43	2.23	2.18	1.07	0.99	12.53	12.80		3.47
784.32		2.31		1.13		12.01			
1568.63	1176.47	2.39	2.35	1.27	1.20	11.54	11.78		3.90
2745.10		2.48		1.50		11.09			
1960.79	2352.95	2.56	2.52	1.67	1.58	10.68	10.89		4.81
3921.58		2.64		2.00		10.29			
2549.03	3235.30	2.73	2.68	2.22	2.11	9.93	10.11		6.00
1960.79		2.81		2.38		9.58			
6274.52	4117.66	2.89	2.85	2.92	2.65	9.26	9.42		7.10

Table A- 11 Full Depth Tests Data (Mortar Sand) – continued

4/17/2003 20DU8-.5									
980									
Vj/Ir	Average Vj/IR	Depth (ft)	Average Depth (ft)	time (min)	Average Time (min)	qapp/σ'v	average qapp/σ'v	average qapp/σ'v for model analysis	Qw/Qp
1272.37		0.09		0.12		349.19			
392.16		0.17		0.15		180.42			
392.16	685.56	0.26	0.17	0.18	0.15	121.28	216.96		6.62
392.16		0.34		0.22		91.15			
196.08	294.12	0.42	0.38	0.23	0.23	72.88	82.01		4.51
784.32		0.51		0.30		60.62			
392.16	588.24	0.59	0.55	0.33	0.32	51.82	56.22	56.22	4.41
392.16		0.67		0.37		45.21			
784.32	588.24	0.76	0.71	0.43	0.40	40.05	42.63		4.27
980.39		0.84		0.52		35.91			
784.32	882.36	0.92	0.88	0.58	0.55	32.52	34.21		4.77
980.39		1.01		0.67		29.69		29.84	5.06
392.16	686.28	1.09	1.05	0.70	0.68	27.30	28.49		4.98
1176.47		1.17	1.17	0.80	0.79	25.24		25.33	5.17
980.39	1078.43	1.26	1.21	0.88	0.84	23.46	24.35		5.29
1176.47		1.34		0.98		21.90			
1372.55	1274.51	1.42	1.38	1.10	1.04	20.52	21.21	20.57	5.76
1176.47		1.51		1.20		19.29			
1372.55	1274.51	1.59	1.55	1.32	1.26	18.20	18.74		6.21
1176.47		1.67		1.42		17.21			
1176.47	1176.47	1.76	1.71	1.52	1.47	16.31	16.76		6.53
392.16		1.84		1.55		15.50			
1176.47	784.32	1.92	1.88	1.65	1.60	14.76	15.13	14.78	6.50
1372.55		2.01		1.77		14.08			
1568.63	1470.59	2.09	2.05	1.90	1.83	13.45	13.76		6.84
392.16		2.17		1.93		12.87			
2549.03	1470.59	2.26	2.21	2.15	2.04	12.34	12.60		7.04
392.16		2.34		2.18		11.84			
4117.66	2254.91	2.42	2.38	2.53	2.36	11.37	11.61		7.57
3333.34		2.51	2.46	2.82	2.61	10.94	11.17		8.08
1176.47	2254.91	2.59	2.55	2.92	2.87	10.54	10.74		8.60
2745.10		2.67		3.15		10.16			
1764.71	2254.91	2.76	2.71	3.30	3.23	9.80	9.98	9.98	9.08
8235.31		2.84		4.00		9.47			
4901.97	6568.64	2.92	2.88	4.42	4.21	9.15	9.31		11.16

45 Deg 7-7-03 10 DU8 0.5	Angled Jet Test								
490									
Vj/Ir	Average Vj/IR	Depth (ft)	Average Depth (ft)	time (min)	Average Time (min)	qapp/σ'v	average qapp/σ'v	average qapp/σ'v for model analysis	Qw/Qp
392.16		0.08		0.07		365.29			
196.08	294.12	0.17	0.13	0.10	0.08	181.85	273.57		2.55
392.16		0.25		0.17		120.70			
294.12	343.14	0.33	0.29	0.22	0.19	90.13	105.42		2.52
294.12		0.42		0.27		71.79			
294.12	294.12	0.50	0.46	0.32	0.29	59.56	65.67		2.44
392.16		0.58		0.38		50.82			
294.12	343.14	0.67	0.63	0.43	0.41	44.27	47.55		2.50
392.16		0.75		0.50		39.17			
196.08	294.12	0.83	0.79	0.53	0.52	35.10	37.14		2.50
392.16		0.92		0.60		31.76			
294.12	343.14	1.00	0.96	0.65	0.63	28.98	30.37		2.50
490.20		1.08		0.73		26.63			
490.20	490.20	1.17	1.13	0.82	0.78	24.62	25.62		2.64
490.20		1.25		0.90		22.87			
980.39	735.30	1.33	1.29	1.07	0.98	21.34	22.10		2.92
1470.59		1.42		1.32		19.99			
882.36	1176.47	1.50	1.46	1.47	1.39	18.79	19.39		3.66
2941.18		1.58		1.97		17.72			
392.16	1666.67	1.67	1.63	2.03	2.00	16.75	17.24		4.71
1274.51		1.75		2.25		15.88			
1176.47	1225.49	1.83	1.79	2.45	2.35	15.09	15.48		5.02
1568.63		1.92		2.72		14.36			
588.24	1078.43	2.00	1.96	2.82	2.77	13.70	14.03		5.41
2549.03		2.08		3.25		13.09			
1666.67	2107.85	2.17	2.13	3.53	3.39	12.52	12.80		6.11
784.32		2.25		3.67		12.00			
784.32	784.32	2.33	2.29	3.80	3.73	11.51	11.76		6.24
2156.87		2.42		4.17		11.06			
784.32	1470.59	2.50	2.46	4.30	4.23	10.64	10.85		6.60
1176.47		2.58		4.50		10.24			
3333.34	2254.91	2.67	2.63	5.07	4.78	9.88	10.06		6.98
3529.42		2.75		5.67		9.53			
6568.64	5049.03	2.83	2.79	6.78	6.23	9.20	9.36		8.54

Table A- 12 Full Depth Tests Data (Mortar Sand) – continued

45 Deg 7-8-03 10 DU8 0.625	Angled Jet Test								
314									
Vj/Ir	Average Vj/IR	Depth (ft)	Average Depth (ft)	time (min)	Average Time (min)	qapp/σ'v	average qapp/σ'v	average qapp/σ'v for model analysis	Qw/Qp
313.73		0.08		0.08		379.30			
125.49	219.61	0.17	0.13	0.12	0.10	188.83	284.06		3.06
376.47		0.25		0.22		125.33			
250.98	313.73	0.33	0.29	0.28	0.25	93.59	109.46		3.28
313.73		0.42		0.37		74.54			
313.73	313.73	0.50	0.46	0.45	0.41	61.84	68.19		3.41
376.47		0.58		0.55		52.77			
376.47	376.47	0.67	0.63	0.65	0.60	45.97	49.37		3.68
376.47		0.75		0.75		40.68			
439.22	407.84	0.83	0.79	0.87	0.81	36.44	38.56		3.91
439.22		0.92		0.98		32.98			
439.22	439.22	1.00	0.96	1.10	1.04	30.10	31.54		4.16
1003.92		1.08		1.37		27.65			
941.18	972.55	1.17	1.13	1.62	1.49	25.56	26.61		5.08
1254.90		1.25		1.95		23.75			
878.43	1066.67	1.33	1.29	2.18	2.07	22.16	22.95		6.13
941.18		1.42		2.43		20.76			
564.71	752.94	1.50	1.46	2.58	2.51	19.51	20.14		6.59
1003.92		1.58		2.85		18.40			
439.22	721.57	1.67	1.63	2.97	2.91	17.40	17.90		6.86
941.18		1.75		3.22		16.49			
627.45	784.32	1.83	1.79	3.38	3.30	15.67	16.08		7.05
815.69		1.92		3.60		14.91			
439.22	627.45	2.00	1.96	3.72	3.66	14.22	14.57		7.16
2007.85		2.08		4.25		13.59			
815.69	1411.77	2.17	2.13	4.47	4.36	13.00	13.29		7.86
878.43		2.25		4.70		12.46			
1003.92	941.18	2.33	2.29	4.97	4.83	11.95	12.21		8.08
1066.67		2.42		5.25		11.49			
941.18	1003.92	2.50	2.46	5.50	5.38	11.05	11.27		8.37
1317.65		2.58		5.85		10.64			
1129.41	1223.53	2.67	2.63	6.15	6.00	10.25	10.45		8.75
1694.12		2.75		6.60		9.89			
1254.90	1474.51	2.83	2.79	6.93	6.77	9.55	9.72		9.28
4329.42		2.92		8.08		9.23			
2823.54	3576.48	3.00	2.96	8.83	8.46	8.93	9.08		10.95

45 Deg 7-8-03 10 DU8 0.8125	Angled Jet Test								
186									
Vj/Ir	Average Vj/IR	Depth (ft)	Average Depth (ft)	time (min)	Average Time (min)	qapp/σ'v	average qapp/σ'v	average qapp/σ'v for model analysis	Qw/Qp
185.64		0.08		0.08		370.00			
185.64	185.64	0.17	0.13	0.17	0.13	184.20	277.10		3.83
148.51		0.25		0.23		122.26			
259.89	204.20	0.33	0.29	0.35	0.29	91.29	106.78		3.83
148.51		0.42		0.42		72.71			
222.76	185.64	0.50	0.46	0.52	0.47	60.33	66.52		3.90
185.64		0.58		0.60		51.48			
259.89	222.76	0.67	0.63	0.72	0.66	44.84	48.16		4.03
148.51		0.75		0.78		39.68			
259.89	204.20	0.83	0.79	0.90	0.84	35.55	37.62		4.07
371.27		0.92		1.07		32.17			
853.93	612.60	1.00	0.96	1.45	1.26	29.36	30.77		5.03
965.31		1.08		1.88		26.98			
1299.46	1132.38	1.17	1.13	2.47	2.18	24.93	25.95		7.41
1039.57		1.25		2.93		23.16			
1373.71	1206.64	1.33	1.29	3.55	3.24	21.62	22.39		9.61
1188.08		1.42		4.08		20.25			
705.42	946.75	1.50	1.46	4.40	4.24	19.03	19.64		11.14
1002.44		1.58		4.85		17.95			
1262.33	1132.38	1.67	1.63	5.42	5.13	16.97	17.46		12.10
2524.66		1.75		6.55		16.09			
2487.53	2506.10	1.83	1.79	7.67	7.11	15.28	15.68		15.20
1893.50		1.92		8.52		14.55			
4789.43	3341.46	2.00	1.96	10.67	9.59	13.87	14.21		18.76

Table A- 13 Full Depth Tests Data (Cherry Branch Sand)

Full Tests - Cherry Branch Sand

5/21/2003 10DU8-.8125									
186									
Vj/Ir	Average Vj/IR	Depth (ft)	Average Depth (ft)	time (min)	Average Time (min)	qapp/σ'v	average qapp/σ'v	average qapp/σ'v for model analysis	Qw/Qp
2203.83		0.06		0.72		655.87			
891.06	1547.44	0.14	0.10	1.12	0.92	275.11	465.49		34.41
1150.95		0.23		1.63		173.87			
1633.60	1392.28	0.31	0.27	2.37	2.00	126.99	150.43		28.51
668.29		0.39		2.67		99.96			
1744.99	1206.64	0.48	0.44	3.45	3.06	82.37	91.16		26.91
1225.20		0.56		4.00		70.01			
1744.99	1485.09	0.64	0.60	4.78	4.39	60.86	65.44		27.94
1076.69		0.73		5.27		53.80		57.33	27.75
2190.51	1633.60	0.81	0.77	6.25	5.76	48.19	51.00		28.69

5/22/2003 10DU8-.625									
313									
Vj/Ir	Average Vj/IR	Depth (ft)	Average Depth (ft)	time (min)	Average Time (min)	qapp/σ'v	average qapp/σ'v	average qapp/σ'v for model analysis	Qw/Qp
5271.57		0.04		0.72		907.78			
690.20	2980.88	0.21	0.13	1.08	0.90	183.36	545.57		27.36
1568.63		0.29		1.50		130.58			
878.43	1223.53	0.38	0.33	1.73	1.62	101.19	115.88		18.52
1694.12		0.46		2.18		82.46			
1380.40	1537.26	0.54	0.50	2.55	2.37	69.49	75.98		18.09
1505.89		0.63		2.95		59.97			
1631.38	1568.63	0.71	0.67	3.38	3.17	52.69	56.33	56.33	18.17
2258.83		0.79		3.98		46.94			
1317.65	1788.24	0.88	0.83	4.33	4.16	42.28	44.61		19.09
2509.81		0.96		5.00		38.43			
941.18	1725.49	1.04	1.00	5.25	5.13	35.20	36.81		19.61
2635.30		1.13		5.95		32.44			
1443.14	2039.22	1.21	1.17	6.33	6.14	30.07	31.26		20.15
2572.56		1.29	1.25	7.02	6.68	28.00		29.04	20.44
1819.61	2196.08	1.38	1.33	7.50	7.26	26.18	27.09		20.84
2572.56		1.46		8.18		24.57		26.25	20.84
2447.06	2509.81	1.54	1.50	8.83	8.51	23.14	23.85		21.71
3137.26		1.63		9.67		21.85			
2635.30	2886.28	1.71	1.67	10.37	10.02	20.68	21.27		23.01
1756.87		1.79		10.83		19.63		20.16	23.15
1882.36	1819.61	1.88	1.83	11.33	11.08	18.67	19.15		23.14
1568.63		1.96		11.75		17.79			
1882.36	1725.49	2.04	2.00	12.25	12.00	16.98	17.38		22.97
2258.83		2.13		12.85		16.23			
2133.34	2196.08	2.21	2.17	13.42	13.13	15.55	15.89		23.21
3701.97		2.29		14.40		14.91		15.23	24.06
4329.42	4015.70	2.38	2.33	15.55	14.98	14.31	14.61		24.57

Table A- 14 Full Depth Tests Data (Cherry Branch Sand) – continued

5/22/2003 20DU8-.8125 371									
Vj/Ir	Average Vj/IR	Depth (ft)	Average Depth (ft)	time (min)	Average Time (min)	qapp/σ'v	average qapp/σ'v	average qapp/σ'v for model analysis	Qw/Qp
1588.27		0.06		0.27		649.34			
668.29	1128.28	0.15	0.10	0.42	0.34	276.66	463.00		25.17
519.78		0.23		0.53		175.22			
445.53	482.66	0.31	0.27	0.63	0.58	127.91	151.56		16.51
371.27		0.40		0.72		100.52			
519.78	445.53	0.48	0.44	0.83	0.78	82.67	91.59		13.58
594.04		0.56		0.97		70.10			
445.53	519.78	0.65	0.60	1.07	1.02	60.78	65.44		12.89
668.29		0.73		1.22		53.59		57.19	12.78
668.29	668.29	0.81	0.77	1.37	1.29	47.88	50.74		12.84
891.06		0.90		1.57		43.23			
668.29	779.67	0.98	0.94	1.72	1.64	39.37	41.30		13.42
891.06		1.06		1.92		36.11			
965.31	928.18	1.15	1.10	2.13	2.03	33.33	34.72		14.05
668.29		1.23		2.28		30.93			
519.78	594.04	1.31	1.27	2.40	2.34	28.83	29.88	29.88	14.12
742.55		1.40		2.57		26.98			
668.29	705.42	1.48	1.44	2.72	2.64	25.35	26.17	26.17	14.08
371.27		1.56		2.80		23.88			
891.06	631.17	1.65	1.60	3.00	2.90	22.56	23.22		13.85
1039.57		1.73		3.23		21.38			
816.80	928.18	1.81	1.77	3.42	3.33	20.30	20.84	20.33	14.38
965.31		1.90		3.63		19.31			
2004.88	1485.09	1.98	1.94	4.08	3.86	18.41	18.86		15.26
1336.59		2.06		4.38		17.58			
1188.08	1262.33	2.15	2.10	4.65	4.52	16.81	17.20		16.44
1707.86		2.23		5.03		16.11			
891.06	1299.46	2.31	2.27	5.23	5.13	15.45	15.78		17.32
965.31		2.40		5.45		14.84		15.14	17.43
1336.59	1150.95	2.48	2.44	5.75	5.60	14.27	14.55		17.60
1113.82		2.56		6.00		13.74			
1188.08	1150.95	2.65	2.60	6.27	6.13	13.24	13.49		18.04
1188.08		2.73		6.53		12.77			
816.80	1002.44	2.81	2.77	6.72	6.63	12.33	12.55		18.32
2079.13		2.90		7.18		11.91			
891.06	1485.09	2.98	2.94	7.38	7.28	11.52	11.72		18.99
1485.09		3.06		7.72		11.15			
2153.39	1819.24	3.15	3.10	8.20	7.96	10.80	10.97		19.64
891.06		3.23		8.40		10.46			
1336.59	1113.82	3.31	3.27	8.70	8.55	10.15	10.31	10.00	20.03
2376.15		3.40		9.23		9.85			
2895.93	2636.04	3.48	3.44	9.88	9.56	9.56	9.70		21.30
1782.11		3.56		10.28		9.29			
2079.13	1930.62	3.65	3.60	10.75	10.52	9.03	9.16		22.35

5/27/2003 10DU8-.5 490									
Vj/Ir	Average Vj/IR	Depth (ft)	Average Depth (ft)	time (min)	Average Time (min)	qapp/σ'v	average qapp/σ'v	average qapp/σ'v for model analysis	Qw/Qp
2107.09		0.13		0.55		299.55			
1078.43		0.21		0.73		180.61			
784.32	1323.28	0.29	0.21	0.87	0.72	128.96	203.04		12.99
1568.63		0.38		1.13		100.08			
882.36	1225.49	0.46	0.42	1.28	1.21	81.64	90.86		11.03
1274.51		0.54		1.50		68.84			
1078.43	1176.47	0.63	0.59	1.68	1.59	59.44	64.14		10.40
1372.55		0.71		1.92		52.24		55.84	10.32
1764.71	1568.63	0.79	0.75	2.22	2.07	46.55	49.40		10.51
2156.87		0.88		2.58		41.94			
1176.47	1666.67	0.96	0.92	2.78	2.68	38.13	40.04		11.18
2058.83		1.04		3.13		34.93			
1176.47	1617.65	1.13	1.09	3.33	3.23	32.20	33.57		11.40
1666.67		1.21		3.62		29.85		31.03	11.44
1470.59	1568.63	1.29	1.25	3.87	3.74	27.80	28.82		11.44
2941.18		1.38	1.38	4.37	4.27	26.00		26.06	11.86
1176.47	2058.83	1.46	1.42	4.57	4.47	24.40	25.20		12.05
2941.18		1.54		5.07		22.97			
1862.75	2401.97	1.63	1.59	5.38	5.23	21.70	22.33		12.62
3137.26		1.71		5.92		20.54			
1470.59	2303.93	1.79	1.75	6.17	6.04	19.49	20.02	20.02	13.20
2058.83		1.88		6.52		18.54			
784.32	1421.57	1.96	1.92	6.65	6.58	17.67	18.10		13.14
2549.03		2.04		7.08		16.87			
1274.51	1911.77	2.13	2.09	7.30	7.19	16.13	16.50		13.20
2549.03		2.21		7.73		15.44			
1764.71	2156.87	2.29	2.25	8.03	7.88	14.81	15.13	15.13	13.40
2745.10		2.38		8.50		14.22			
1764.71	2254.91	2.46	2.42	8.80	8.65	13.67	13.95		13.69

Table A- 15 Full Depth Tests Data (Cherry Branch Sand) – continued

6/27/2003 10DU8-.5 490									
Vj/Ir	Average Vj/IR	Depth (ft)	Average Depth (ft)	time (min)	Average Time (min)	qapp/σ'v	average qapp/σ'v	average qapp/σ'v for model analysis	Qw/Qp
2157.73		0.08		0.37		448.58			
588.24	1372.98	0.17	0.12	0.47	0.42	223.27	335.92		12.77
490.20		0.25		0.55		148.19			
294.12	392.16	0.33	0.29	0.60	0.58	110.65	129.42		7.55
392.16		0.42		0.67		88.13			
392.16	392.16	0.50	0.46	0.73	0.70	73.11	80.62		5.85
490.20		0.58		0.82		62.39			
490.20	490.20	0.67	0.62	0.90	0.86	54.35	58.37	54.94	5.26
392.16		0.75		0.97		48.09			
294.12	343.14	0.83	0.79	1.02	0.99	43.09	45.59		4.80
588.24		0.92		1.12		38.99			
392.16	490.20	1.00	0.96	1.18	1.15	35.58	37.29		4.60
1078.43		1.08		1.37		32.69			
392.16	735.30	1.17	1.12	1.43	1.40	30.22	31.45	30.33	4.77
1176.47		1.25		1.63		28.07			
686.28	931.37	1.33	1.29	1.75	1.69	26.20	27.13	26.27	5.02
1470.59		1.42		2.00		24.54			
980.39	1225.49	1.50	1.46	2.17	2.08	23.07	23.80		5.47
1764.71		1.58		2.47		21.75			
1470.59	1617.65	1.67	1.62	2.72	2.59	20.57	21.16	20.60	6.11
2156.87		1.75		3.08		19.49			
1960.79	2058.83	1.83	1.79	3.42	3.25	18.52	19.01		6.95
2058.83		1.92		3.77		17.63			
1568.63	1813.73	2.00	1.96	4.03	3.90	16.81	17.22		7.63
2450.99		2.08		4.45		16.06			
1568.63	2009.81	2.17	2.12	4.72	4.58	15.37	15.72	15.39	8.26
1960.79		2.25		5.05		14.73			
1862.75	1911.77	2.33	2.29	5.37	5.21	14.13	14.43		8.71
3039.22		2.42		5.88		13.58			
1078.43	2058.83	2.50	2.46	6.07	5.98	13.06	13.32		9.31
3137.26		2.58		6.60		12.58			
2941.18	3039.22	2.67	2.62	7.10	6.85	12.12	12.35		10.00
3039.22		2.75		7.62		11.70			
2549.03	2794.12	2.83	2.79	8.05	7.83	11.29	11.49		10.75
3823.54		2.92		8.70		10.92			
2843.14	3333.34	3.00	2.96	9.18	8.94	10.56	10.74		11.58
7156.88		3.08		10.40		10.22			
2941.18	5049.03	3.17	3.12	10.90	10.65	9.90	10.06	9.91	13.05
9509.83		3.25		12.52		9.60			
10784.34	10147.08	3.33	3.29	14.35	13.43	9.31	9.45		15.63

Table A- 16 Full Depth Tests Data (Mortar Sand + Kaolinite)

Full Depth Tests - Mortar Sand + Kaolinite

7-15-03 10KM8-0.5

490

Vj/Ir	Average Vj/IR	Depth (ft)	Average Depth (ft)	time (min)	Average Time (min)	qapp/σ'v	average qapp/σ'v	Qw/Qp
294.12		0.08		0.05		330.77		
294.12	294.12	0.17	0.13	0.10	0.08	164.66	247.72	2.30
294.12		0.25		0.15		109.30		
294.12	294.12	0.33	0.29	0.20	0.18	81.61	95.45	2.30
392.16		0.42		0.27		65.00		
588.24	490.20	0.50	0.46	0.37	0.32	53.93	59.47	2.65
980.39		0.58		0.53		46.02		
980.39	980.39	0.67	0.63	0.70	0.62	40.09	43.05	3.78
1568.63		0.75	0.71	0.97	0.83	35.47		4.94
980.39	1274.51	0.83	0.79	1.13	1.05	31.78	33.63	5.08
1078.43		0.92		1.32		28.76	30.27	
294.12	686.28	1.00	0.96	1.37	1.34	26.24	27.50	5.36
1274.51		1.08		1.58		24.11		
882.36	1078.43	1.17	1.13	1.73	1.66	22.29	23.20	5.65
1176.47		1.25		1.93		20.71		
1176.47	1176.47	1.33	1.29	2.13	2.03	19.32	20.02	6.03
2352.95		1.42		2.53		18.10		
1470.59	1911.77	1.50	1.46	2.78	2.66	17.02	17.56	6.98
4117.66		1.58		3.48		16.05		
1764.71	2941.18	1.67	1.63	3.78	3.63	15.17	15.61	8.56
2450.99		1.75		4.20		14.38		
1176.47	1813.73	1.83	1.79	4.40	4.30	13.66	14.02	9.19
1470.59		1.92		4.65		13.00		
1372.55	1421.57	2.00	1.96	4.88	4.77	12.40	12.70	9.32
1078.43		2.08		5.07		11.85		
980.39	1029.41	2.17	2.13	5.23	5.15	11.34	11.59	9.28
1470.59		2.25		5.48		10.86		
1078.43	1274.51	2.33	2.29	5.67	5.58	10.42	10.64	9.32

8-5-0310KM8-0.8125

186

Vj/Ir	Average Vj/IR	Depth (ft)	Average Depth (ft)	time (min)	Average Time (min)	qapp/σ'v	average qapp/σ'v	Qw/Qp
631.17		0.08		0.28		344.65		
334.15		0.17		0.43		171.58		
556.91	507.41	0.25	0.17	0.68	0.47	113.88	210.04	10.72
816.80		0.33		1.05		85.04		
668.29	742.55	0.42	0.38	1.35	1.20	67.73	76.38	12.26
1188.08	928.18	0.50	0.46	1.88	1.62	56.19	61.96	13.51
816.80	1002.44	0.58	0.54	2.25	2.07	47.95	52.07	14.61
1522.22		0.67		2.93		41.77		
1782.11	1652.17	0.75	0.71	3.73	3.33	36.96	39.37	19.07
2970.19		0.83		5.07		33.12		
2747.42	2858.81	0.92	0.88	6.30	5.68	29.97	31.54	24.88

8-6-0310KM8-.625

314

Vj/Ir	Average Vj/IR	Depth (ft)	Average Depth (ft)	time (min)	Average Time (min)	qapp/σ'v	average qapp/σ'v	Qw/Qp
690.20		0.08		0.18		338.95		
690.20	690.20	0.17	0.13	0.37	0.28	168.74	253.84	8.43
376.47		0.25		0.47		112.00		
627.45	501.96	0.33	0.29	0.63	0.55	83.63	97.82	7.22
439.22		0.42		0.75		66.61		
313.73	376.47	0.50	0.46	0.83	0.79	55.26	60.94	6.62
1003.92		0.58		1.10		47.16		
878.43	941.18	0.67	0.63	1.33	1.22	41.08	44.12	7.46
564.71		0.75	0.71	1.48		36.35	38.71	7.58
1003.92	784.32	0.83	0.79	1.75	1.62	32.57	34.46	7.82
941.18		0.92		2.00		29.47		8.36
2635.30	1788.24	1.00	0.96	2.70	2.35	26.89	28.18	9.39
752.94		1.08		2.90		24.71		
1066.67	909.81	1.17	1.13	3.18	3.04	22.84	23.78	10.36
815.69		1.25		3.40		21.22		
1819.61	1317.65	1.33	1.29	3.88	3.64	19.80	20.51	10.80
941.18		1.42		4.13		18.55		
1568.63	1254.90	1.50	1.46	4.55	4.34	17.44	17.99	11.40
690.20		1.58		4.73		16.44		
1192.16	941.18	1.67	1.63	5.05	4.89	15.55	15.99	11.53
1192.16		1.75		5.37		14.74		
3513.73	2352.95	1.83	1.79	6.30	5.83	14.00	14.37	12.47
3890.21		1.92		7.33		13.33		
5333.35	4611.78	2.00	1.96	8.75	8.04	12.71	13.02	15.73

Data Analysis and Model Development Data

Table A- 17 Data Analysis and Model Development Data (Concrete Sand)

Depth Analysis																				
	Depth (ft)	Time (min)	Vj/IR	Qw/Qp	Depth (ft)	Time (min)	Vj/IR	Qw/Qp	Depth (ft)	Time (min)	Vj/IR	Qw/Qp	Depth (ft)	Time (min)	Vj/IR	Qw/Qp	Depth (ft)	Time (min)	Vj/IR	Qw/Qp
5/29/2003 10DW8-.5	0.50	1.10	1176.47	9.04	1.00	3.70	4264.72	14.67	1.50	n/a	n/a	n/a	2.00	n/a	n/a	n/a	2.50	n/a	n/a	n/a
6/2/2003 10DW8-.625	0.50				1.00				1.50				2.00	n/a	n/a	n/a	2.50	n/a	n/a	n/a
6/25/03 10DW8-.625	0.50	4.63	7435.31	47.24	1.00				1.50				2.00	n/a	n/a	n/a	2.50	n/a	n/a	n/a
5/29/2003 20DW8-.8125	0.50	0.65	519.78	8.74	1.00	2.03	1707.86	14.50	1.50	5.18	4937.94	28.30	2.00	n/a	n/a	n/a	2.50	n/a	n/a	n/a
5/29/2003 20DW8-.5	0.50	0.33	588.24	5.50	1.00	0.89	2941.18	7.17	1.50	1.57	2156.87	8.26	2.00	2.75	1470.59	10.79	2.50	5.60	1470.59	17.49
5/30/2003 20DW8-.625	0.50	0.48	941.18	8.08	1.00	1.42	2007.85	11.32	1.50	4.14	1631.38	21.76	2.00	5.98	2321.57	25.55	2.50	n/a	n/a	n/a
6/3/2003 20DW8-.625	0.50	0.49	878.43	8.22	1.00	1.43	1819.61	11.39	1.50	3.00	3011.77	17.79	2.00	3.00	3011.77	17.79	2.50			

Bearing Pressure Analysis																				
	Depth (ft)	Time (min)	Qw/Qp	qapp/σ'v	Depth (ft)	Time (min)	Qw/Qp	qapp/σ'v	Depth (ft)	Time (min)	Qw/Qp	qapp/σ'v	Depth (ft)	Time (min)	Qw/Qp	qapp/σ'v	Depth (ft)	Time (min)	Qw/Qp	qapp/σ'v
5/29/2003 10DW8-.5	0.5	1.1	9.0	59.5	1.0	3.7	14.7	27.8	1.5	n/a	n/a		2.0	n/a	n/a		2.5	n/a	n/a	
6/2/2003 10DW8-.625	0.5				1.0				1.5				2.0	n/a	n/a		2.5	n/a	n/a	
6/25/03 10DW8-.625	0.5	4.6	47.2	74.0	1.0				1.5				2.0	n/a	n/a		2.5	n/a	n/a	
5/29/2003 20DW8-.8125	0.5	0.7	8.7	47.5	1.0	2.0	14.5	24.5	1.5	5.2	28.3	18.3	2.0	n/a	n/a		2.5	n/a	n/a	
5/29/2003 20DW8-.5	0.5	0.3	5.5	59.9	1.0	0.9	7.2	27.5	1.5	1.6	8.3	17.5	2.0	2.8	10.8	12.7	2.5	5.6	17.5	9.794778
5/30/2003 20DW8-.625	0.5	0.5	8.1	61.4	1.0	1.4	11.3	28.4	1.5	4.1	21.8	18.1	2.0	6.0	25.5	14.5	2.5	n/a	n/a	
6/3/2003 20DW8-.625	0.5	0.5	8.2	61.3	1.0	1.4	11.4	28.4	1.5	3.0	17.8	20.6	2.0				2.5			

Table A- 18 Data Analysis and Model Development Data (Mortar Sand)

Full Depth Tests - Mortar Sand

Test Description	Jet Velocity (ft/min)	Pile Dia. (in)	Ap (ft^2)	Dj (in)	Aj (ft^2)	Final Depth of Insertion (ft)	Ap/Aj	Q (ft^3/min)	Pile Volume (ft^3)	Time	Qw/Qp (Total)
4/15/2003 10DU8-.8125	186	8	0.35	0.81	0.0072	0.76	48.47	1.34	0.27	7.00	35.28
4/15/2003 20DU8-.8125	370	8	0.35	0.81	0.0072	2.43	48.47	2.67	0.85	6.45	20.30
4/16/2003 10DU8-.5	490	8	0.35	0.50	0.0027	1.21	128.00	1.34	0.42	5.83	18.45
4/16/2003 20DU8-.5	978	8	0.35	0.50	0.0027	2.90	128.00	2.67	1.01	2.90	7.65
4/17/2003 20DU8-.5	978	8	0.35	0.50	0.0027	2.92	128.00	2.67	1.02	4.42	11.57
4/17/2003 20DU8-.625	626	8	0.35	0.63	0.0043	2.56	81.92	2.67	0.89	4.45	13.28
4/11/2003 10DU8-.8125	186	8	0.35	0.81	0.0072	0.49	48.47	1.34	0.17	2.07	16.18
5/8/2003 20DU8-.625	626	8	0.35	0.63	0.0043	2.36	81.92	2.67	0.82	3.97	12.65
45 Deg 7-7-03 10 DU8 0.5	490	8	0.35	0.50	0.0027	2.83	128.00	1.34	0.99	6.78	9.17
45 Deg 7-8-03 10 DU8 0.625	314	8	0.35	0.63	0.0043	3.00	81.92	1.34	1.05	8.83	11.28
45 Deg 7-8-03 10 DU8 0.8125	186	8	0.35	0.81	0.0072	2.00	48.47	1.34	0.70	10.67	20.43

Test Description	Depth (ft)	Time (min)	Qw/Qp	qapp/σ'v	Depth (ft)	Time (min)	Qw/Qp	qapp/σ'v	Depth (ft)	Time (min)	Qw/Qp	qapp/σ'v
4/15/2003 10DU8-.8125	0.50	3.00	22.51	59.71	1.00				1.50			
4/15/2003 20DU8-.8125	0.50				1.00		4.89	28.48	1.50			
4/16/2003 10DU8-.5	0.50	0.77	5.87	61.79	1.00	3.45	13.21	29.92	1.50			
4/16/2003 20DU8-.5	0.50				1.00				1.50			
4/17/2003 20DU8-.5	0.50	0.32	4.41	56.22	1.00	0.68	4.98	28.49	1.50	1.26	6.21	18.74
4/17/2003 20DU8-.625	0.50	0.38	5.67	52.76	1.00	0.94	7.08	28.31	1.50	1.61	8.10	18.44
4/11/2003 10DU8-.8125	0.50	2.07	16.06		1.00				1.50			
5/8/2003 20DU8-.625	0.50	0.38	6.07	62.55	1.00	0.83	6.41	29.73	1.50	1.72	8.85	19.15
45 Deg 7-7-03 10 DU8 0.5	0.50	0.29	2.44	65.67	1.00	0.63	2.50	30.37	1.50	1.39	3.66	19.39
45 Deg 7-8-03 10 DU8 0.625	0.50	0.41	3.41	68.19	1.00	1.04	4.16	31.54	1.50	2.51	6.59	20.14
45 Deg 7-8-03 10 DU8 0.8125	0.50	0.47	3.90	66.52	1.00	1.26	5.03	30.77	1.50	4.24	11.14	19.64

Test Description	Depth (ft)	Time (min)	Qw/Qp	qapp/σ'v	Depth (ft)	Time (min)	Qw/Qp	qapp/σ'v	Depth	Time	Qw/Qp	qapp/σ'v
4/15/2003 10DU8-.8125	2.00				2.50				3.00			
4/15/2003 20DU8-.8125	2.00				2.50				3.00			
4/16/2003 10DU8-.5	2.00				2.50				3.00			
4/16/2003 20DU8-.5	2.00				2.50				3.00			
4/17/2003 20DU8-.5	2.00	1.83	6.84	13.76	2.50	2.61	8.08	11.17	3.00	4.21	11.16	9.31
4/17/2003 20DU8-.625	2.00	3.09	11.71	13.47	2.50	4.38	13.31	10.48	3.00			
4/11/2003 10DU8-.8125	2.00				2.50				3.00			
5/8/2003 20DU8-.625	2.00	2.98	11.50	13.91	2.50				3.00			
45 Deg 7-7-03 10 DU8 0.5	2.00	2.77	5.41	14.03	2.50	4.23	6.60	10.85	3.00	6.23	8.54	9.36
45 Deg 7-8-03 10 DU8 0.625	2.00	3.66	7.16	14.57	2.50	5.38	8.37	11.27	3.00	8.46	10.95	9.08
45 Deg 7-8-03 10 DU8 0.8125	2.00	9.59	18.76	14.21						3.00		

Test Description	Jet Velocity (ft/min)	qapp/σ'v	Qw/Qp	qapp/σ'v	Qw/Qp	qapp/σ'v	Qw/Qp	qapp/σ'v	Qw/Qp	qapp/σ'v	Qw/Qp	qapp/σ'v
4/15/2003 10DU8-.8125	186											
4/15/2003 20DU8-.8125	370											
4/16/2003 10DU8-.5	490	56.50	5.87	29.92	13.21	26.47	16.60					
4/16/2003 20DU8-.5	978											
4/17/2003 20DU8-.5	978	56.22	4.41	29.84	5.06	25.33	5.17	20.57	5.76	14.76	6.50	9.98
4/17/2003 20DU8-.625	626	53.58	5.67	30.99	6.29	26.04	7.35	20.28	7.78	15.22	9.79	10.48
4/11/2003 10DU8-.8125	186											
5/8/2003 20DU8-.625	626	53.00	6.08	29.73	6.41	26.25	6.90	20.38	8.01	15.33	10.97	

Table A- 19 Data Analysis and Model Development Data (Cherry Branch Sand)

Full Tests - Cherry Branch Sand

Test Description	Depth	Time	Vj/IR	Qw/Qp	Depth	Time	Vj/IR	Qw/Qp	Depth	Time	Vj/IR	Qw/Qp
5/21/2003 10DU8-.8125	0.50	3.45	1744.99	26.91	1.00				1.50			
5/22/2003 10DU8-.625	0.50	2.37	1537.26	18.09	1.00	5.13	1725.49	19.61	1.50	8.51	2509.81	21.71
5/22/2003 20DU8-.8125	0.50	0.78	445.53	13.58	1.00	1.64	779.67	13.42	1.50	2.64	705.42	14.08
5/27/2003 10DU8-.5	0.50	1.21	1225.49	11.03	1.00	2.68	1666.67	11.18	1.50	4.47	2058.83	12.05
6/27/2003 10DU8-.5	0.50	0.70	392.16	5.85	1.00	1.15	490.20	4.60	1.50	2.08	1225.49	5.47

Test Description	Depth	Time	Vj/IR	Qw/Qp	Depth	Time	Vj/IR	Qw/Qp	Depth	Time	Vj/IR	Qw/Qp
5/21/2003 10DU8-.8125	2.00				2.50				3.00			
5/22/2003 10DU8-.625	2.00	12.00	1725.49	22.97	2.50	14.98	4015.70	24.57	3.00			
5/22/2003 20DU8-.8125	2.00	3.86	1485.09	15.26	2.50	5.60	1150.95	17.60	3.00	7.28	1485.09	18.99
5/27/2003 10DU8-.5	2.00	6.58	1421.57	13.14	2.50	8.65	2254.91	13.69	3.00			
6/27/2003 10DU8-.5	2.00	3.90	1813.73	7.63	2.50	5.98	2058.83	9.31	3.00	8.94	3333.34	11.58

Test Description	Depth	Time	Vj/IR	Qw/Qp
5/21/2003 10DU8-.8125	3.50			
5/22/2003 10DU8-.625	3.50			
5/22/2003 20DU8-.8125	3.50	9.56	2351.40	21.30169834
5/27/2003 10DU8-.5	3.50			
6/27/2003 10DU8-.5	3.50			

Test Description	Jet Velocity, Vj (ft.min)	qapp/σ'v	Qw/Qp	qapp/σ'v	Qw/Qp	qapp/σ'v	Qw/Qp	qapp/σ'v	Qw/Qp	qapp/σ'v	Qw/Qp	qapp/σ'v	Qw/Qp
5/21/2003 10DU8-.8125	186	57.33	27.75										
5/22/2003 10DU8-.625	313	56.33	18.17	29.04	20.44	26.25	20.84	20.16	23.15	15.23	24.06		
5/22/2003 20DU8-.8125	371	57.19	12.78	29.88	14.12	26.17	14.08	20.33	14.38	15.14	17.43	10.00	20.03
5/27/2003 10DU8-.5	490	55.84	10.32	31.03	11.44	26.06	11.86	20.02	13.20	15.13	13.40		13.69
6/27/2003 10DU8-.5	490	54.94	5.26	30.33	4.77	26.27	5.02	20.60	6.11	15.39	8.26	9.91	13.05

Table A- 20 Data Analysis (Mortar Sand + Kaolinite)

Full Depth Tests - Mortar Sand + Kaolinite

Test Description	Jet Velocity (ft/min)	Pile Dia. (in)	Ap (ft^2)	Dj (in)	Aj (ft^2)	Final Depth of Insertion (ft)	Ap/Aj	Q (ft^3/min)	Pile Volume (ft^3)	Time	Qw/Qp (Total)
7-15-03 10KM8-0.5	490	8.00	0.35	0.50	0.0027	2.33	128.00	1.34	0.81	5.67	9.30
8-5-0310KM8-0.8125	186	8.00	0.35	0.81	0.0072	0.92	48.47	1.34	0.32	6.30	26.32
8-6-0310KM8-.625	314	8.00	0.35	0.63	0.0043	2.00	81.92	1.34	0.70	8.75	16.76

Test Description	Depth (ft)	Time (min)	Qw/Qp	Depth (ft)	Time (min)	Qw/Qp	Depth (ft)	Time (min)	Qw/Qp	Depth (ft)	Time (min)	Qw/Qp
7-15-03 10KM8-0.5	0.50	0.32	2.65	1.00	1.34	5.36	1.50	2.66	6.98	2.00	4.77	9.32
8-5-0310KM8-0.8125	0.50	1.62	13.51	1.00	5.68		1.50			2.00		
8-6-0310KM8-.625	0.50	0.79	6.62	1.00	2.35	9.39	1.50	4.34	11.40	2.00	8.04	15.73

Depth Control Tests

Table A- 21 Depth Control Data Analysis and Model Development (Concrete Sand)

Depth Control Tests - Concrete Sand

Test Description	Jet Velocity (ft/min)	Pile Dia. (in)	Pile Area, Ap (ft^2)	Jet Dia., Dj (in)	Jet Area, Aj (ft^2)	Inst. Depth (ft)	Ap/Aj	Qw (ft^3/min)	Pile Volume (ft^3)	Time (min)	Qp/Qj (Total)
5/29/2003 10DW8-.5	490.20	8.00	0.35	0.50	0.00273	1.00	128.00	1.34	0.35	3.93	0.066
6/25/2003 20DW8-.5	980.00	8.00	0.35	0.50	0.00273	1.00	128.00	2.67	0.35	0.50	0.261
6/25/2003 20DW8-.625	627.00	8.00	0.35	0.63	0.00426	1.00	81.92	2.67	0.35	1.70	0.077
6/25/2003 20DW8-.813	371.00	8.00	0.35	0.81	0.00720	1.00	48.47	2.67	0.35	1.42	0.092

Test Description	Jet Velocity (ft/min)	Qw (ft^3/min)	Pile Volume(ft^3)	Debris Volume, Vdebris (ft^3)	Debris Area, Adebris (ft^2)	Vdebris/Vpile	Qw/Qp	Insertion Rate, IR (ft/min)	Vdebris/Vwtotal	Adebris*Dp/Vw	VwTotal
5/29/2003 10DW8-.5	490	1.34	0.35	0.50	4.03	1.42	15.07	0.26	0.09	10.57	5.26
6/25/2003 20DW8-.5	980	2.67	0.35	0.58	5.62	1.67	3.82	2.09	0.44	2.29	1.34
6/25/2003 20DW8-.625	627	2.67	0.35	0.66	5.37	1.88	13.00	0.65	0.14	6.91	4.54
6/25/2003 20DW8-.813	371	2.67	0.35	0.63	4.64	1.82	10.84	0.70	0.17	5.97	3.78

Table A- 22 Depth Control Data Analysis and Model Development (Mortar Sand)

Depth Control - Mortar Sand

Test Description	Jet Velocity (ft/min)	Pile Dia. (in)	Pile Area, Ap (ft^2)	Jet Dia., Dj (in)	Jet Area, Aj (ft^2)	Inst. Depth (ft)	Ap/Aj	Qw (ft^3/min)	Pile Volume (ft^3)	Time (min)	Qw/Qp (Total)
8/6/2003 10DU8-0.5	490	8.00	0.35	0.50	0.0027	1.00	128.00	1.34	0.35	1.42	0.18
8/6/2003 10DU8-0.625	314	8.00	0.35	0.63	0.0043	1.00	81.92	1.34	0.35	6.25	0.04
8/6/2003 20DU8-0.5	980	8.00	0.35	0.50	0.0027	1.00	128.00	2.67	0.35	0.52	0.25
8/6/2003 20DU8-0.813	371	8.00	0.35	0.81	0.0072	1.00	48.47	2.67	0.35	0.78	0.17

Test Description	Jet Velocity (ft/min)	Qw (ft^3/min)	Pile Volume(ft^3)	Debris Volume, Vdebris (ft^3)	Debris Area, Adebris (ft^2)	Vdebris/Vpile	Qw/Qp	Insertion Rate, IR (ft/min)	Vdebris/Vwtotal	Adebris*Dp/ Vwtotal	VwTotal
8/6/2003 10DU8-0.5	490	1.34	0.35	0.42	5.08	1.21	5.43	0.72	0.22	1.79	1.89
8/6/2003 10DU8-0.625	314	1.34	0.35	0.45	4.43	1.29	23.94	0.17	0.05	0.35	8.36
8/6/2003 20DU8-0.5	980	2.67	0.35	0.48	5.84	1.37	3.96	1.92	0.35	2.82	1.38
8/6/2003 20DU8-0.813	371	2.67	0.35	0.42	5.81	1.20	6.00	1.29	0.20	1.85	2.09

Table A- 23 Depth Control Data Analysis and Model Development (Cherry Branch Sand)

Depth Control Tests - Cherry Branch Sand

Test Description	Jet Velocity (ft/min)	Pile Dia. (in)	Pile Area, Ap (ft^2)	Jet Dia., Dj (in)	Jet Area, Aj (ft^2)	Inst. Depth (ft)	Ap/Aj	Qw (ft^3/min)	Pile Volume (ft^3)	Time (min)	Qw/Qp (Total)
5/21/2003 10DU8-.8125	186	8	0.35	0.81	0.0072	0.81	48.47	1.34	0.28	6.25	29.54
6/27/2003 10DU8-.5	490	8	0.35	0.50	0.0027	1.00	128.00	1.34	0.35	1.60	6.13
6/26/2003 10DU8-.625	314	8	0.35	0.63	0.0043	1.00	81.92	1.34	0.35	3.45	13.21
6/26/2003 20DU8-.625	627	8	0.35	0.63	0.0043	1.00	81.92	2.67	0.35	1.02	7.77
6/26/2003 20DU8-.813	371	8	0.35	0.81	0.0072	1.00	48.47	2.67	0.35	1.43	10.95

Test Description	Jet Velocity (ft/min)	Qw (ft^3/min)	Pile Volume(ft^3)	Debris Volume, Vdebris (ft^3)	Debris Area, Adebris (ft^2)	Vdebris/V pile	Qw/Qp	Insertion Rate, IR (ft/min)	Vdebris/V wtotal	Adebris*Dp/ Vwtotal	VwTotal
5/21/2003 10DU8-.8125	186	1.34	0.28	0.45	5.84	1.58	29.54	0.13	0.05	0.47	8.36
6/27/2003 10DU8-.5	490	1.34	0.35	0.49	6.38	1.40	6.13	0.61	0.23	1.99	2.14
6/26/2003 10DU8-.625	314	1.34	0.35	0.54	7.17	1.54	13.21	0.29	0.12	1.04	4.61
6/26/2003 20DU8-.625	627	2.67	0.35	0.63	6.80	1.80	7.77	0.99	0.23	1.67	2.71
6/26/2003 20DU8-.813	371	2.67	0.35	0.39	5.65	1.12	10.95	0.71	0.10	0.99	3.82

Table A- 24 Depth Control Data Analysis and Model Development (Mortar Sand + Kaolinite)

Depth Control Tests- Mortar Sand + Kaolinite

Test Description	Jet Velocity (ft/min)	Pile Dia. (in)	Pile Area, Ap (ft^2)	Jet Dia., Dj (in)	Jet Area, Aj (ft^2)	Inst. Depth (ft)	Ap/Aj	Qw (ft^3/min)	Pile Volume (ft^3)	Time (min)	Qw/Qp (Total)
8-5-03-10KM8-0.5	490	8.00	0.35	0.50	0.0027	1.00	128.00	1.34	0.35	1.33	0.20
8-5-03-10KM8-0.813	186	8.00	0.35	0.81	0.0072	1.00	48.47	1.34	0.35	6.30	0.04
8-5-03-20KM8-0.813	371	8.00	0.35	0.81	0.0072	1.00	48.53	2.67	0.35	1.08	0.12
8-5-03-20KM8-0.5	980	8.00	0.35	0.50	0.0027	1.00	128.00	2.67	0.35	0.50	0.26

Test Description	Jet Velocity (ft/min)	Qw (ft^3/min)	Pile Volume(ft^3)	Debris Volume, Vdebris (ft^3)	Debris Area, Adebris (ft^2)	Vdebris/V pile	Qw/Qp	Insertion Rate, IR (ft/min)	Vdebris/V wtotal	Adebris*D p/Vwtotal	VwTotal
8-5-03-10KM8-0.5	490	1.34	0.35	0.37	5.27	1.07	5.11	0.75	0.21	1.97	1.78
8-5-03-10KM8-0.813	186	1.34	0.35	0.32	3.57	0.92	24.13	0.16	0.04	0.28	8.42
8-5-03-20KM8-0.813	371	2.67	0.35	0.42	4.97	1.21	8.30	0.92	0.15	1.14	2.90
8-5-03-20KM8-0.5	980	2.67	0.35	0.43	5.57	1.24	3.83	2.00	0.32	2.78	1.34